AD-A077 504 LOS ALAMOS SCIENTIFIC LAB N MEX F/G 4/2
ACTIVITIES OF THE SPECIAL WEATHER ADVISORY SERVICE.(U)
JUL 53 G J NEWGARDEN

UNCLASSIFIED AEC-WT-705 NL

| OF |
ADA
077504

PHOTOGRAPH THIS SHEET

ADA077504

DTIC ACCESSION NUMBER

III

LEVEL

INVENTORY

AEC

WT-705

DOCUMENT IDENTIFICATION

DISTRIBUTION STATEMENT A

Approved for public release;
Distribution Unlimited

DISTRIBUTION STATEMENT

ACCESSION FOR

NTIS GRA&I ☒

DTIC TAB ☐

UNANNOUNCED ☐

JUSTIFICATION

Per ltr. on file

BY

DISTRIBUTION /

AVAILABILITY CODES

DIST	AVAIL AND/OR SPECIAL	
A		

DISTRIBUTION STAMP

DDC
RECEIVED
DEC 3 1979
D

DATE ACCESSIONED

79 11 21 043

DATE RECEIVED IN DTIC

PHOTOGRAPH THIS SHEET AND RETURN TO DTIC-DDA-2

DTIC FORM OCT 79 70A

DOCUMENT PROCESSING SHEET

WT-705

Copy No. 201 A

Operation
UPSHOT-KNOTHOLE

NEVADA PROVING GROUNDS

March - June 1953

ACTIVITIES OF THE SPECIAL WEATHER ADVISORY SERVICE

LOS ALAMOS SCIENTIFIC LABORATORY
UNIVERSITY of CALIFORNIA

If this report is no longer needed, return
AEC Technical Information Service
P. O. Box 401
Oak Ridge, Tennessee

UNCLASSIFIED

~~CONFIDENTIAL~~

WT-705

This document consists of 98 pages
No. 201 of 255 copies, Series A

Report to the Test Director

ACTIVITIES OF THE SPECIAL WEATHER ADVISORY SERVICE

By

George J. Newgarden III
Major, USAF

Los Alamos Scientific Laboratory
University of California
July 1953

~~RESTRICTED DATA~~

~~This document contains restricted data as defined in the Atomic Energy Act of 1946. Its transmittal or the disclosure of its contents in any manner to an unauthorized person is prohibited.~~

~~CONFIDENTIAL~~

~~SECURITY INFORMATION~~

UNCLASSIFIED

ABSTRACT

Certain weather advisory functions were delegated to the Group H-6 (LASL) Weather Section during test activities at the Nevada Proving Grounds. Techniques utilized in performing these functions are outlined, and the actual advisories, forecasts, and analyses issued are made a matter of record.

The weather advisory functions outlined herein were fulfilled by Lt Col C. A. Spohn through Upshot-Knothole 8, at which time Lt Col Spohn received transfer orders and was superseded by his assistant, Maj George J. Newgarden III.

CONTENTS

ILLUSTRATIONS

ILLUSTRATIONS (Continued)

ILLUSTRATIONS (Continued)

ACTIVITIES OF THE SPECIAL WEATHER ADVISORY SERVICE

1 GENERAL

The Weather Section of the Health Division of the Los Alamos Scientific Laboratory was delegated the responsibility to provide certain specialized weather advisory service for the Advisory Panel during Operation Upshot-Knothole. In addition, the Weather Section maintained close liaison with the Radiological-Safety (Rad-Safe) Group on those items which were of special interest to that organization. Generally, the same functions were performed as in Operations Buster-Jangle and Tumbler-Snapper. The specific functions are as follows:

1.1 Preshot Functions

1. **Preparation of fall-out forecasts and plots.**
2. **Forecasts of maximum bomb-cloud height.**
3. **Assistance to the CAA representative in determining necessary airspace closure.**

Forecasts of bomb-cloud trajectory, which would normally be a function of this group, were made by the Air Weather Service forecast team at Mercury Forecast Center, under the direction of Lt Col DeWitt Morgan, chief forecaster.

1.2 Postshot Functions

1. **Preparation of additional fall-out plots, as required.**
2. **Computation of cloud heights.**
3. **Recommendations for changes in CAA airspace closure.**
4. **Analysis of cloud trajectories.**

Postshot analysis of fall-out was also carried out, but, since this was frequently completed a considerable time after the shot, it is not considered an integral part of the test advisory service. However, postshot fall-out analysis charts are included in this report.

2 FALL-OUT FORECASTS AND PLOTS

Forecast fall-out patterns were prepared at 2100 local time on D−1 day for briefings given the Advisory Panel. These forecasts were based on the wind forecast for the target area at shot time, as prepared by the Mercury Forecast Center. (See the Appendix to Activities of the Special Weather Advisory Service, Operation Buster-Jangle Report, WT-418, for a description of the technique of preparation of fall-out forecasts.) In addition, fall-out plots were prepared based on all wind soundings made at the Control Point between 2100 local time and shot time. These preshot fall-out plots and the postshot plots were primarily for the use of the controller of the offsite monitoring section of the Rad-Safe Group in positioning his monitors.

Since fall-out plots are based on single station winds aloft (i.e., the Control Point at Nevada Proving Grounds), it must necessarily be assumed that the wind field is constant (i.e., no space-time changes). Obviously such is seldom the case; therefore, upon completion of each test, postshot analysis of fall-out was undertaken. Since wind space-time changes are considered in these analyses, their accuracy is improved considerably. In all cases the postshot analysis fall-out charts included in this report verify very closely the facts obtained by the Rad-Safe offsite monitors.

The various fall-out forecasts, plots, and postshot analyses are shown in Figs. 1 to 48. Discussion of the patterns for each individual shot follows.

2.1 Upshot-Knothole 1 (Figs. 1 to 4)

The briefing forecast indicated fall-out to the northeast. Fall-out plots prepared from the 0100 and 0430 PST wind soundings indicated that the fall-out sector was gradually shifting to the east. The postshot analysis shows that the fall-out did occur almost due east of zero point.

2.2 Upshot-Knothole 2 (Figs. 5 to 8)

The briefing forecast indicated fall-out again to the northeast. Fall-out plots from 0100 and 0330 PST wind soundings indicated a minor shifting of the fall-out sector to a more northerly heading. The postshot analysis shows that the high-level fall-out occurred in the north-northeast quadrant and the low-level fall-out occurred slightly west of north.

2.3 Upshot-Knothole 3 (Figs. 9 to 12)

The briefing forecast indicated fall-out to the southeast. Fall-out plots from 0100 and 0330 PST wind soundings indicated little change. The postshot analysis shows that the fall-out did occur to the southeast; however, there was a marked increase in the horizontal speed of the fall-out.

2.4 Upshot-Knothole 4 (Figs. 13 to 16)

The briefing forecast indicated fall-out to the south-southeast. Fall-out plots from 0330 and 0530 PST wind soundings indicated little change. The postshot analysis shows that the fall-out did occur to the south-southeast, although the high-level fall-out was slightly more easterly than was forecast.

2.5 Upshot-Knothole 5 (Figs. 17 to 20)

The briefing forecast again indicated fall-out to the south-southeast. Fall-out plots from 0100 and 0430 PST wind soundings indicated gradual shifting to the south. The postshot analysis shows that the fall-out did occur to the south-southeast; however, it was more southerly than was forecast.

2.6 Upshot-Knothole 6 (Figs. 21 to 25)

The briefing forecast indicated fall-out to the east-northeast. Fall-out plots from 2330, 0200, and 0420 PST wind soundings indicated a marked shift to the southeast. The postshot analysis shows that the fall-out did occur to the southeast.

2.7 Upshot-Knothole 7 (Figs. 26 to 30)

The briefing forecast indicated fall-out to the east. Fall-out plots from 0115, 0230, and 0415 PST wind soundings indicated a shift to the southeast. The postshot analysis shows that the fall-out occurred to the east-southeast.

2.8 Upshot-Knothole 8 (Figs. 31 to 34)

The briefing forecast again indicated fall-out to the east. Fall-out plots from 0430 and 0815 PDT winds indicated a slight shift to the east-northeast. The postshot analysis shows that the fall-out did occur to the east-northeast.

2.9 Upshot-Knothole 9 (Figs. 35 to 38)

The briefing forecast indicated fall-out to the east. Fall-out plots from 0200 and 0500 PDT wind soundings indicated a slight shift to the northeast, especially the low-level fall-out sector. The postshot analysis shows that the fall-out did occur to the northeast, although high-level fall-out occurred almost due east.

2.10 Upshot-Knothole 10 (Figs. 39 to 43)

The briefing forecast indicated fall-out to the northeast. Fall-out plots from 0200, 0400, and 0815 PDT wind soundings indicated little change. The postshot analysis shows that the fall-out did occur to the northeast but approximately 15° more northerly.

2.11 Upshot-Knothole 11 (Figs. 44 to 48)

The briefing forecast indicated fall-out to the southeast. Fall-out plots from 2330 and 0130 PDT wind soundings indicated a slight shift to the east-southeast. The fall-out plot from the 0500 PDT wind sounding indicated little change in the high-level fall-out sector; however, the plot indicates inconsistency in the low-level fall-out pattern owing to light and variable low-level winds. The postshot analysis shows that high-level fall-out occurred slightly south of east, low-level fall-out occurred around point zero, and the horizontal speed of fall-out decreased markedly.

2.12 Summary

The primary fall-out patterns (i.e., fall-out occurring from the cloud proper and the upper stem) do not show excessive shifts from the briefing forecasts to D day postshot analysis, generally less than 35° with a mean error of approximately 27°. The low-level fall-out patterns, however, occasionally show extreme shifts, as in Upshot-Knothole 6 and 11. It is the weak gradient type of pressure pattern at low levels which presents the meteorologist with the most difficult problem in forecasting wind direction.

3 CLOUD-HEIGHT FORECASTS AND DETERMINATIONS

A forecast of anticipated maximum cloud height was prepared immediately preceding the fall-out forecast and was included in the material presented at the briefing. These cloud-height forecasts were used to determine the levels from which fall-out could be expected, to determine the levels of concern for the CAA airspace closure, and to determine the levels for sampling by aircraft samplers.

3.1 Forecast Techniques

The forecasts were made using regression equations derived from Ranger, Buster-Jangle, and Tumbler-Snapper data. Independent variables were bomb yield, wind speed, atmospheric lapse rate, and height of tropopause (for yields greater than 10 kt only).

3.2 Determination Techniques

Beginning at 1 min after shot time and continuing at 1-min intervals up to approximately

15 min, elevation angles to both top and base of the bomb cloud were obtained by theodolite. These were combined with the wind data closest to zero time to determine the cloud height by the following method. An initial cloud height was determined from the elevation angle. The base line was then corrected by applying the 1-min cloud drift indicated by the wind flow in the layer through which the cloud was rising. This new base-line distance and the elevation angle then yielded a second approximation. Since these 1-min corrections to the cloud height were rarely in excess of 1500 ft, the second approximation yielded as much accuracy as the method justified.

Any errors in the technique are due to the assumptions that wind data taken about 10 miles from point zero, and as much as an hour earlier or later than shot time, represented the wind layer through which the cloud passed and that all theodolite sightings are really made on the top and base of the cloud. This latter item is of less importance if the cloud is moving away from the theodolite location, but when the cloud approaches the theodolite it becomes of major importance since it is more difficult for the observers to take a correct sight. Nonetheless it is believed that these results are more accurate than cloud-height estimates made by test aircraft pilots who are basing their estimates on pressure-altimeter readings, which may be off by several thousand feet at higher elevations. During the Upshot-Knothole test series, two simultaneous theodolite readings, one from the CP and one from the old Ranger CP, were obtained from Upshot-Knothole 1 through 10. The cloud-growth curves included in this report are based on the mean values of the two theodolite readings. Since Upshot-Knothole 11 was a night shot, theodolite data are not available. However, corrected data obtained for Upshot-Knothole 11 by test aircraft are as follows: maximum height of top of cloud, 42,700 ft MSL; maximum height of base of cloud, 35,000 ft MSL.

3.3 Results

Figure 49 shows the forecast and computed cloud heights for Upshot-Knothole. (Heights for Upshot-Knothole 11 are based on aircraft reports.) For nine of the shots the mean forecast error was approximately ±2000 ft. In the case of Upshot-Knothole 4, however, the cloud top was forecast 8000 ft lower than it occurred. This shot was a high-level air burst for which the cloud-top regression equation was not designed as it is when based on tower shots. The result of this high-level air burst suggests that the amount and rate of rise of the cloud are also dependent on the atmosphere pressure level at burst height. In the case of Upshot-Knothole 6 the cloud top was forecast 8000 ft higher than it occurred. Preliminary data indicate that the actual yield of the bomb was somewhat lower than anticipated and used in the regression equation. Other cloud-height forecast errors are due to inaccurate forecasts of wind speeds, atmospheric lapse rate, and tropopause height.

Figures 50 to 59 show individual cloud-growth curves as computed from theodolite and wind data. It is interesting to note the tendency of the cloud to sink after attaining maximum height.

4 CAA AIRSPACE CLOSURES

4.1 Closure Determination

On the evening prior to each shot a conference was held, immediately following the briefing, to determine the air sectors which would have to be closed to traffic during and after the shot. Participating members in the conference were representatives of the CAA, Test Director, Health Division Meteorological Section, and Rad-Safe Group. At this conference an initial closure plan was determined, based on (1) forecast cloud trajectory at various levels, (2) forecast height of cloud top and base, and (3) a dosage computation developed by T. N. White, LASL, which considered the wind shear, rate of turbulent diffusion, radioactive-decay rate, and the bomb yield.

Following shot time this closure plan was amended as required when reports of tracking aircraft, later wind data, and cloud-height computations indicated that items 1 and/or 2 differed markedly from the forecast values.

It was also necessary to ensure that no dangerous contamination could occur to nonparticipating aircraft and personnel and at the same time to minimize disruption of commercial air schedules. Because of the operating techniques of CAA, the philosophy of the conference was always to plan the closure so that changes would be more likely to release airspace than to close additional airspace, since the former could be done much more rapidly and positively than the latter. Further, last-minute closure of airspace seriously disrupts commercial aircraft service. This ensured that the first requirement would be met, even if the second could not always be.

4.2 Form of Closure Plan

The closure plan had to be drawn up in such a form that it could be easily administered by the CAA control center at Salt Lake City. The form which was devised as meeting this need most completely is described in the following paragraphs.

(a) Flash Circle. A circle, of generally a 50-mile radius, center at 37°N, 116°W, closed at all altitudes for a period of several hours which included shot time. The flash circle was to ensure that no aircraft was close enough to the blast at shot time for the pilot to suffer eye injury or temporary blindness.

(b) Sector. A pie-shaped wedge, the tip at 37°N, 116°W, was marked out to include those elevations and areas of normal outside traffic (i.e., outside the range) in which cloud and debris drift was anticipated while still dangerous.

(c) Warning Circle. A circle of sufficient size to include both the flash circle and the sector was laid out centered on some well-known town. The circle was for the convenience of CAA in alerting pilots as to the region through which flight plans needed to be cleared with the control center. It was the only part of the closure plan which was released to the general public by the CAA control center at Salt Lake City.

(d) High-level Quadrangle (or Triangle). The high-level quadrangle was closed to all aircraft for a considerable period (12 to 15 hr). This region was always much larger than the warning circle and covered the region through which the cloud proper was expected to drift while still hazardous. The base of this region was generally above 26,000 ft and hence was above the level of commercial traffic. Distribution of this notification was handled by the CAA control center at Salt Lake City, which notified those military airfields handling high-level traffic.

The closure plans for the Upshot-Knothole series are included as Figs. 60 to 70. Owing to complexity of corrections, all changes to a given closure plan are listed in the figure legends.

5 CLOUD TRAJECTORIES

Following each shot a cloud-trajectory analysis was carried out. Appropriate levels were selected to cover the vertical extent of the cloud, within the limits as imposed by the wind data available. For the selected levels, constant-level wind charts were plotted and analyzed, by streamline analysis, at 6-hr intervals (i.e., the intervals at which synoptic wind soundings are made at the various meteorological stations nationwide). The cloud was then moved at each level as indicated by the streamlines and isotachs, assuming that the analyzed field was unchanged during the 6-hr period (taken as 3 hr before and after synoptic time). For this reason the cloud trajectories sometimes show abrupt changes in direction or speed at the change from one 6-hr period to the next. The trajectories were usually computed for 24 hr, or until the cloud was several hundred miles from the site. Figures 71 to 81 show the plotted trajectories for the Upshot-Knothole test series.

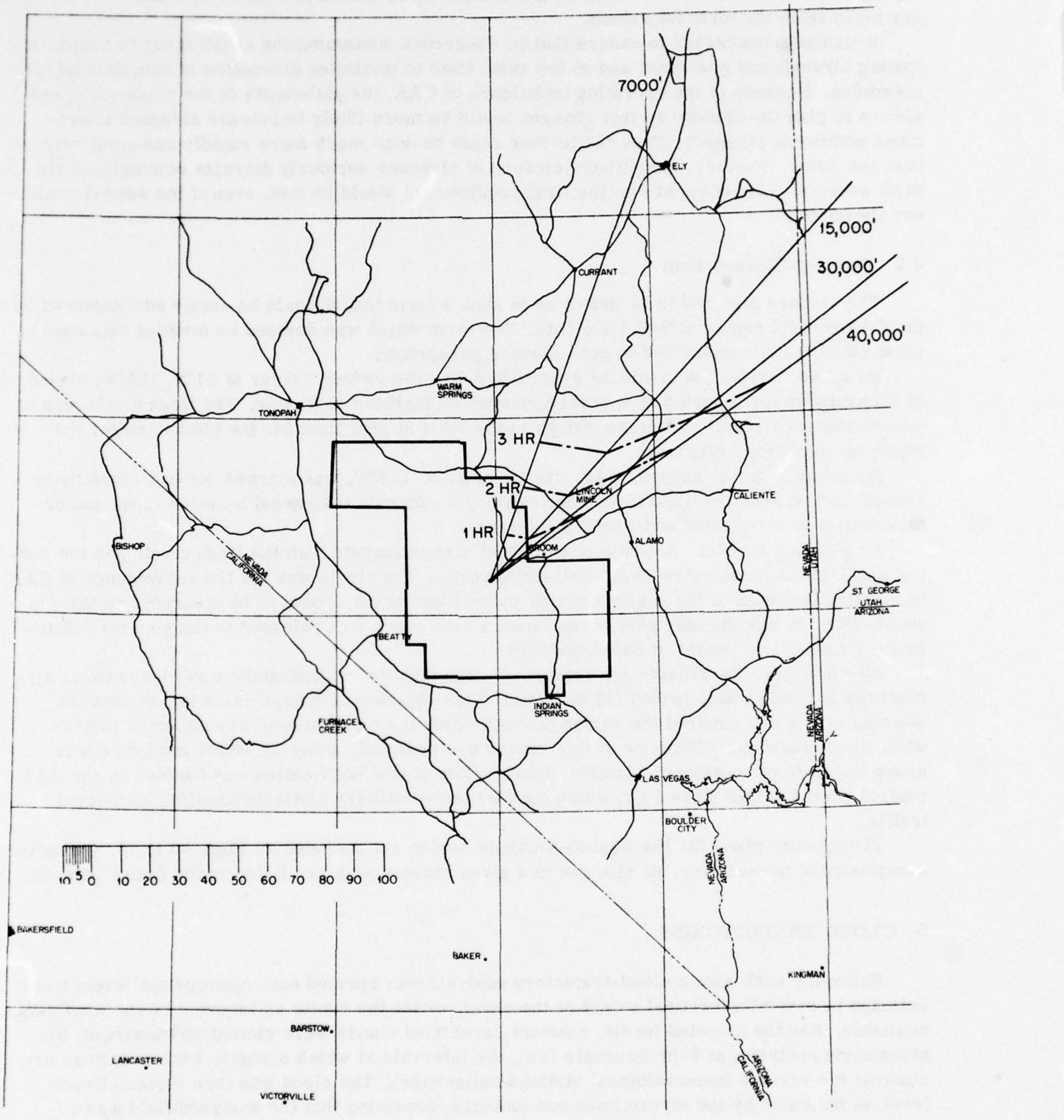

Fig. 1 — Fall-out forecast for Upshot-Knothole 1, prepared from briefing wind forecast at 2100 PST, 16 March 1953, valid at 0520 PST, 17 March 1953.

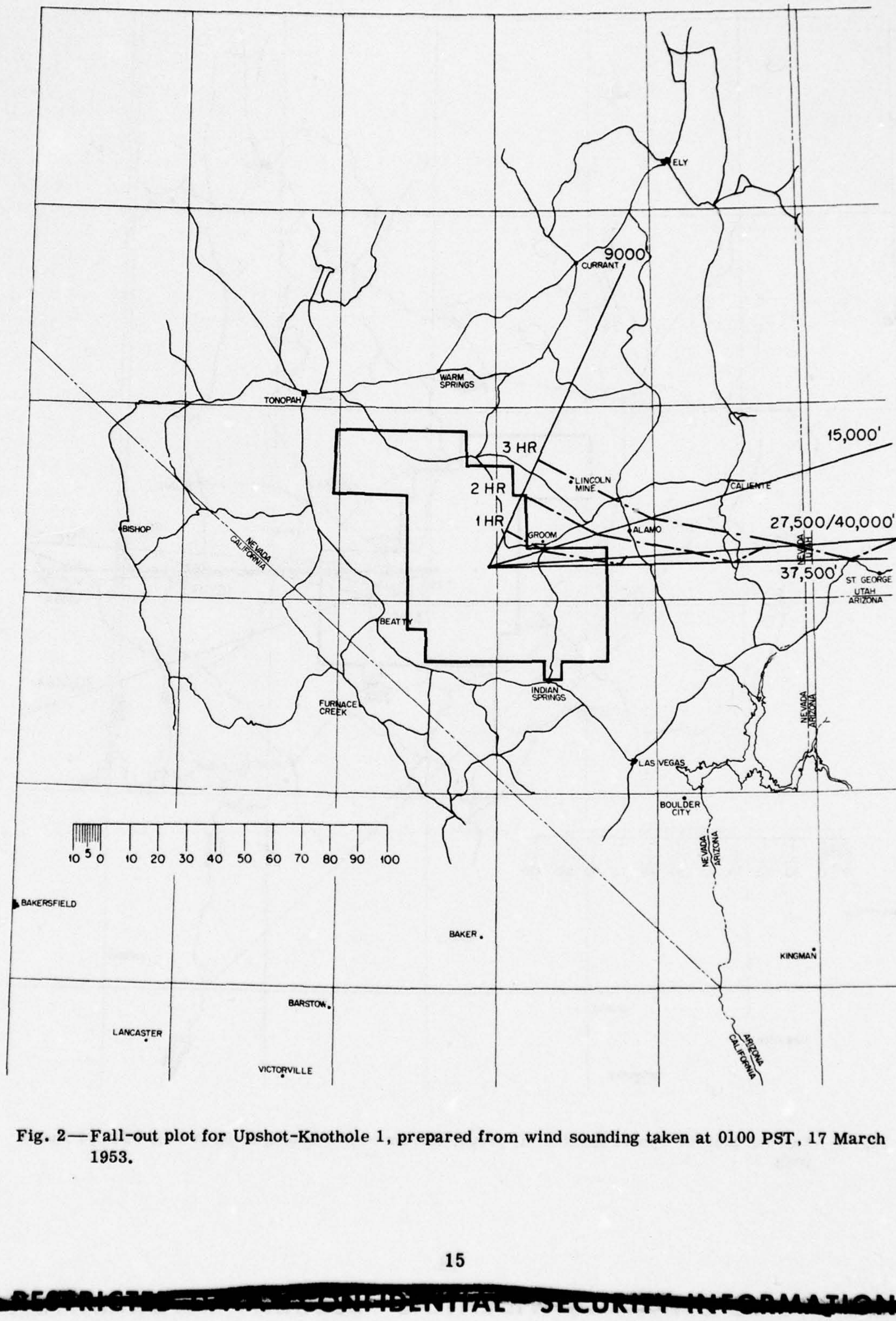

Fig. 2—Fall-out plot for Upshot-Knothole 1, prepared from wind sounding taken at 0100 PST, 17 March 1953.

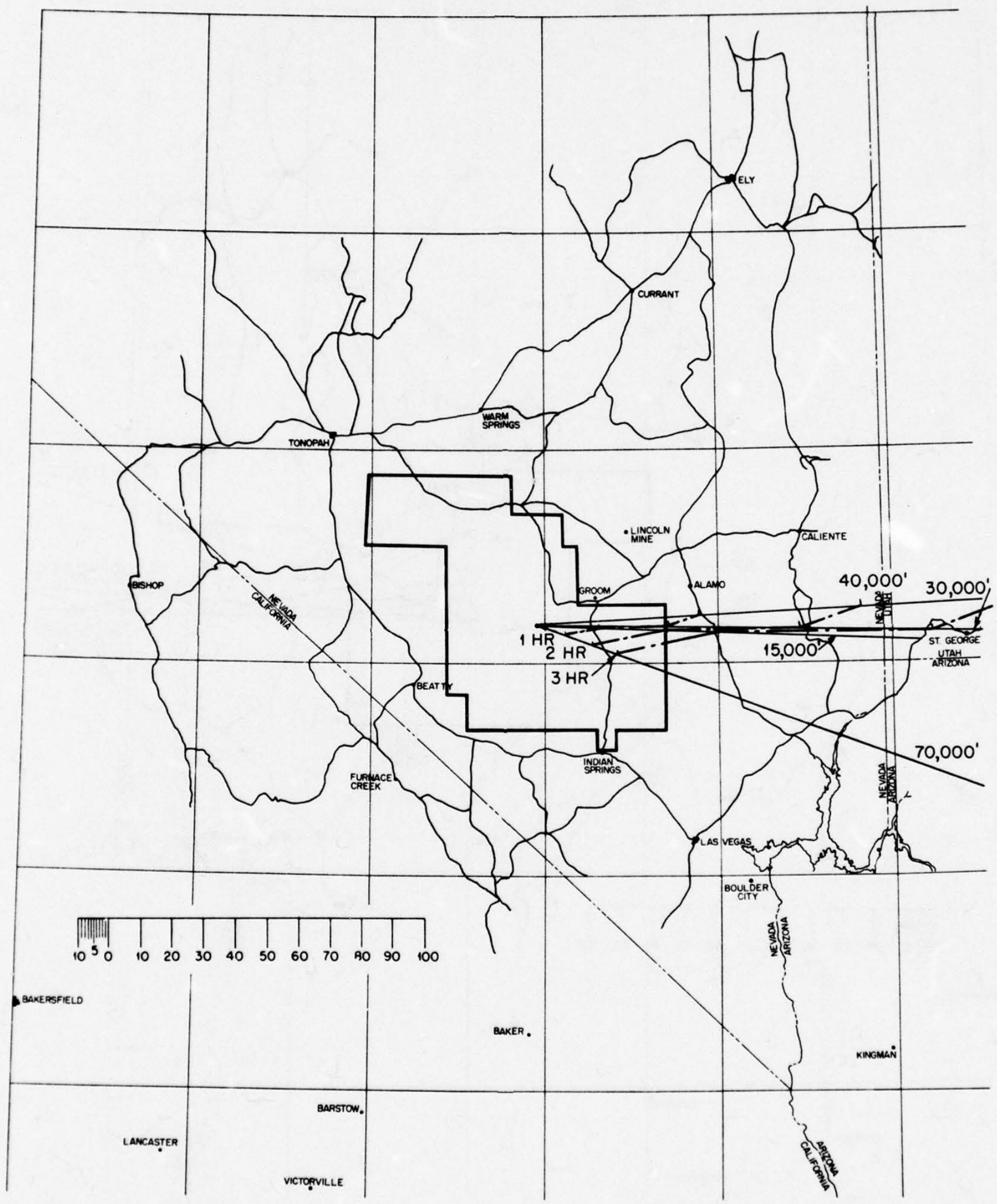

Fig. 3—Fall-out plot for Upshot-Knothole 1, prepared from wind sounding taken at 0400 PST, 17 March 1953.

[redacted]

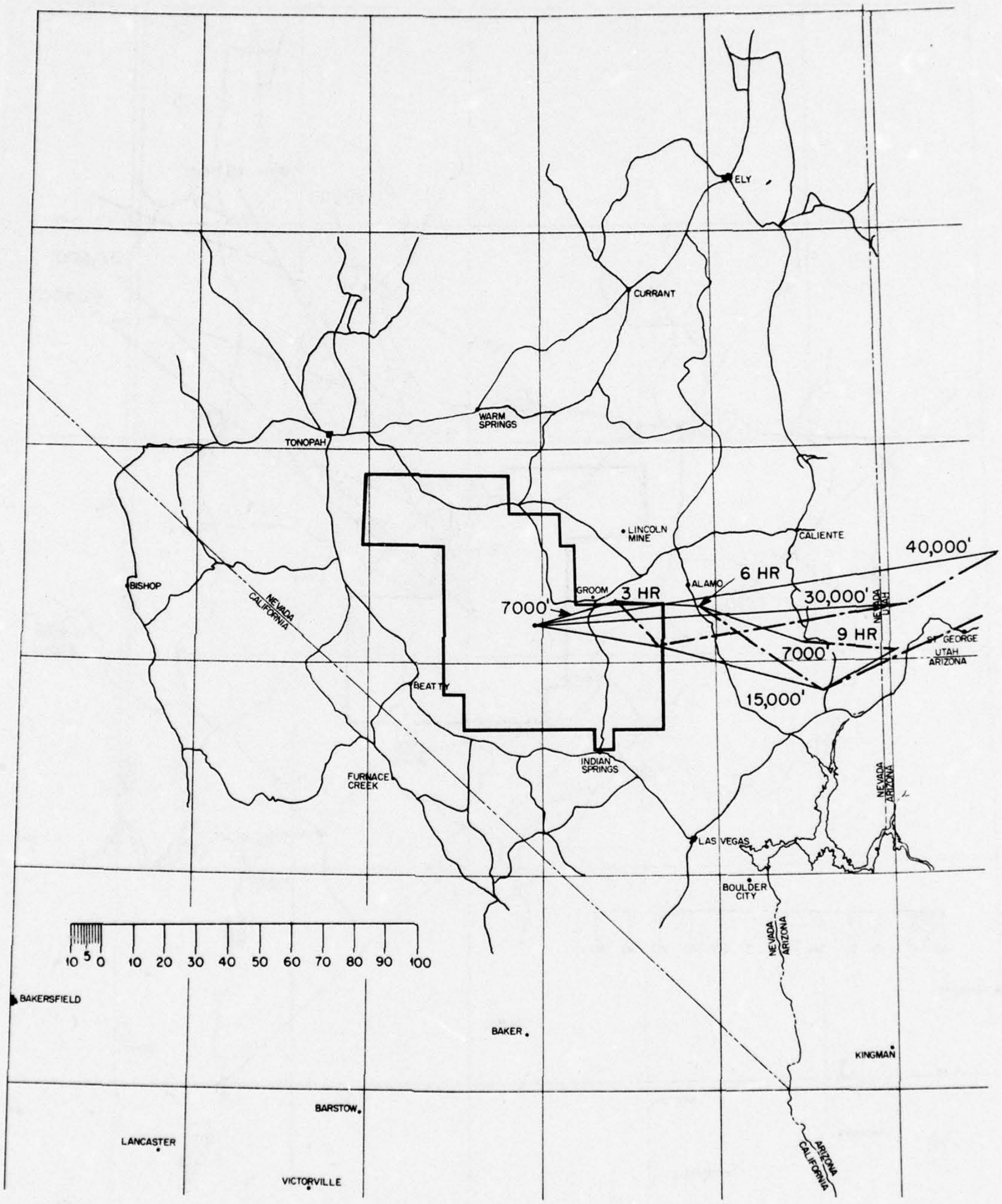

Fig. 4—Postshot analysis of fall-out for Upshot-Knothole 1.

~~RESTRICTED DATA — CONFIDENTIAL — SECURITY INFORMATION~~

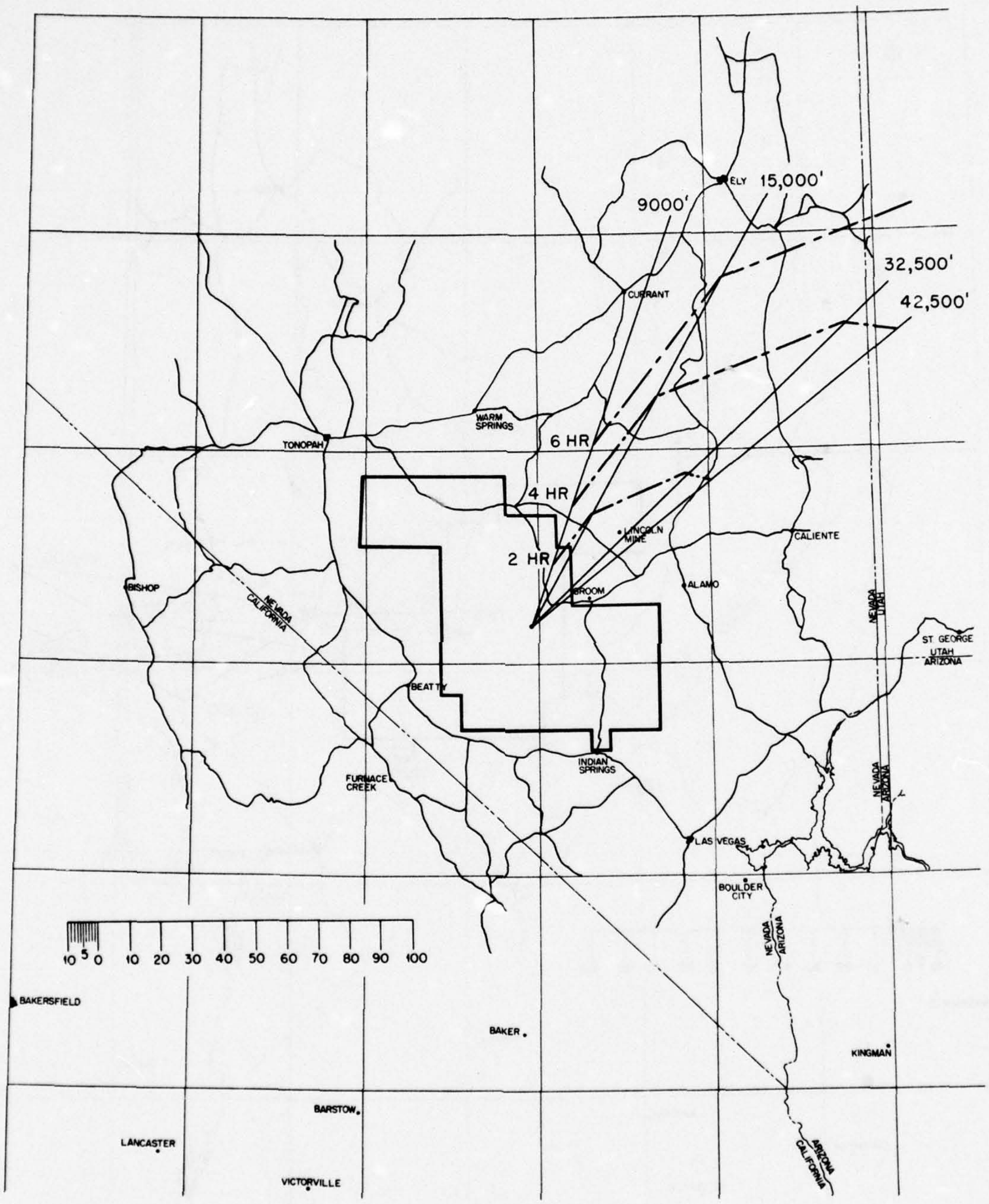

Fig. 5—Fall-out forecast for Upshot-Knothole 2, prepared from briefing wind forecast at 2100 PST, 23 March 1953, valid at 0510 PST, 24 March 1953.

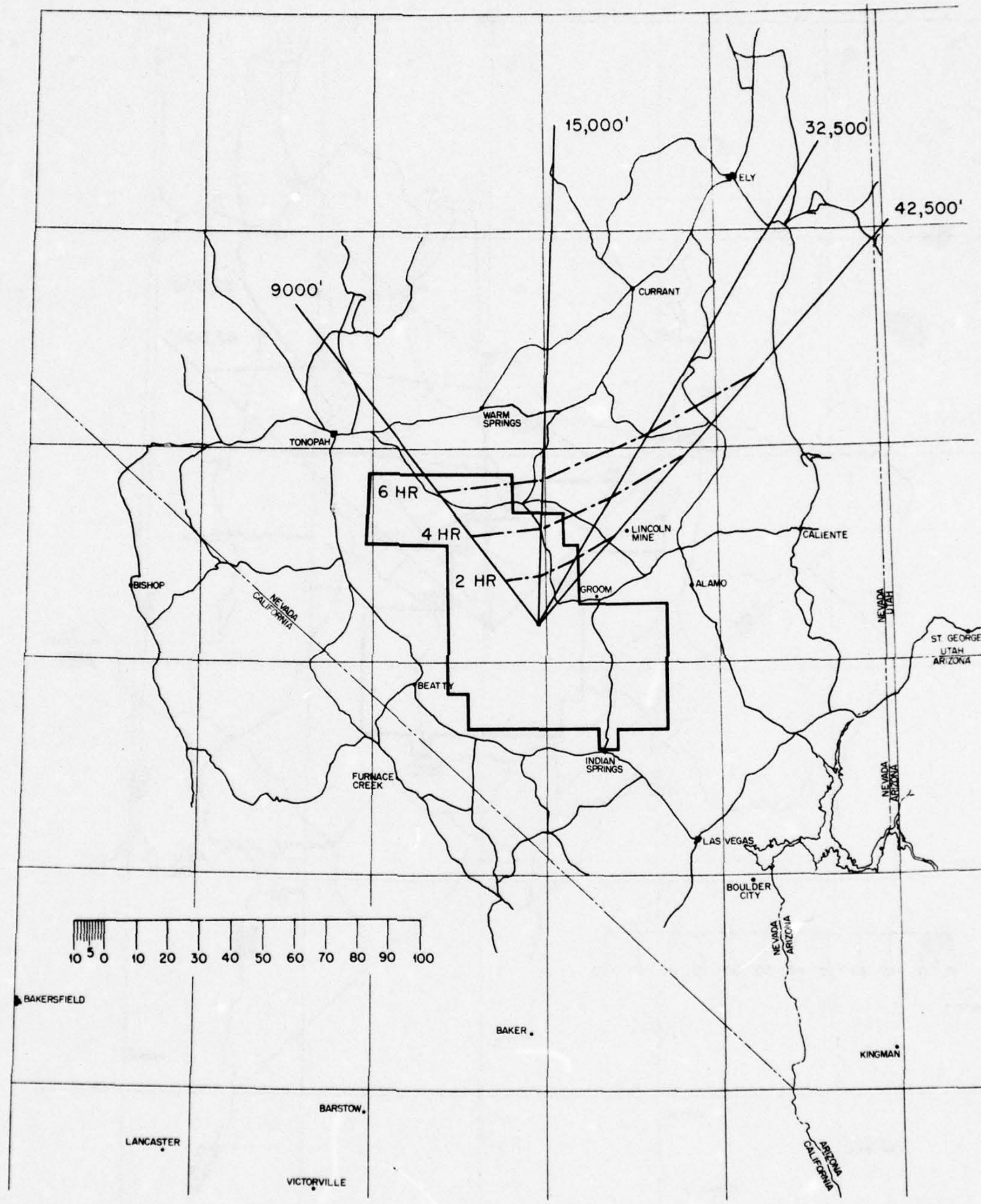

Fig. 6—Fall-out plot for Upshot-Knothole 2, prepared from wind sounding taken at 0100 PST, 24 March 1953.

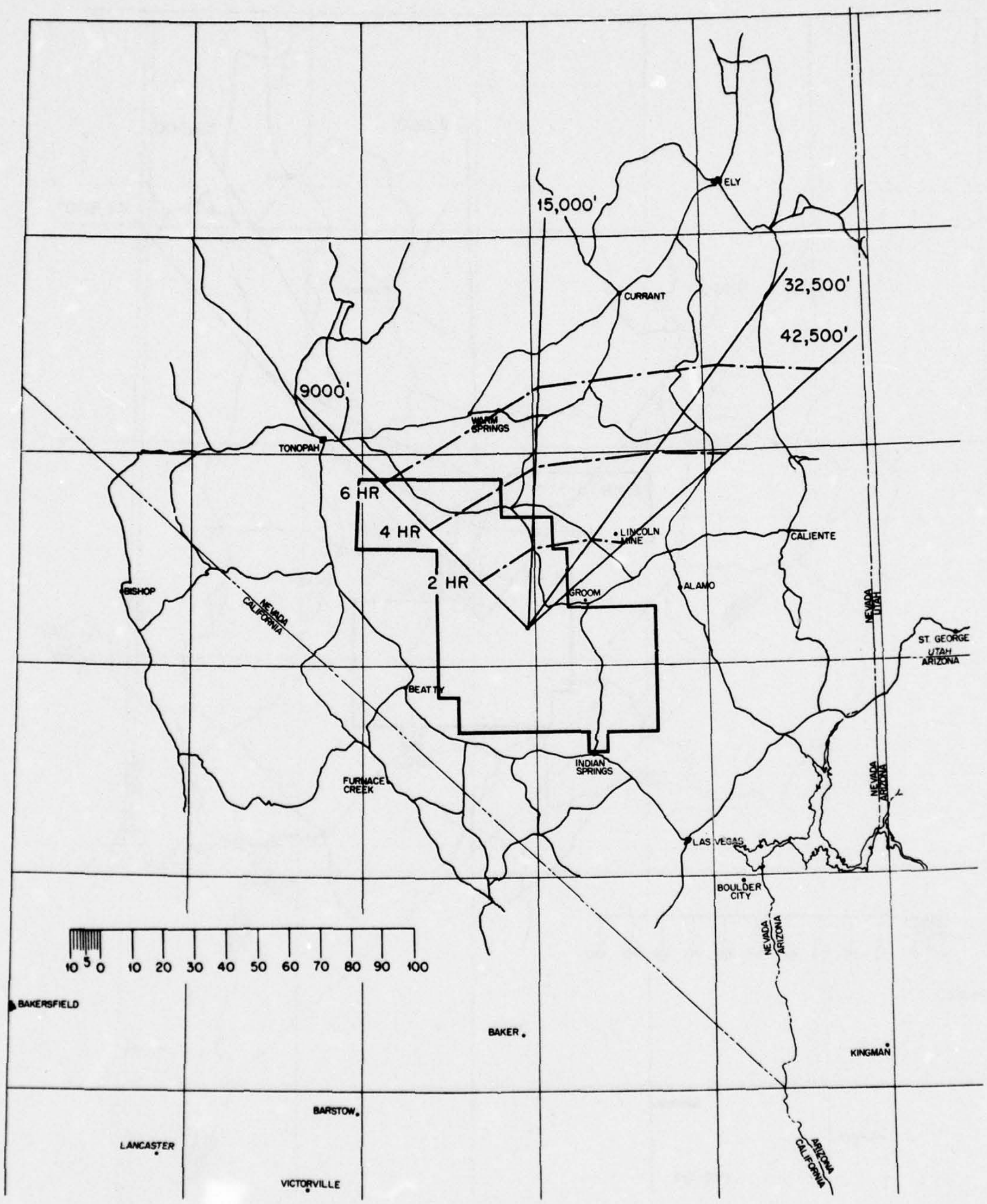

Fig. 7—Fall-out plot for Upshot-Knothole 2, prepared from wind sounding taken at 0330 PST, 24 March 1953.

[redacted]

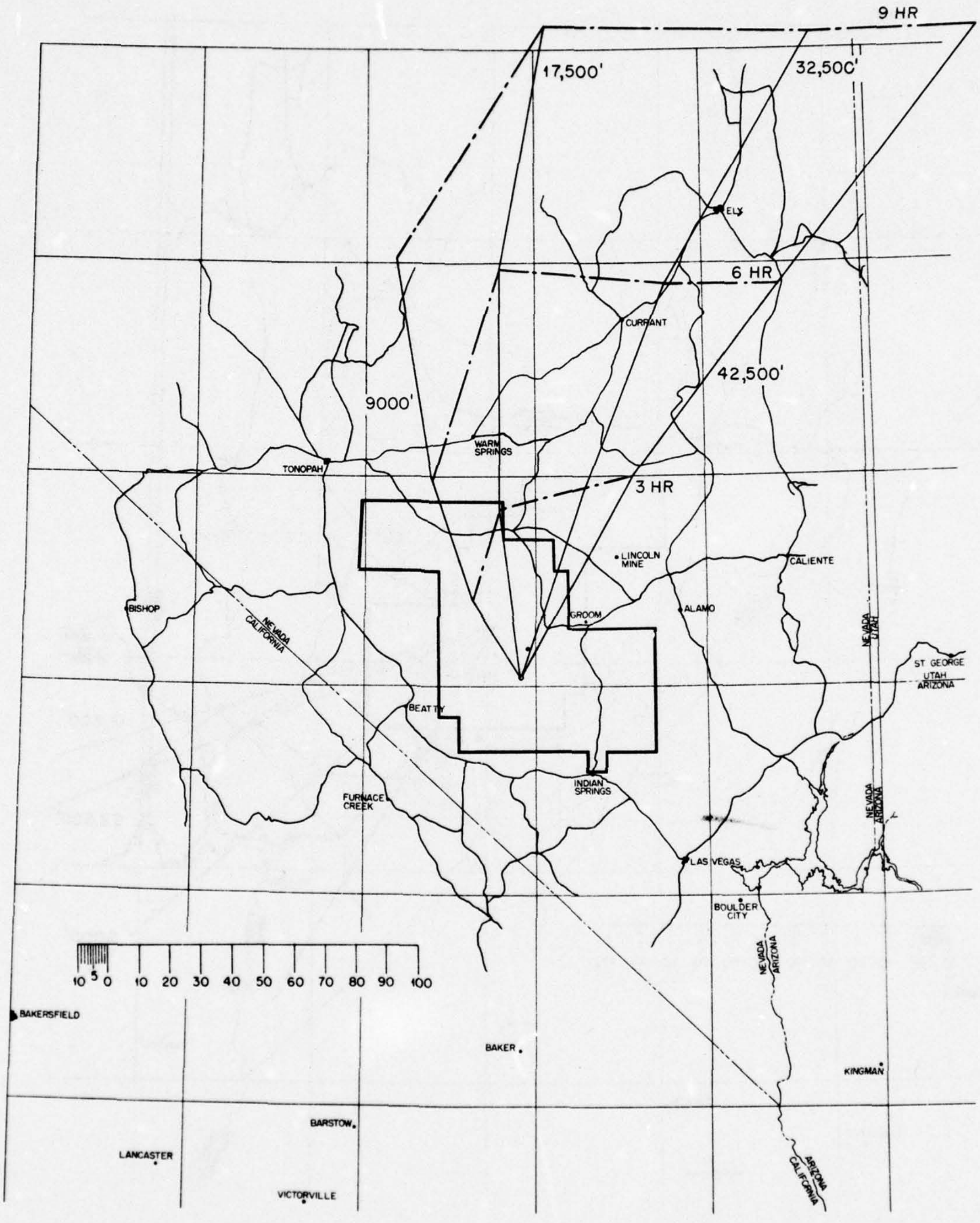

Fig. 8—Postshot analysis of fall-out for Upshot-Knothole 2.

[redacted]

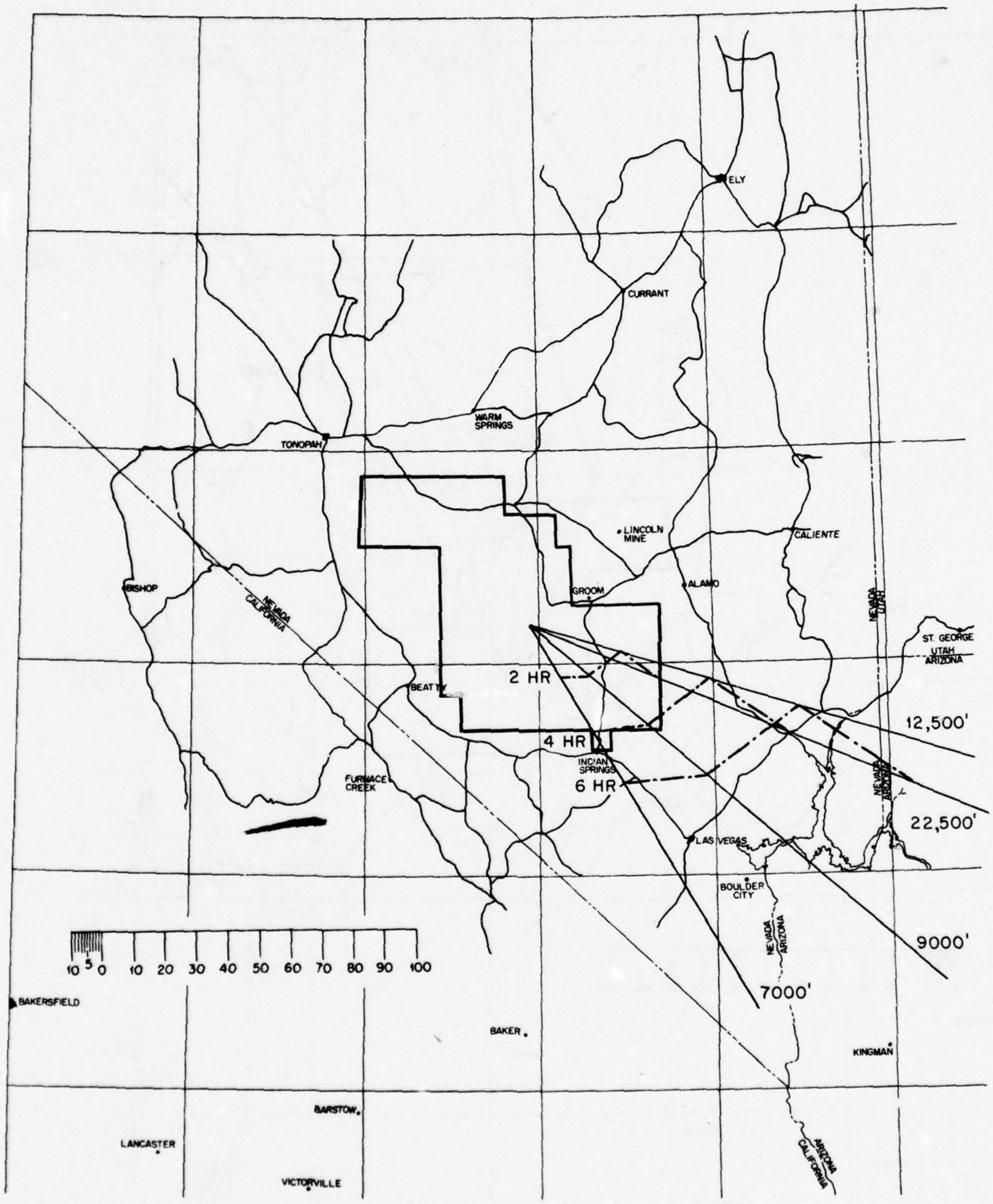

Fig. 9—Fall-out forecast for Upshot-Knothole 3, prepared from briefing wind forecast at 2100 PST, 30 March 1953, valid at 0500 PST, 31 March 1953.

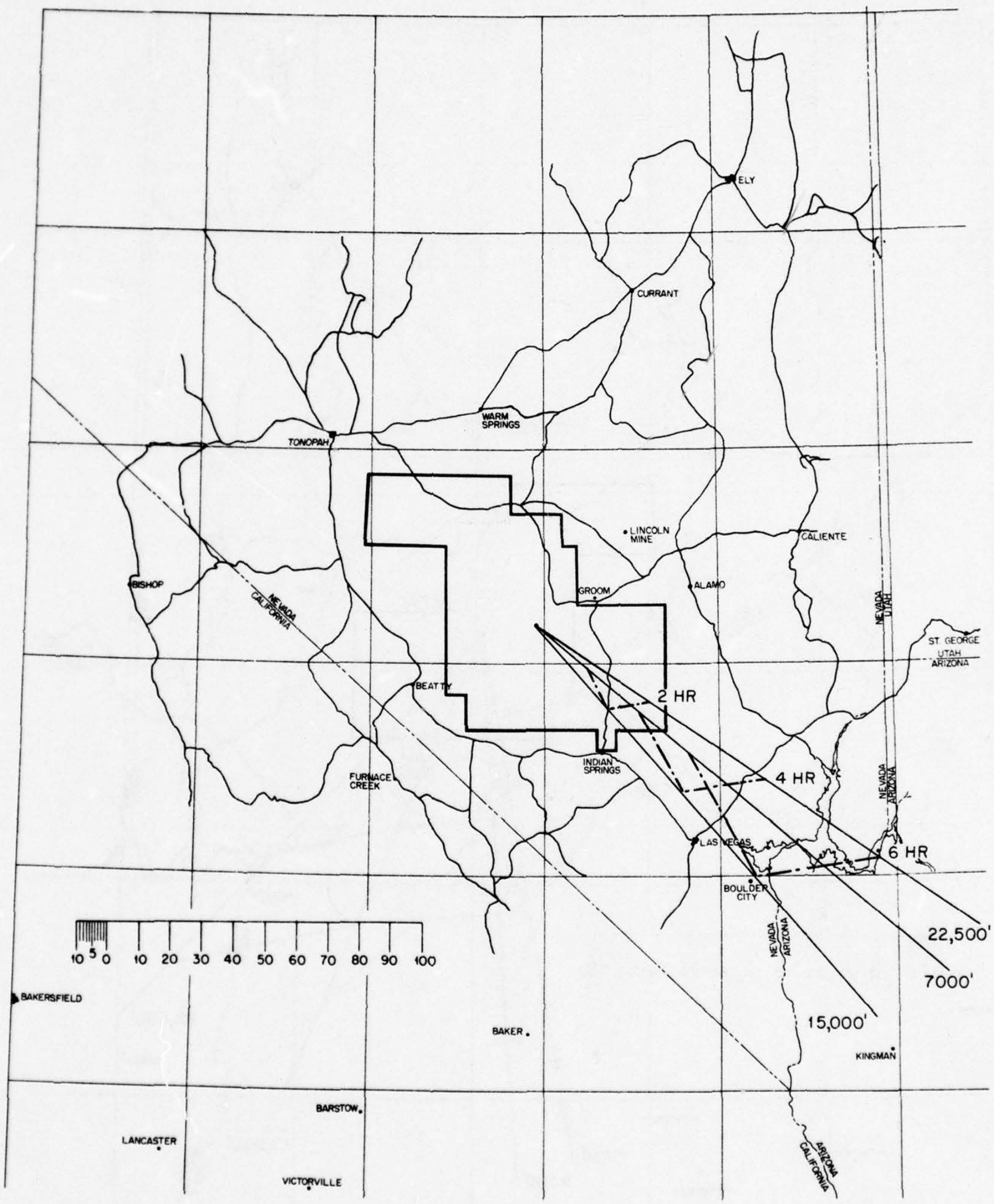

Fig. 10—Fall-out plot for Upshot-Knothole 3, prepared from wind sounding taken at 0100 PST, 31 March 1953.

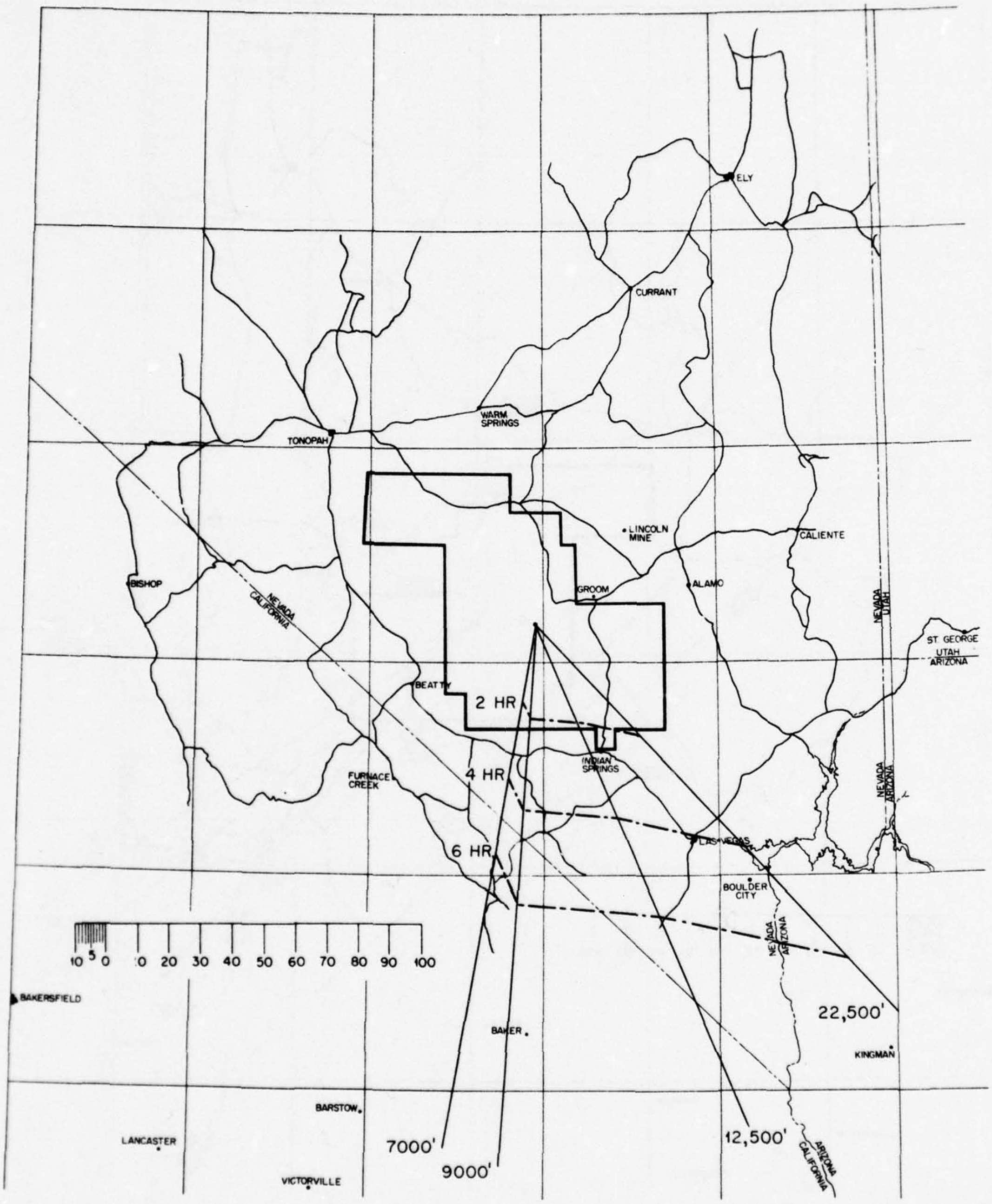

Fig. 11—Fall-out plot for Upshot-Knothole 3, prepared from wind sounding taken at 0330 PST, 31 March 1953.

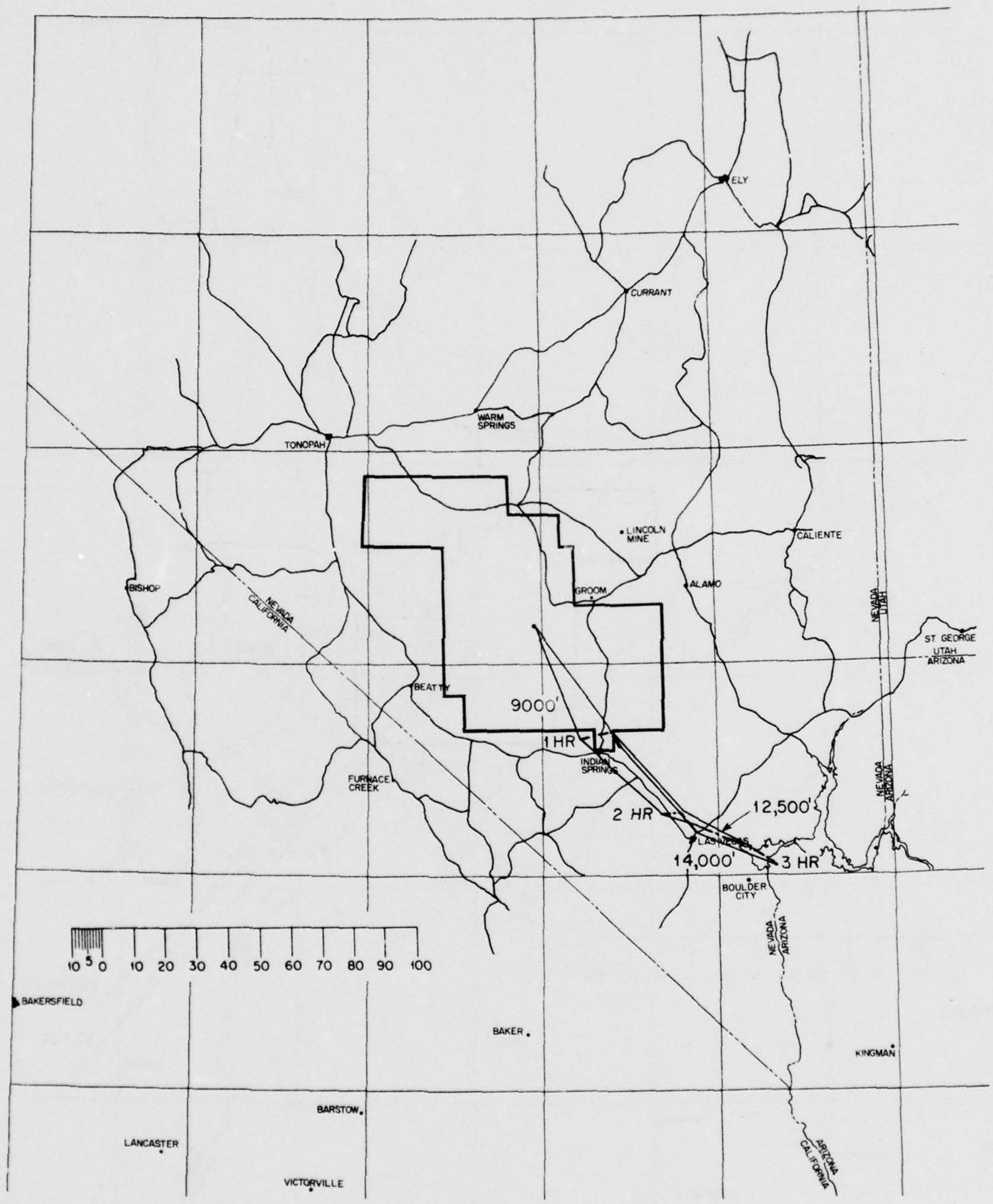

Fig. 12—Postshot analysis of fall-out for Upshot-Knothole 3.

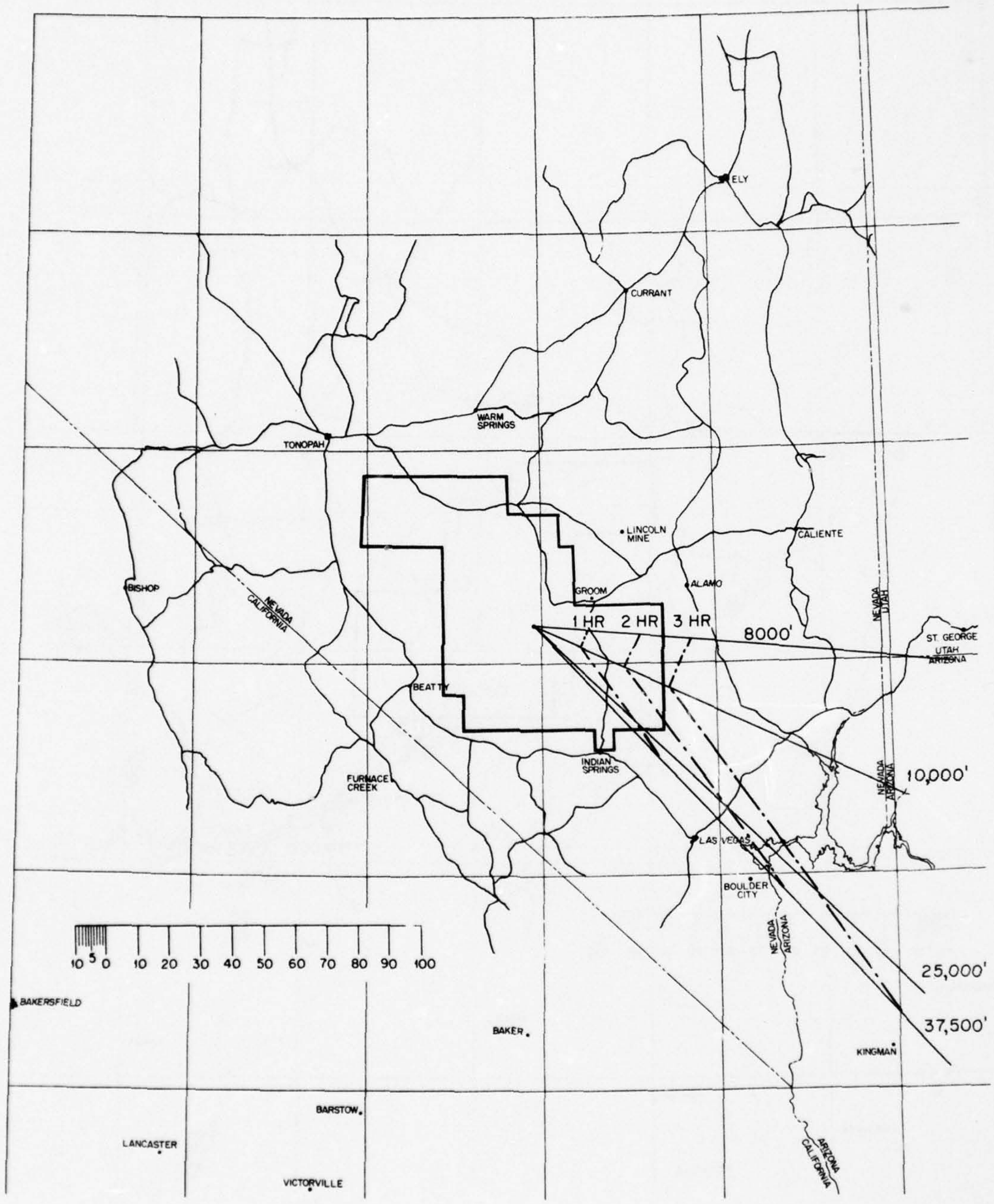

Fig. 13—Fall-out forecast for Upshot-Knothole 4, prepared from briefing wind forecast at 2100 PST, 5 April 1953, valid at 0730 PST, 6 April 1953.

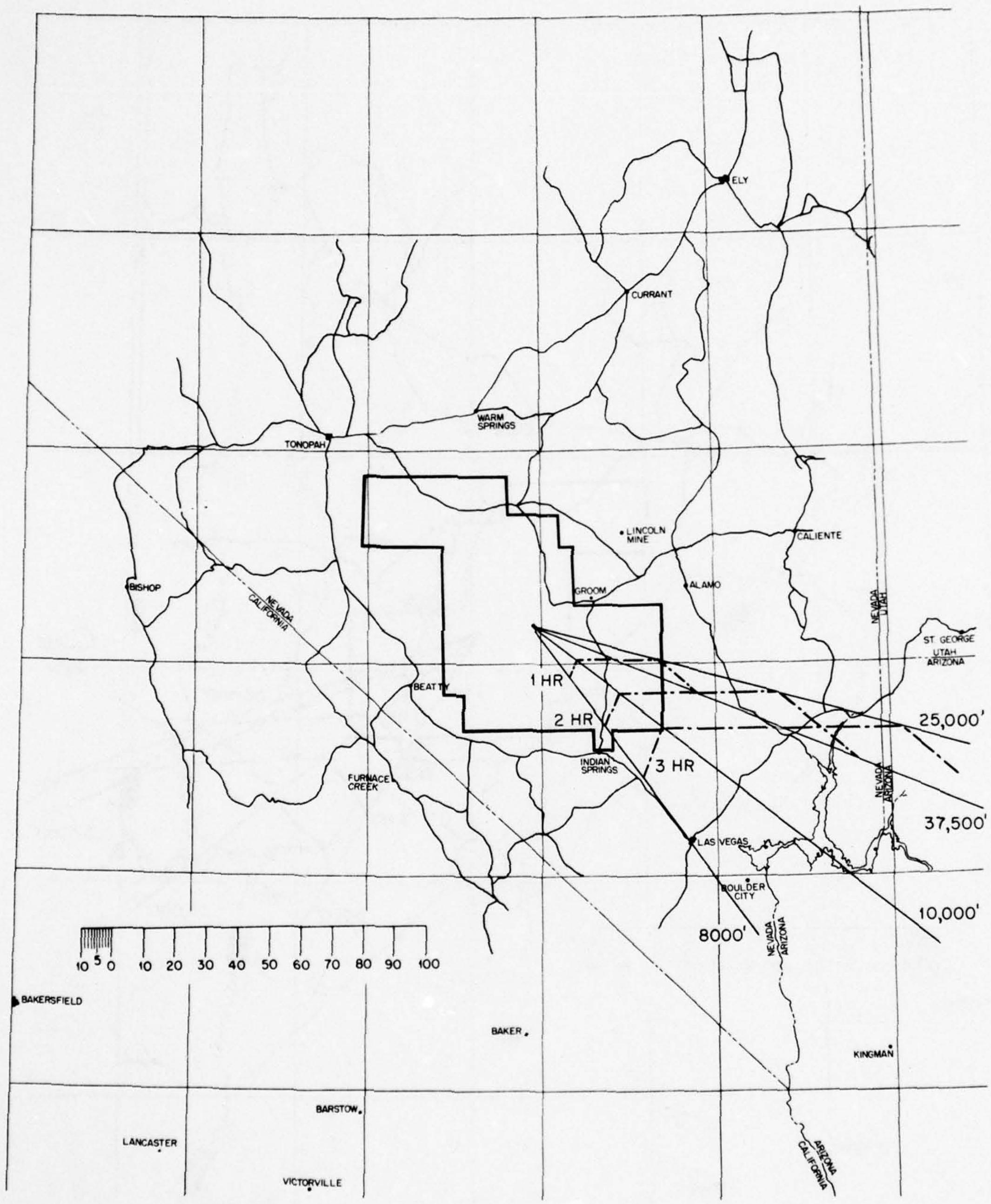

Fig. 14—Fall-out plot for Upshot-Knothole 4, prepared from wind sounding taken at 0330 PST, 6 April 1953.

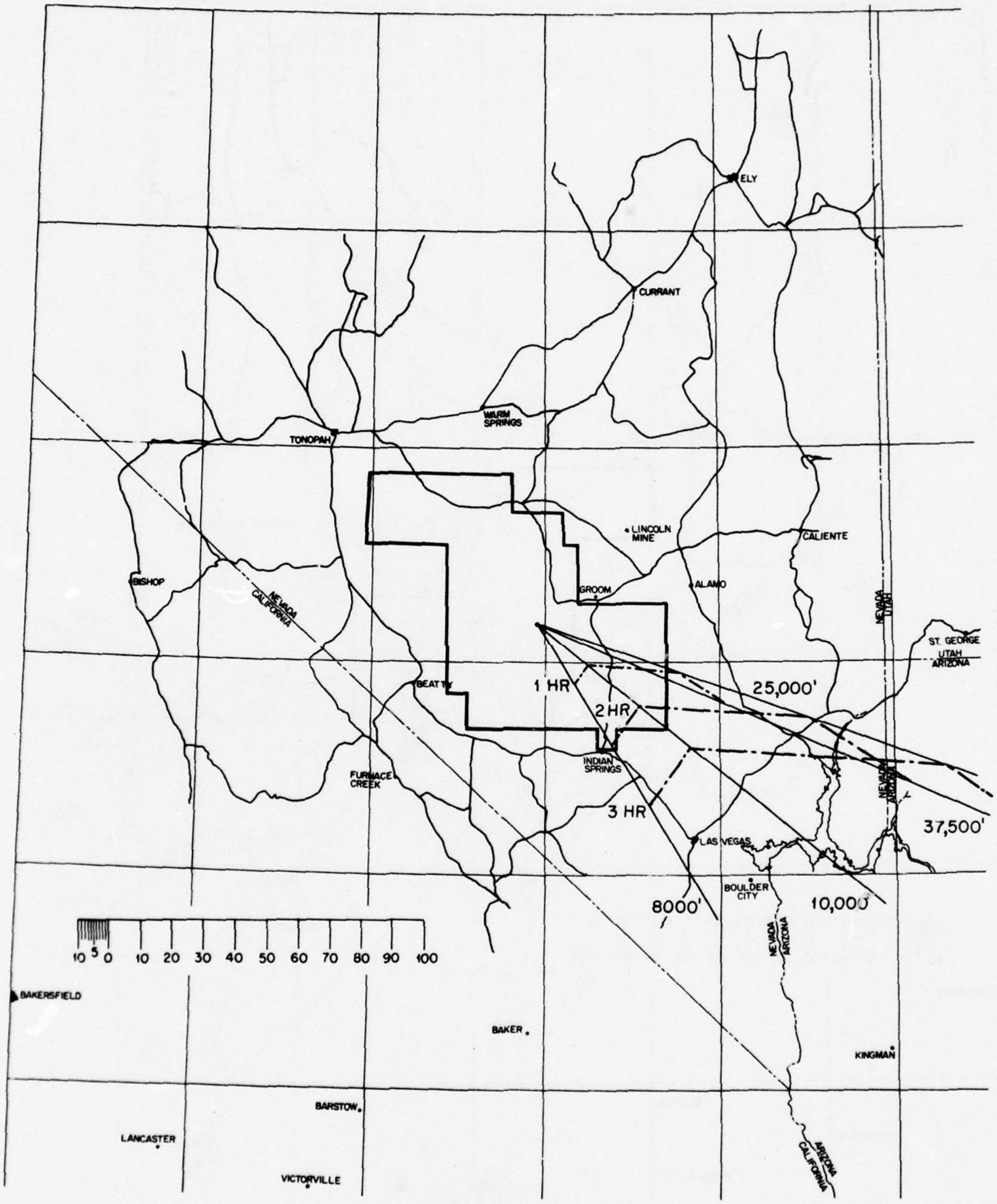

Fig. 15—Fall-out plot for Upshot-Knothole 4, prepared from wind sounding taken at 0530 PST, 6 April 1953.

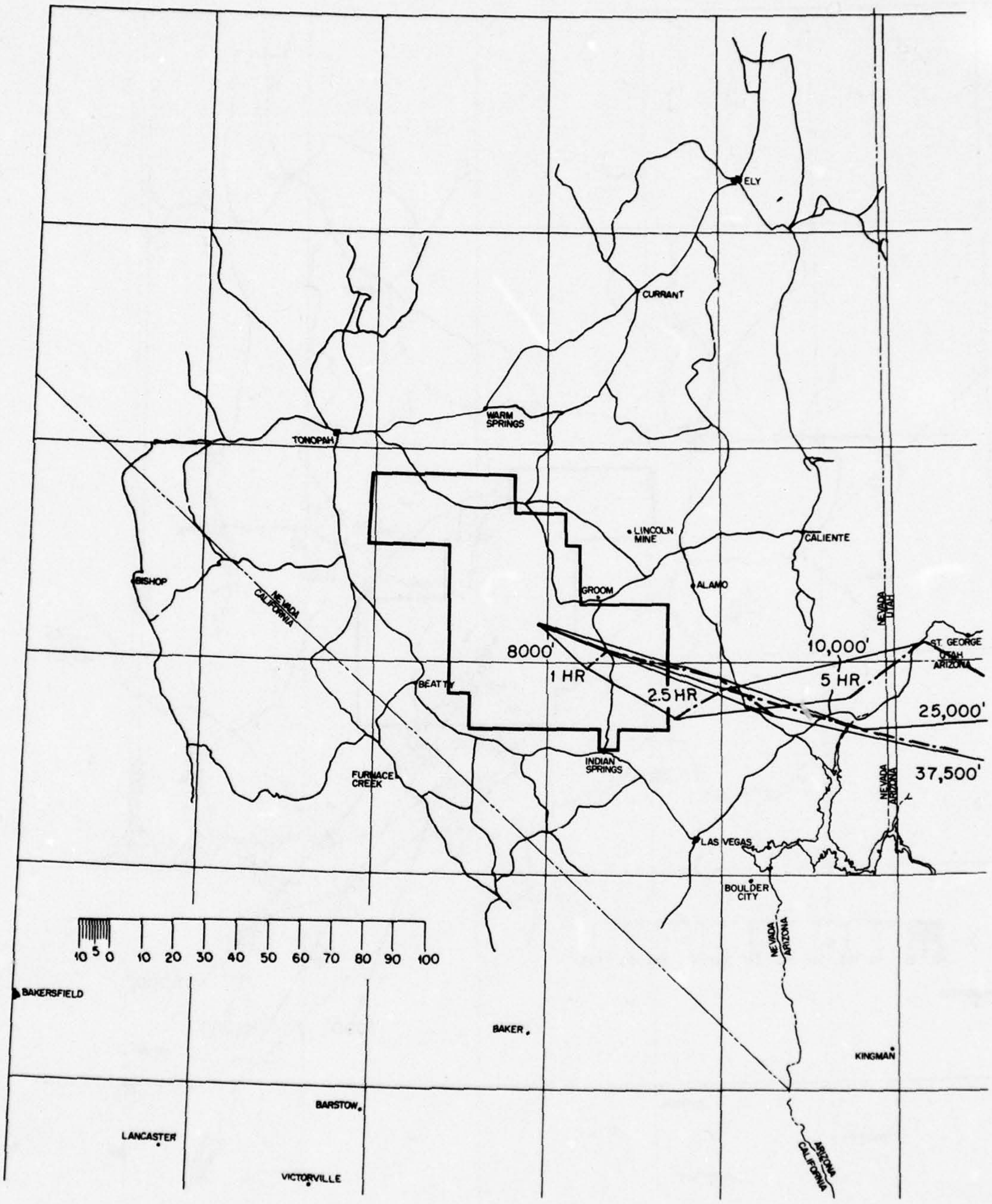

Fig. 16—Postshot analysis of fall-out for Upshot-Knothole 4.

[redacted]

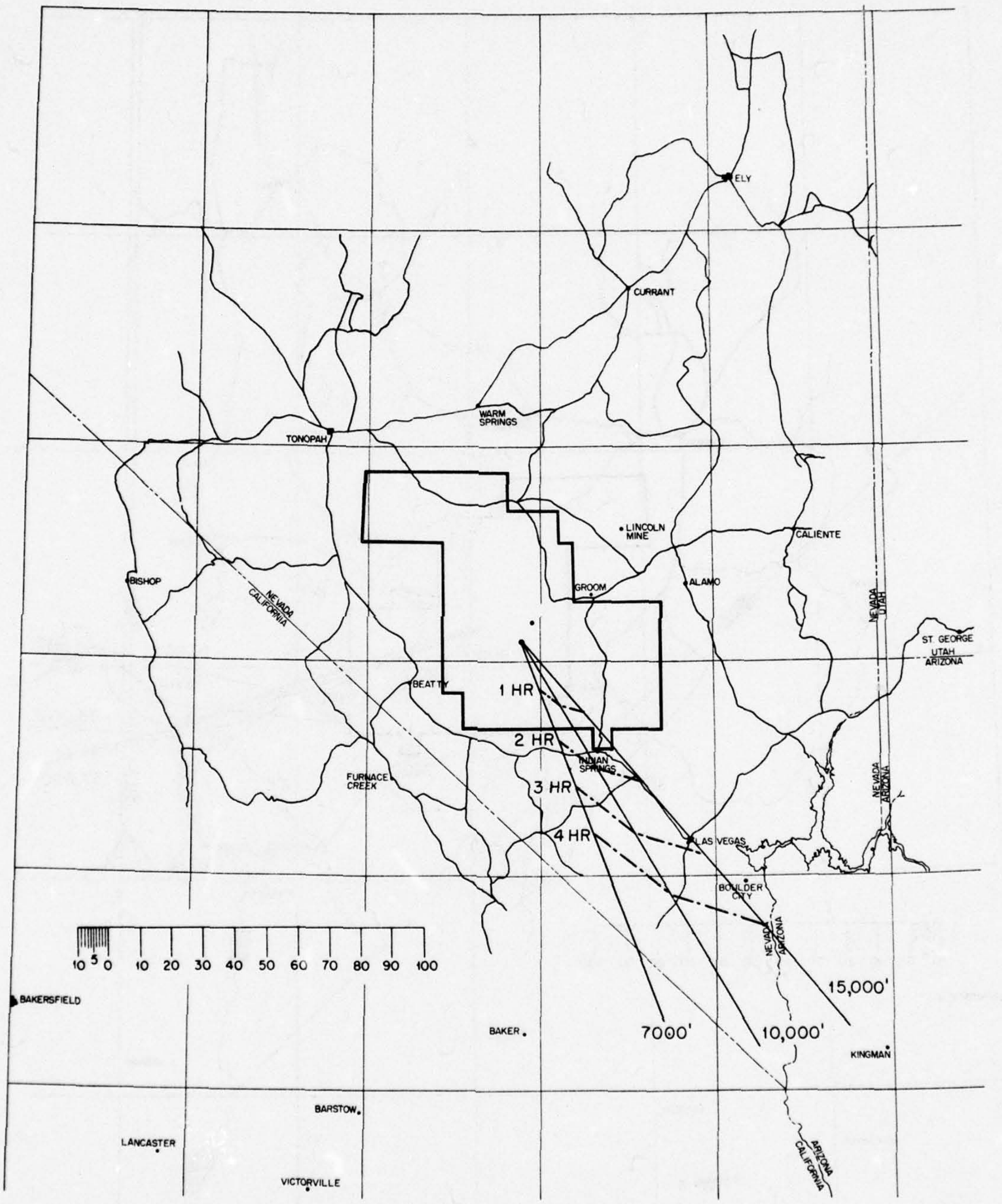

Fig. 17—Fall-out forecast for Upshot-Knothole 5, prepared from briefing wind forecast at 2100 PST, 10 April 1953, valid at 0430 PST, 11 April 1953.

[redacted]

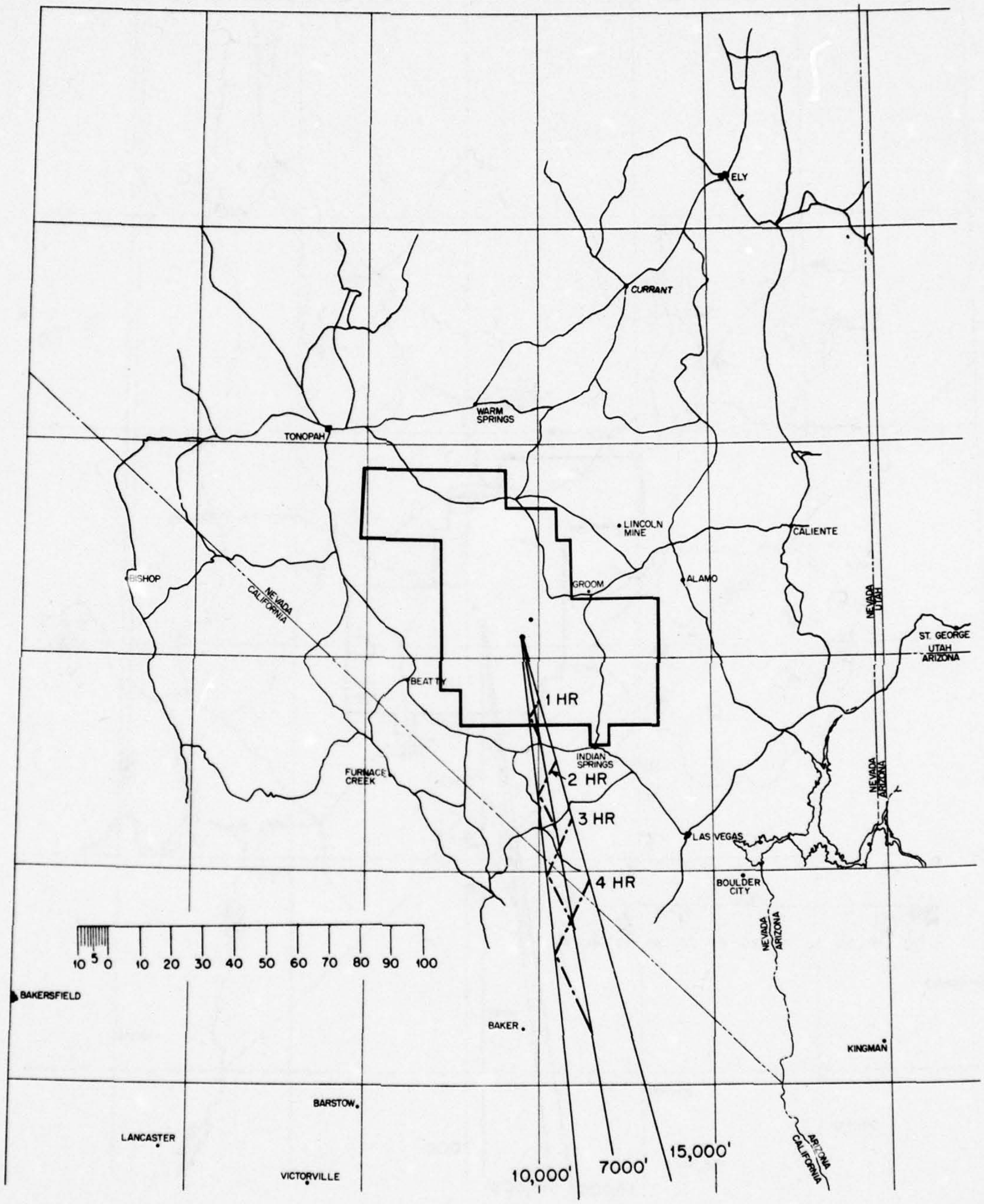

Fig. 18—Fall-out plot for Upshot-Knothole 5, prepared from wind sounding taken at 0100 PST, 11 April 1953.

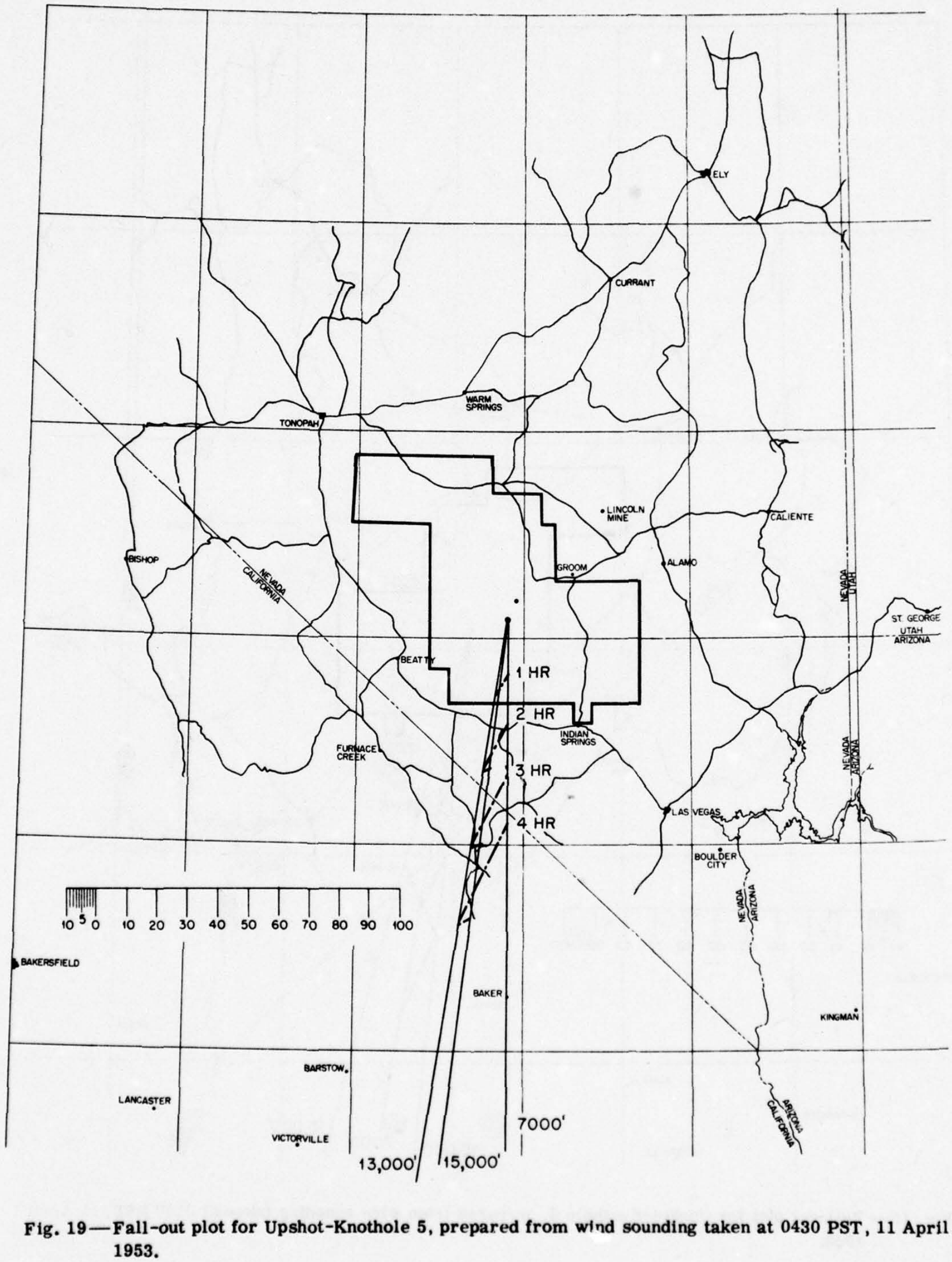

Fig. 19—Fall-out plot for Upshot-Knothole 5, prepared from wind sounding taken at 0430 PST, 11 April 1953.

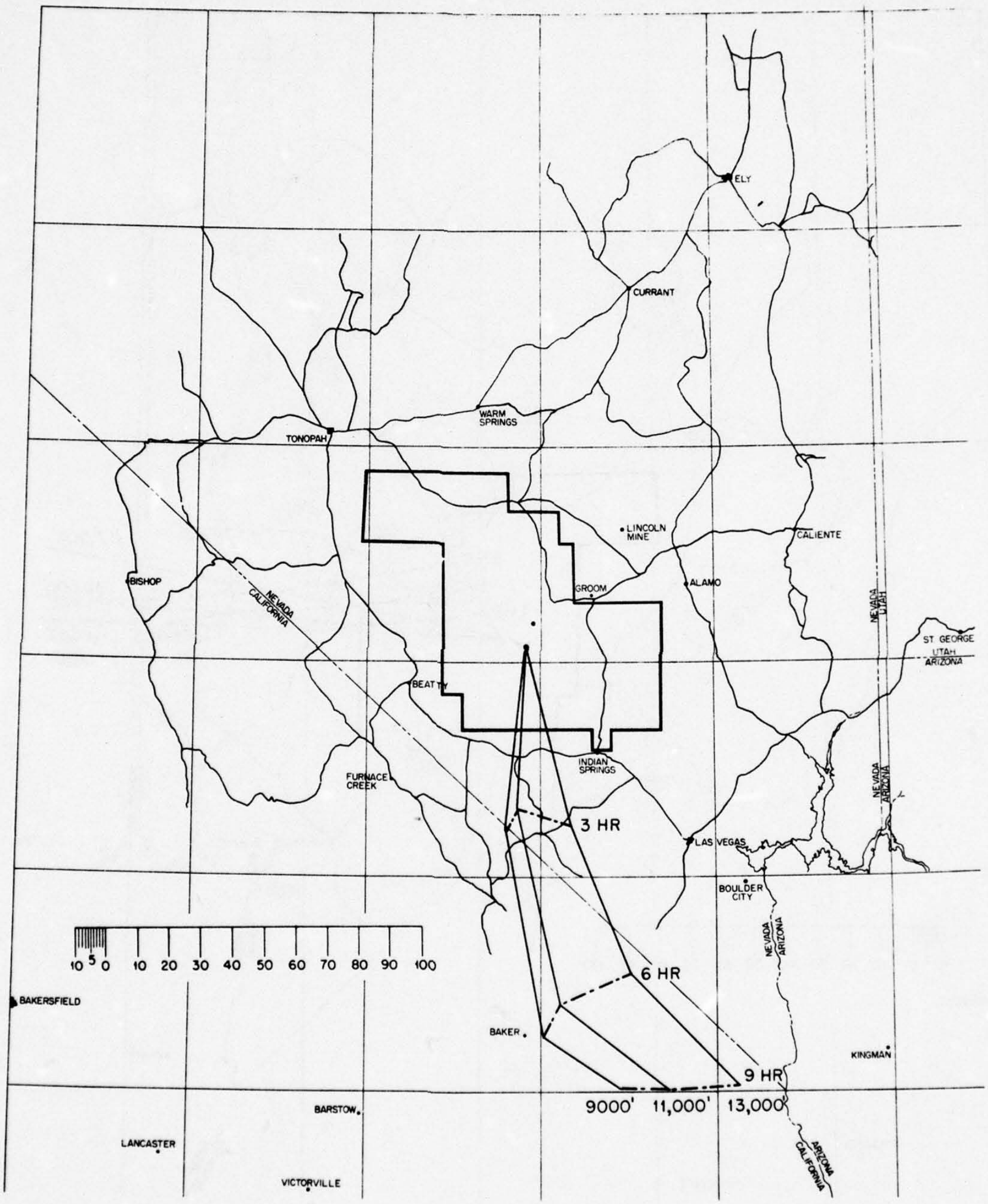

Fig. 20—Postshot analysis of fall-out for Upshot-Knothole 5.

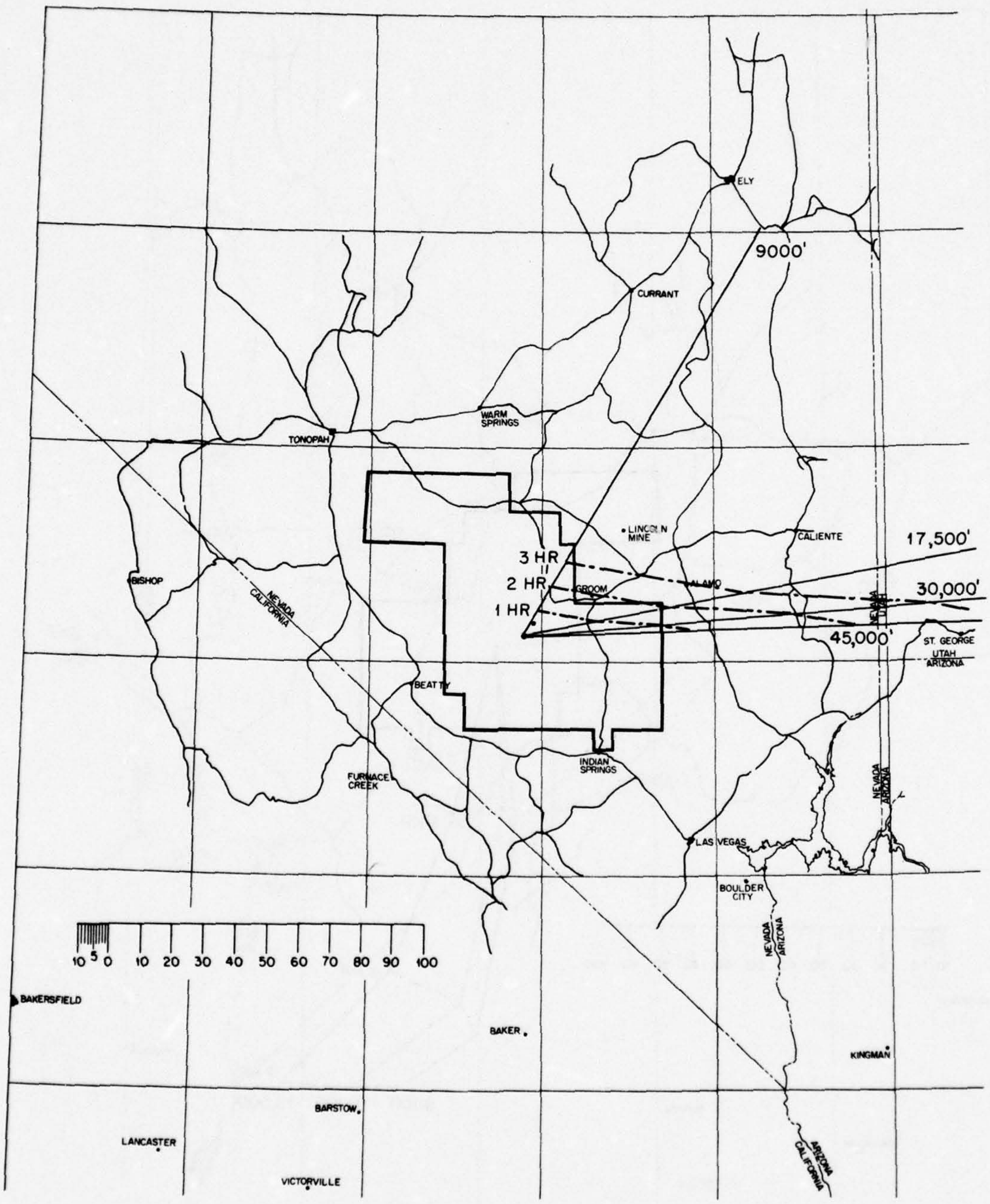

Fig. 21—Fall-out forecast for Upshot-Knothole 6, prepared from briefing wind forecast at 2100 PST, 17 April 1953, valid at 0435 PST, 18 April 1953.

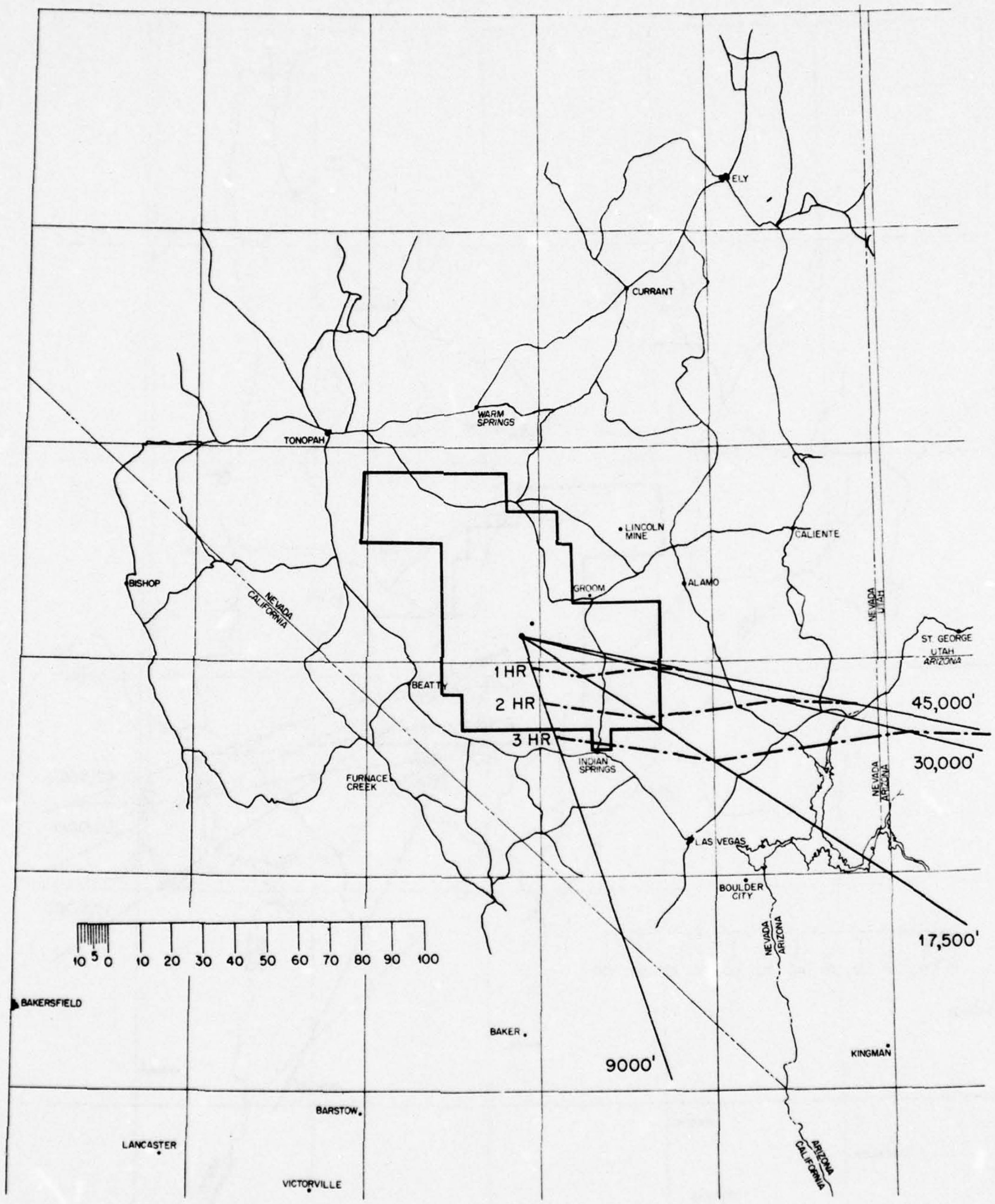

Fig. 22—Fall-out plot for Upshot-Knothole 6, prepared from wind sounding taken at 2330 PST, 17 April 1953.

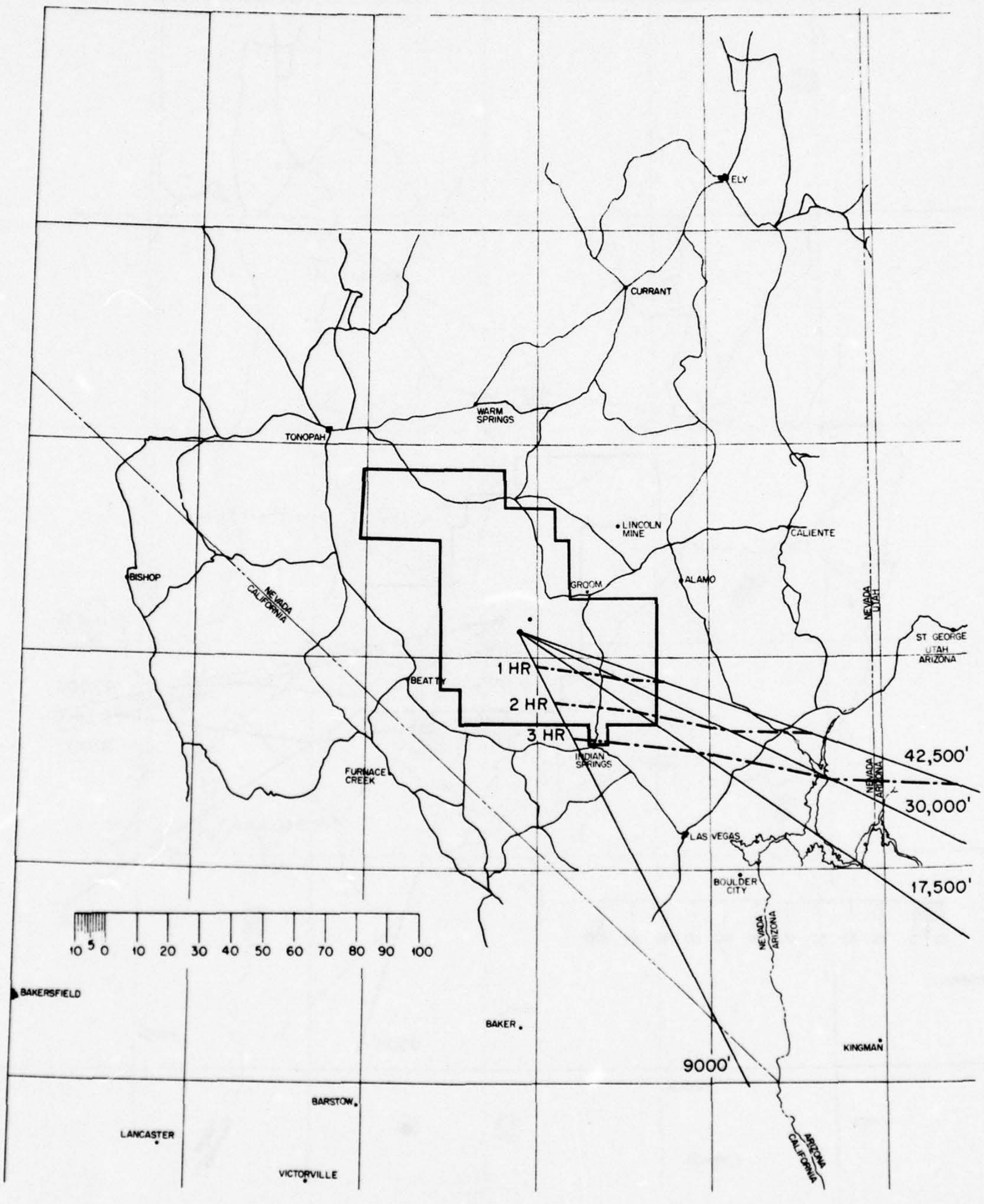

Fig. 23—Fall-out plot for Upshot-Knothole 6, prepared from wind sounding taken at 0200 PST, 18 April 1953.

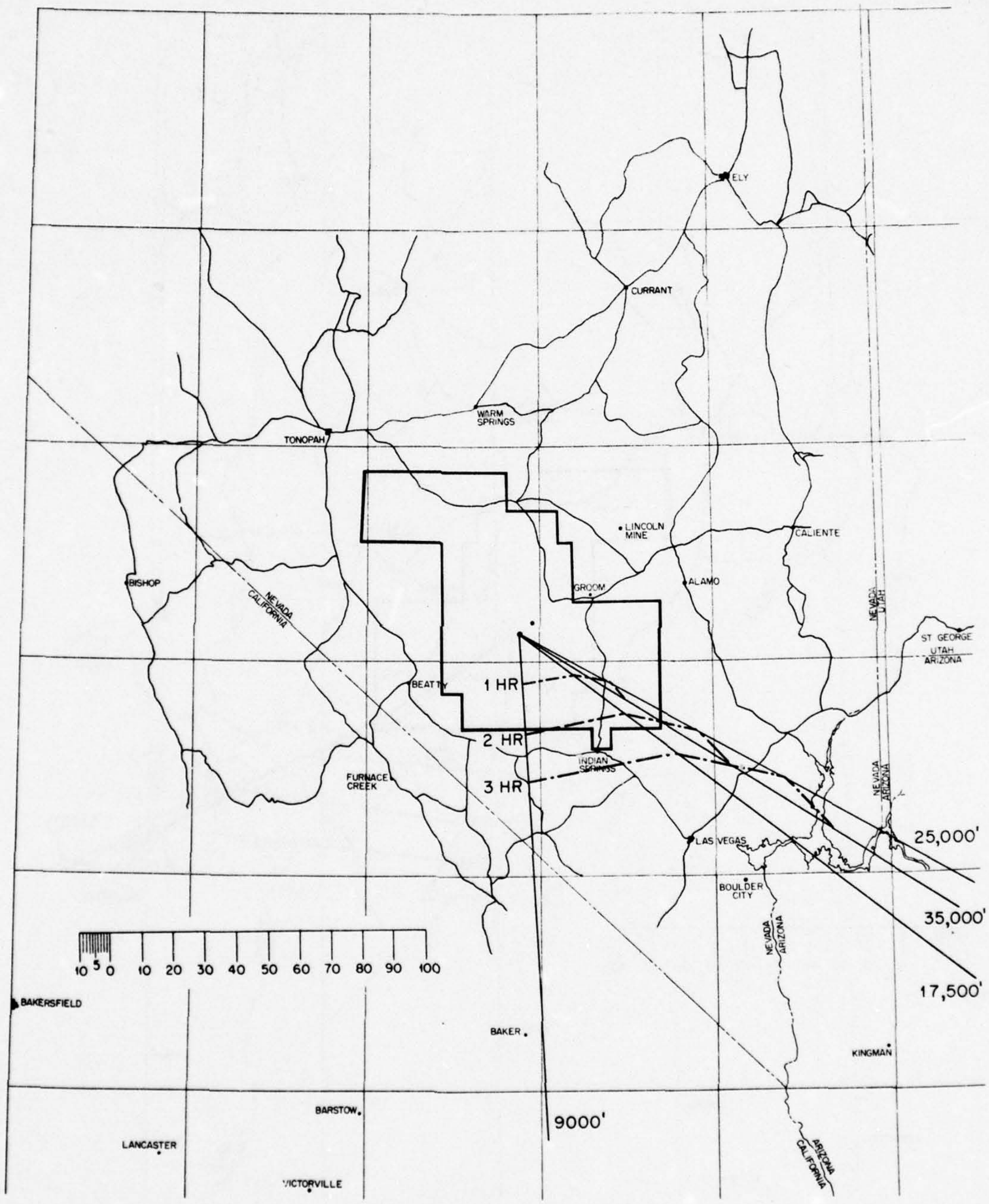

Fig. 24—Fall-out plot for Upshot-Knothole 6, prepared from wind sounding taken at 0420 PST, 18 April 1953.

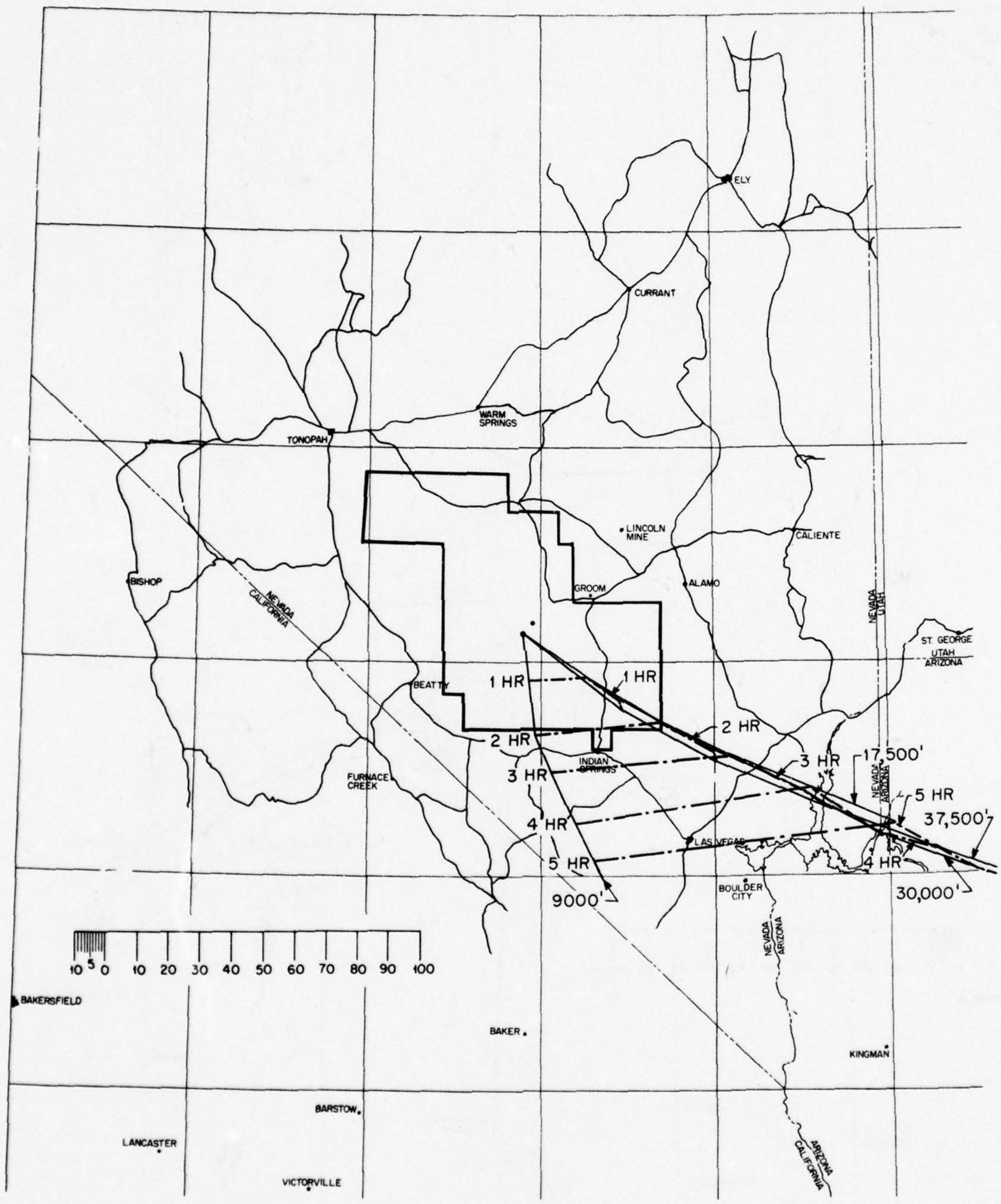

Fig. 25—Postshot analysis of fall-out for Upshot-Knothole 6.

[redacted]

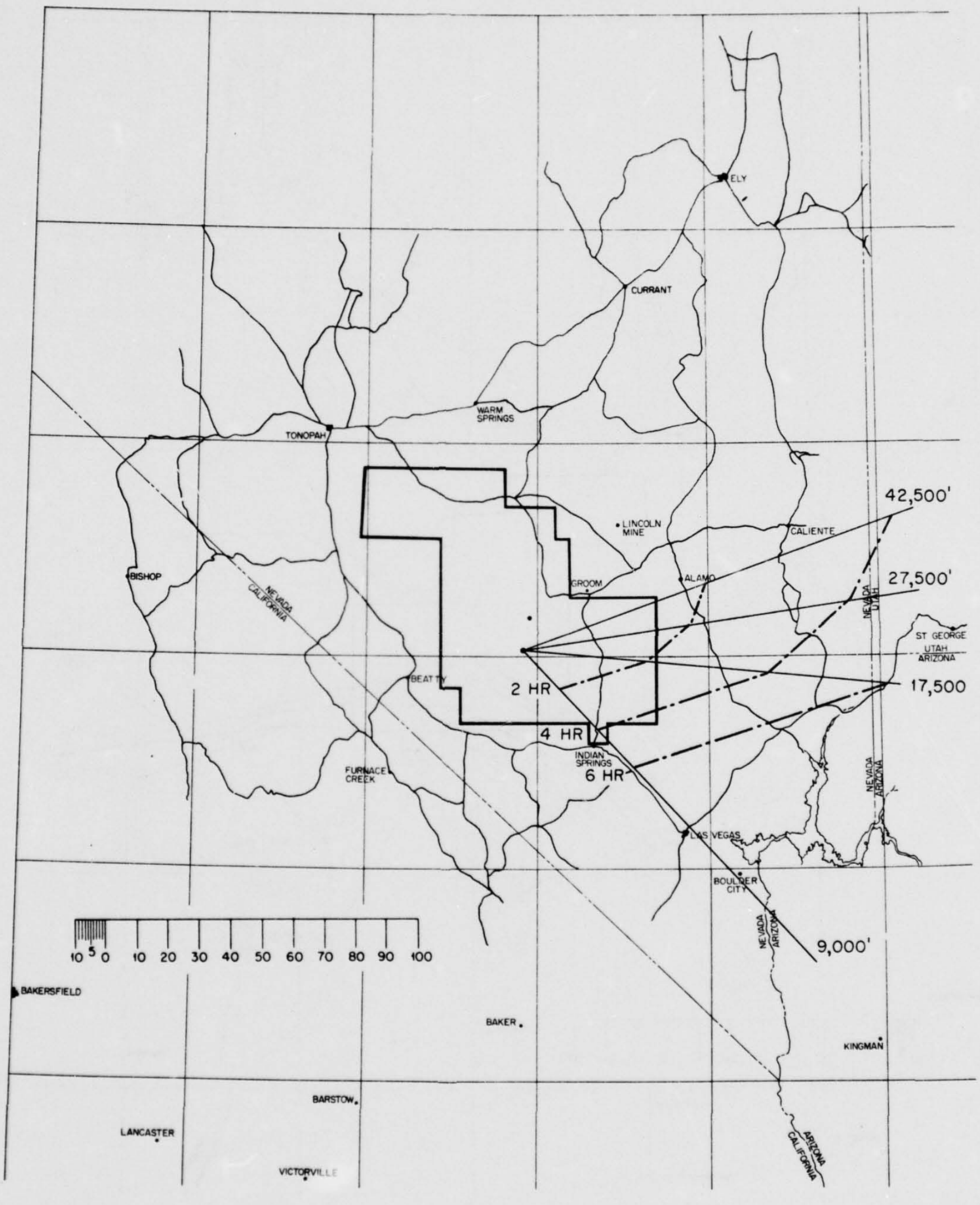

Fig. 26—Fall-out forecast for Upshot-Knothole 7, prepared from briefing wind forecast at 2100 PST, 24 April 1953, valid at 0430 PST, 25 April 1953.

[redacted]

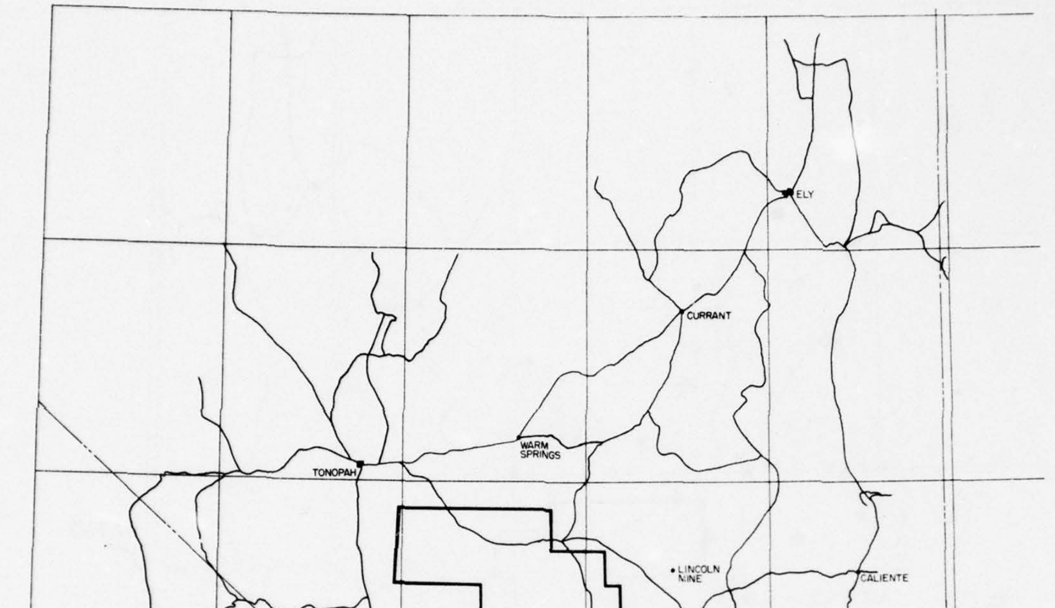

Fig. 27—Fall-out plot for Upshot-Knothole 7, prepared from wind sounding taken at 0115 PST, 25 April 1953.

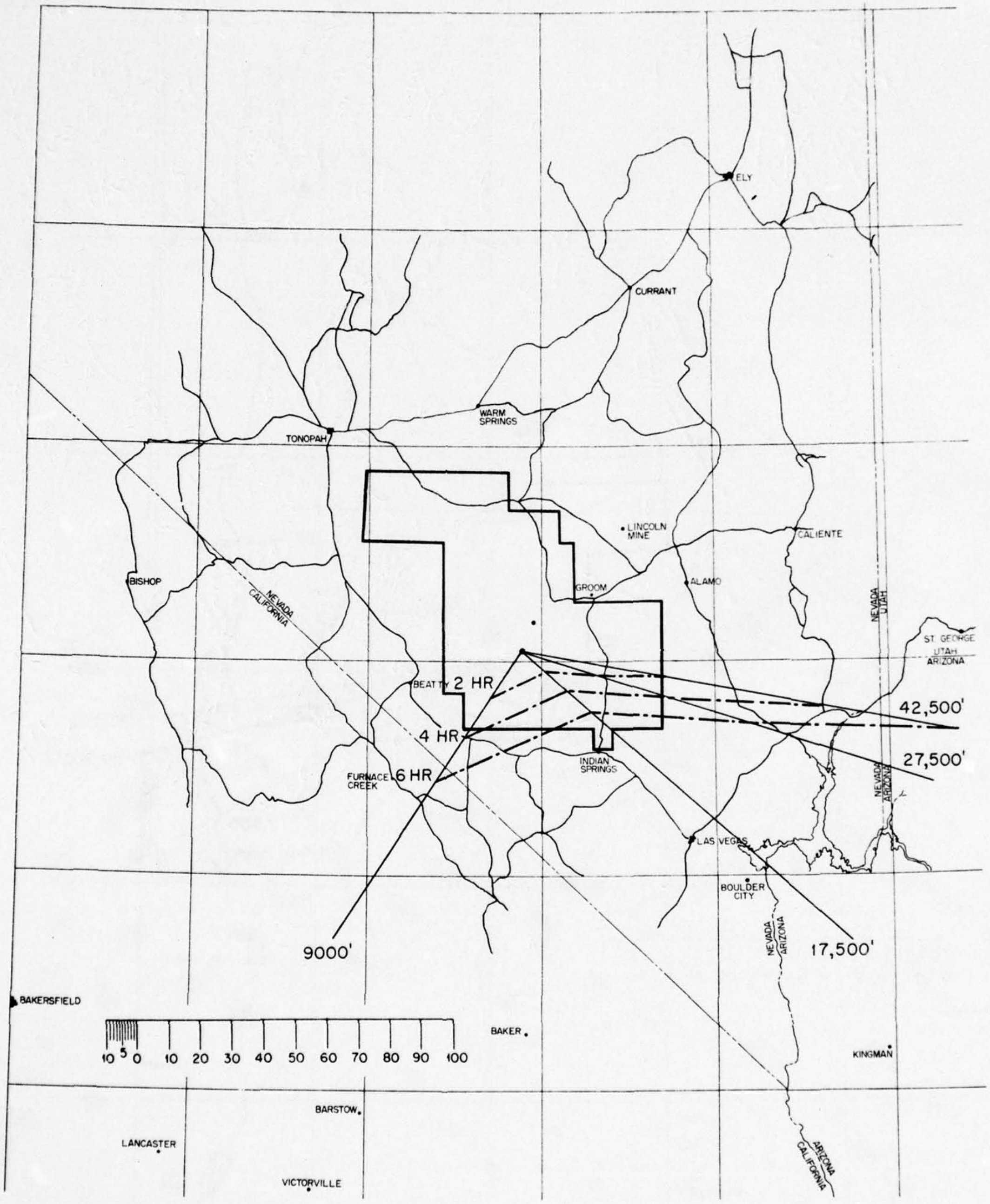

Fig. 28—Fall-out plot for Upshot-Knothole 7, prepared from wind sounding taken at 0230 PST, 25 April 1953.

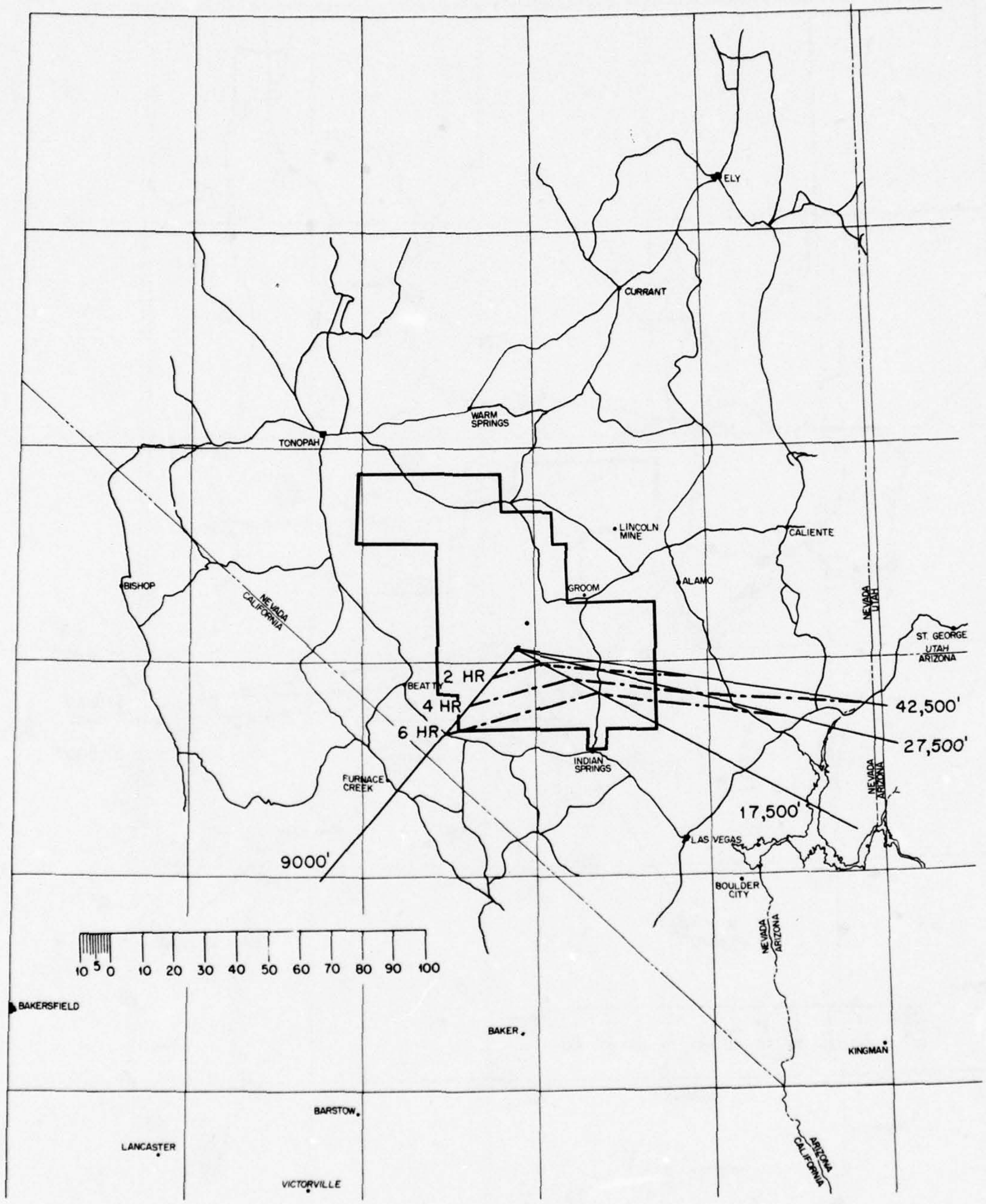

Fig. 29—Fall-out plot for Upshot-Knothole 7, prepared from wind sounding taken at 0415 PST, 25 April 1953.

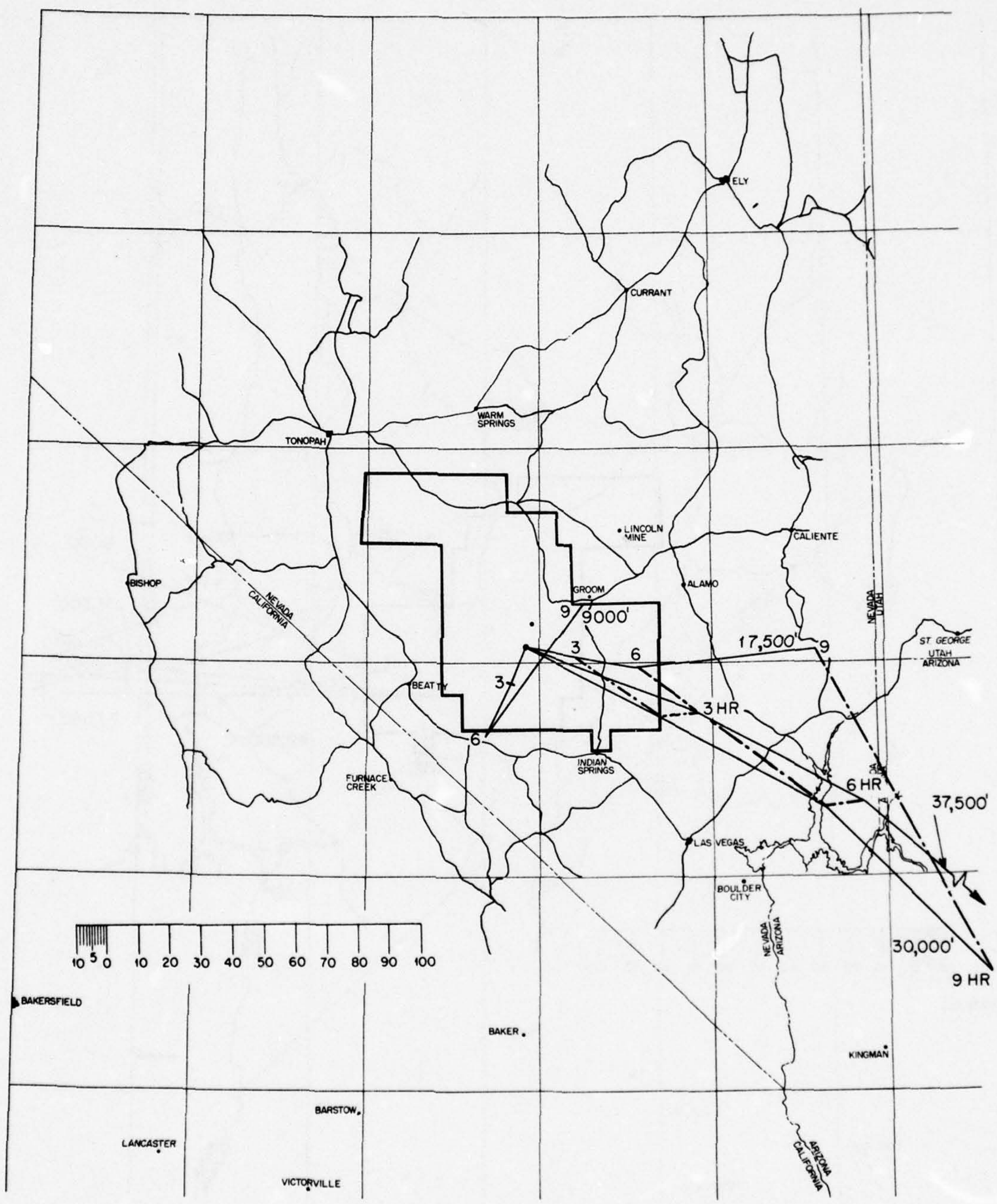

Fig. 30—Postshot analysis of fall-out for Upshot-Knothole 7.

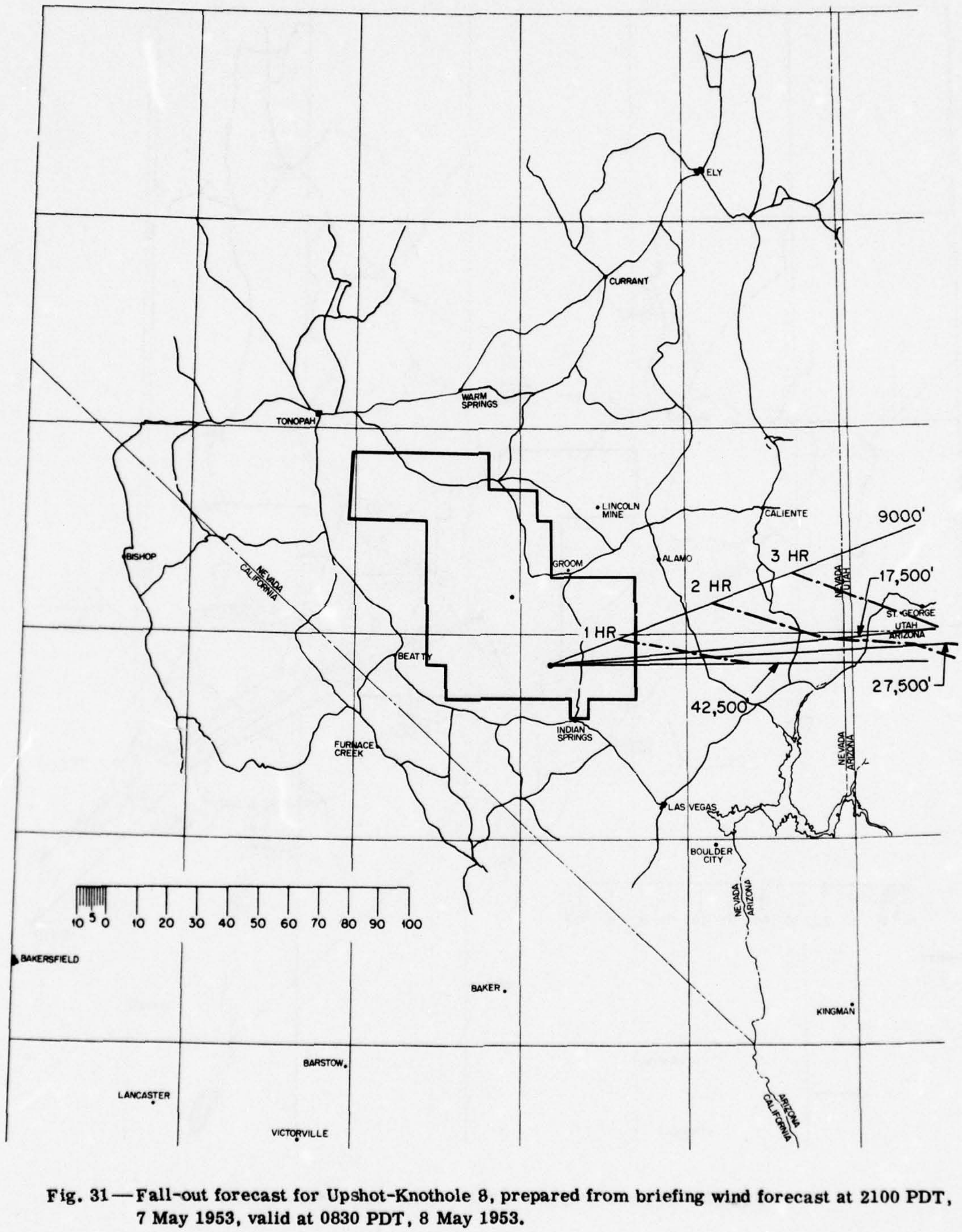

Fig. 31—Fall-out forecast for Upshot-Knothole 8, prepared from briefing wind forecast at 2100 PDT, 7 May 1953, valid at 0830 PDT, 8 May 1953.

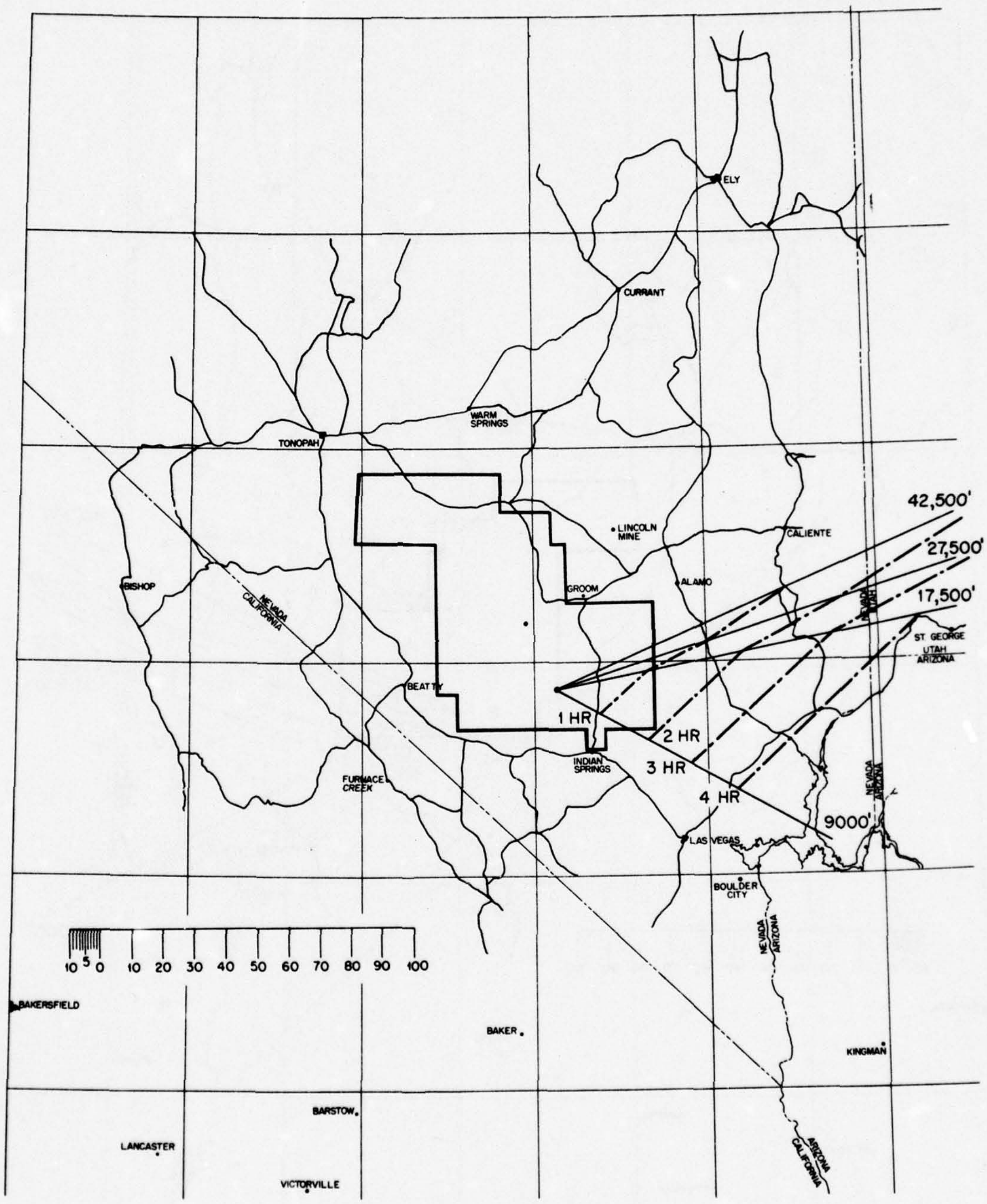

Fig. 32—Fall-out plot for Upshot-Knothole 8, prepared from wind sounding taken at 0430 PDT, 8 May 1953.

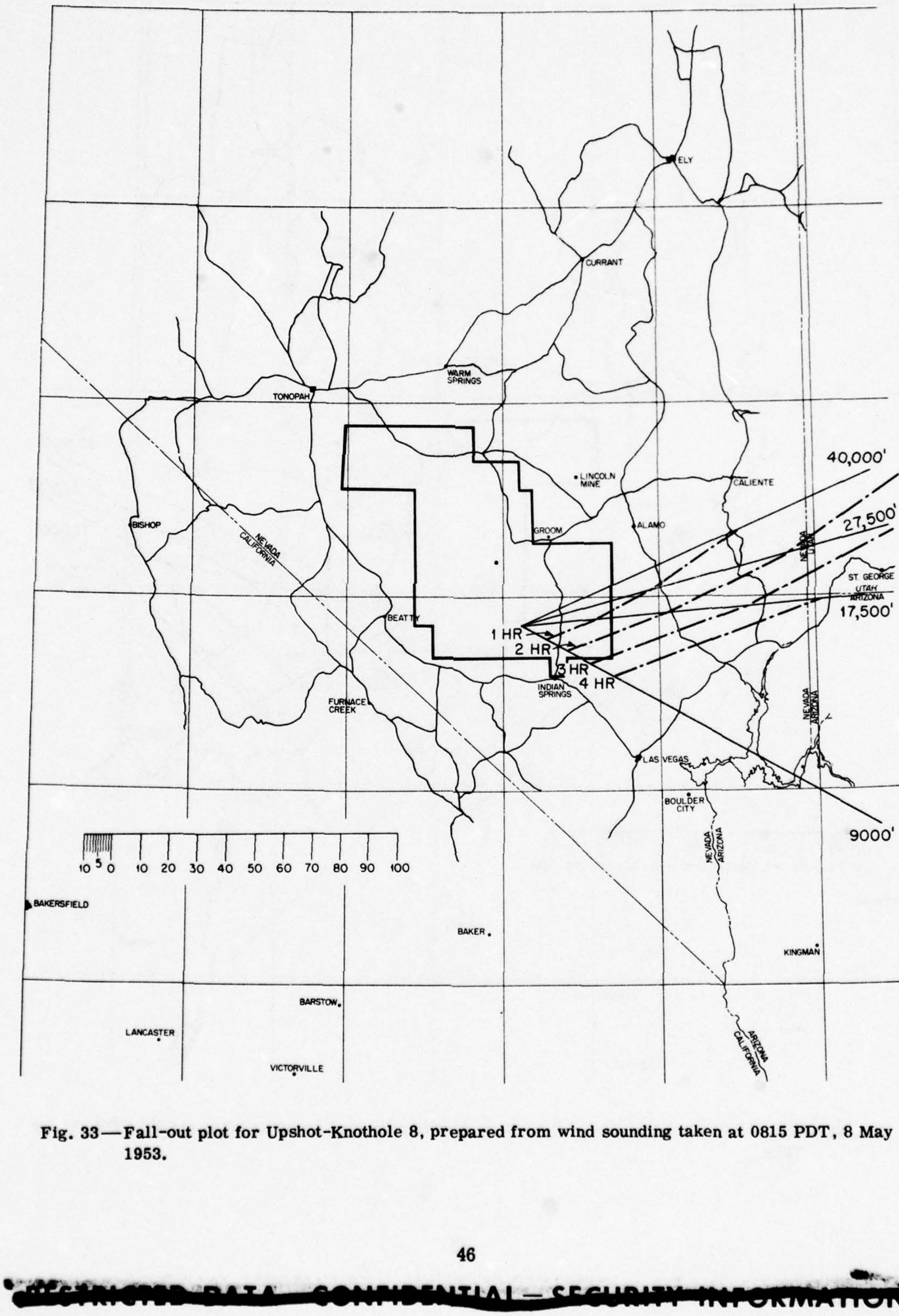

Fig. 33—Fall-out plot for Upshot-Knothole 8, prepared from wind sounding taken at 0815 PDT, 8 May 1953.

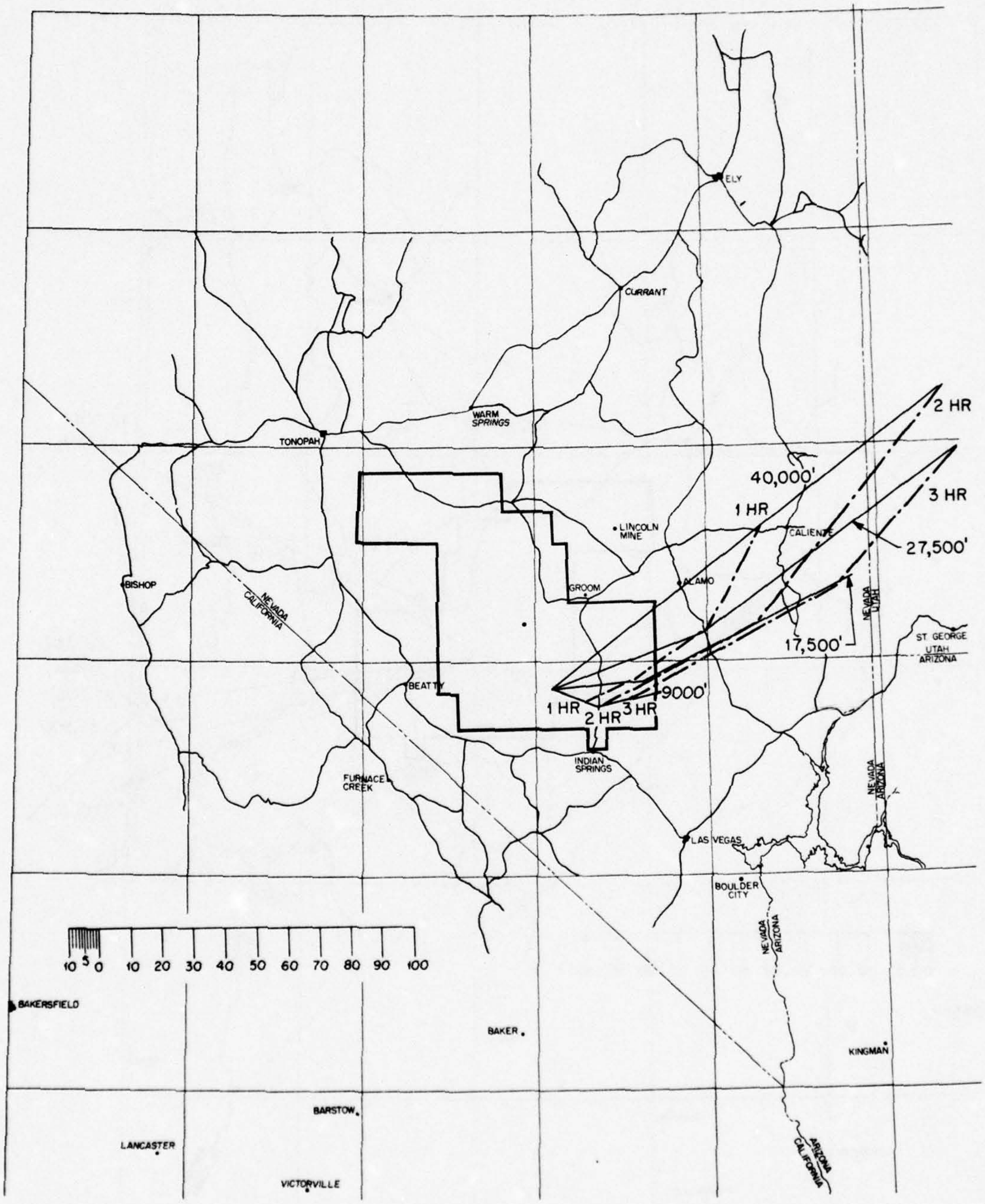

Fig. 34—Postshot analysis of fall-out for Upshot-Knothole 8.

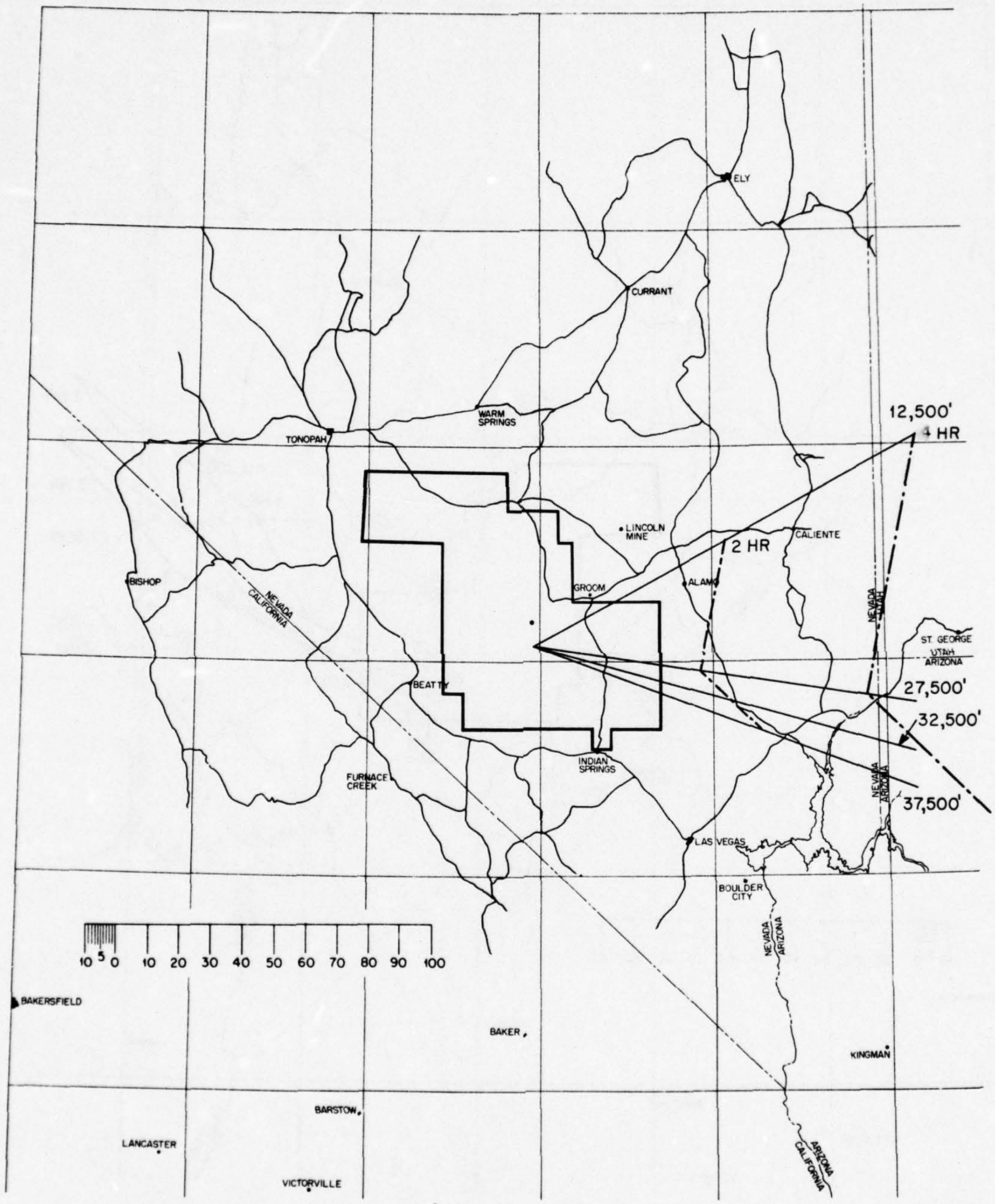

Fig. 35—Fall-out forecast for Upshot-Knothole 9, prepared from briefing wind forecast at 2100 PDT, 18 May 1953, valid at 0505 PDT, 19 May 1953.

[redacted]

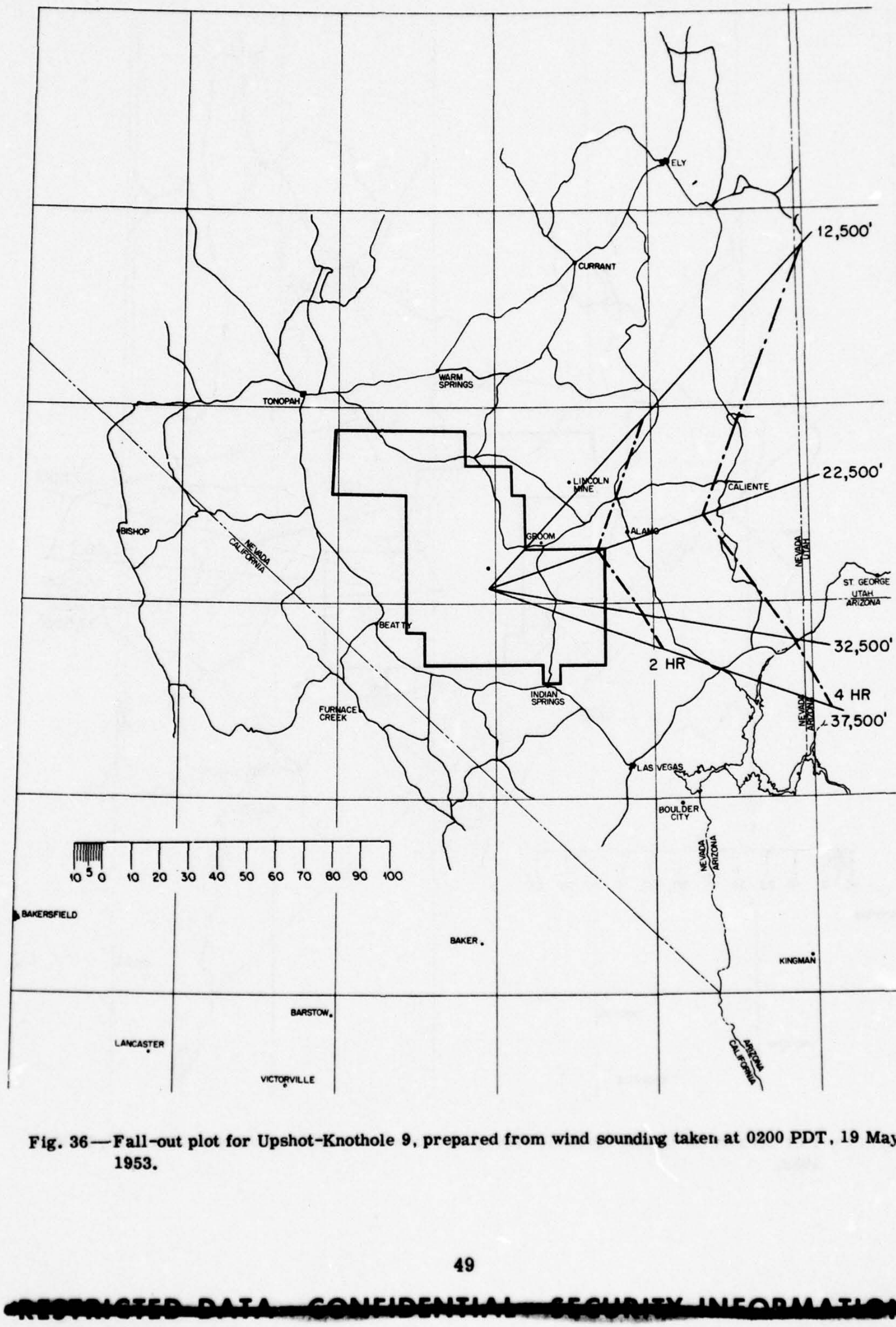

Fig. 36—Fall-out plot for Upshot-Knothole 9, prepared from wind sounding taken at 0200 PDT, 19 May 1953.

[redacted]

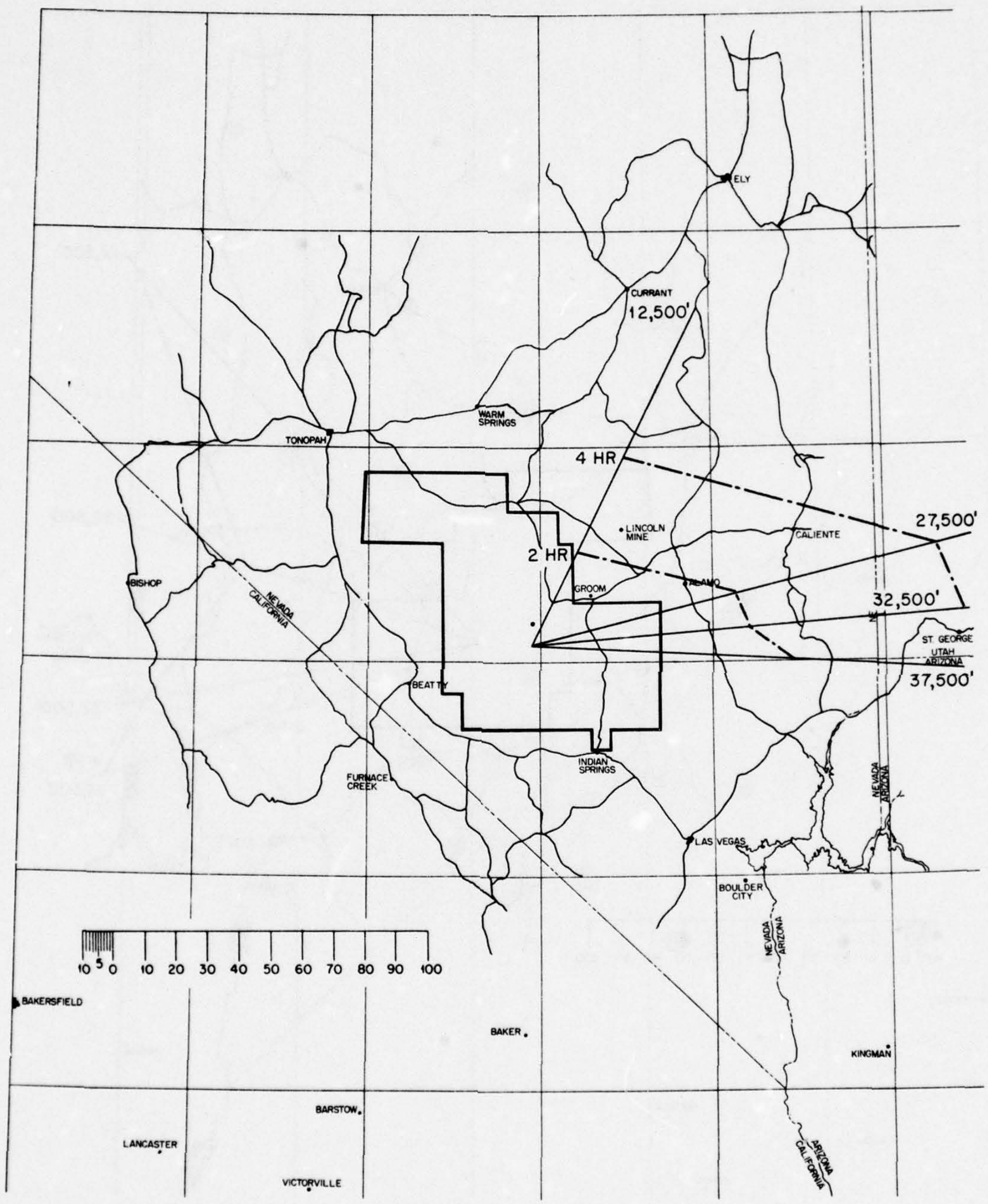

Fig. 37—Fall-out plot for Upshot-Knothole 9, prepared from wind sounding taken at 0500 PDT, 19 May 1953.

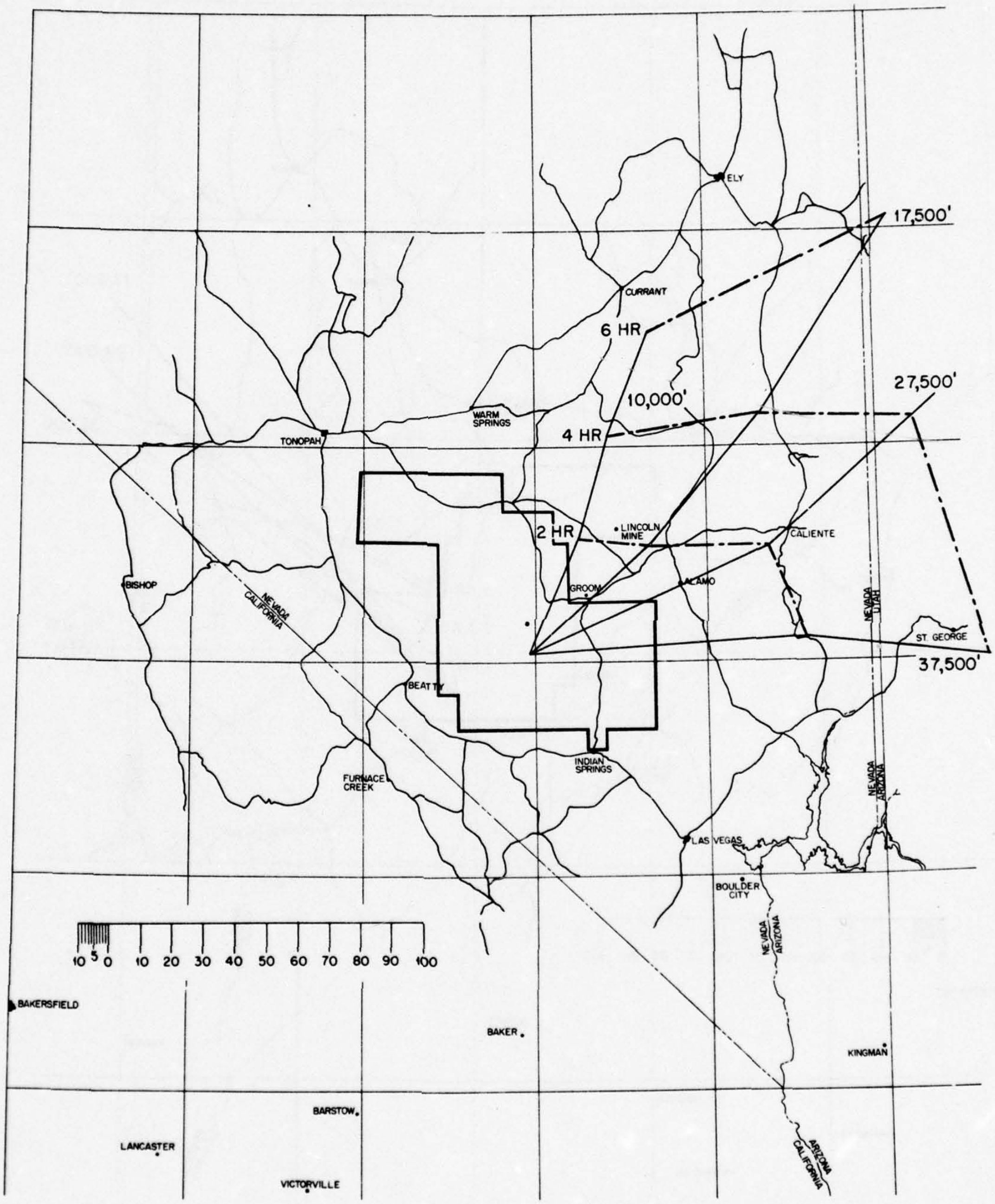

Fig. 38—Postshot analysis of fall-out for Upshot-Knothole 9.

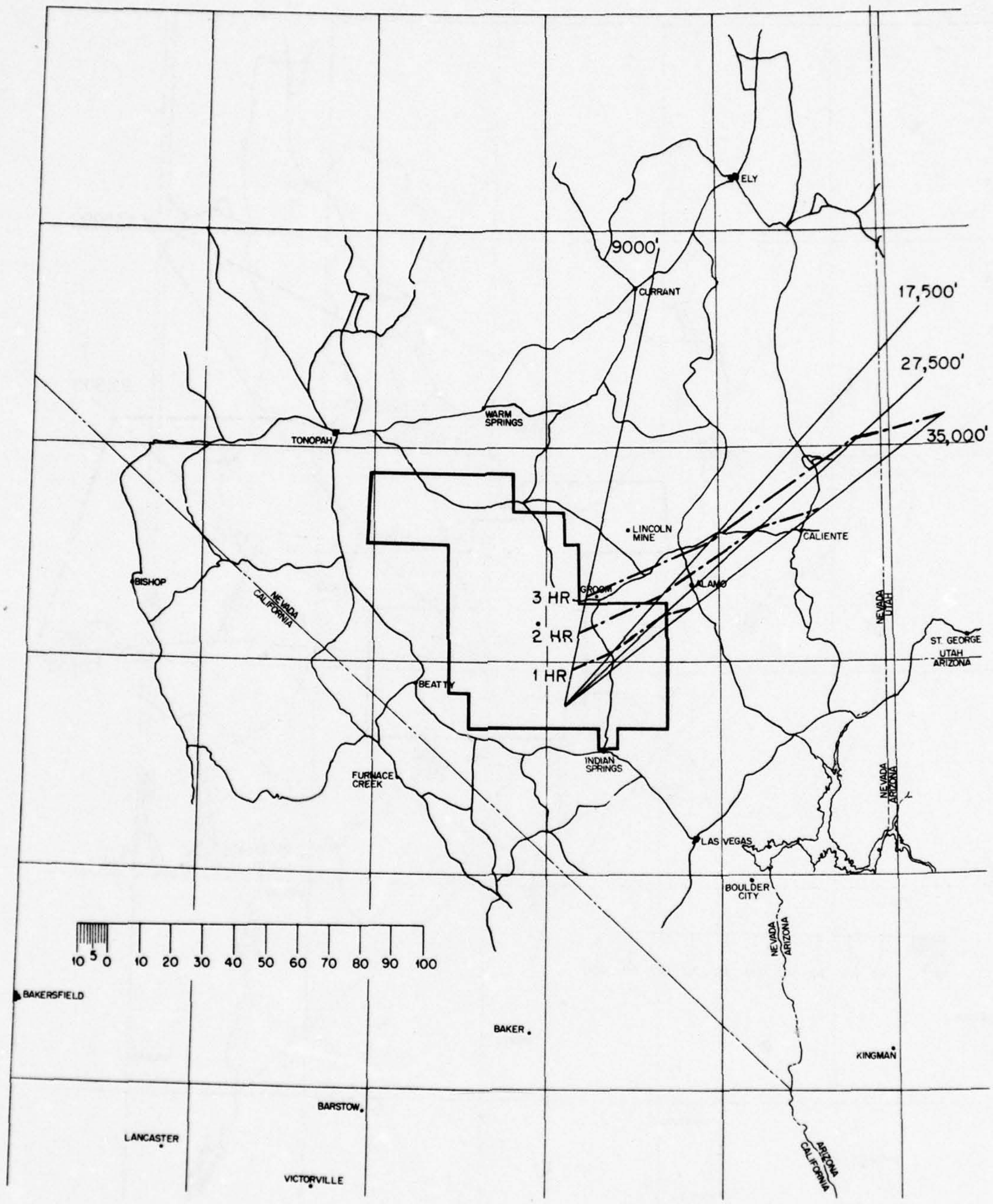

Fig. 39—Fall-out forecast for Upshot-Knothole 10, prepared from briefing wind forecast at 2100 PDT, 24 May 1953, valid at 0830 PDT, 25 May 1953.

[redacted]

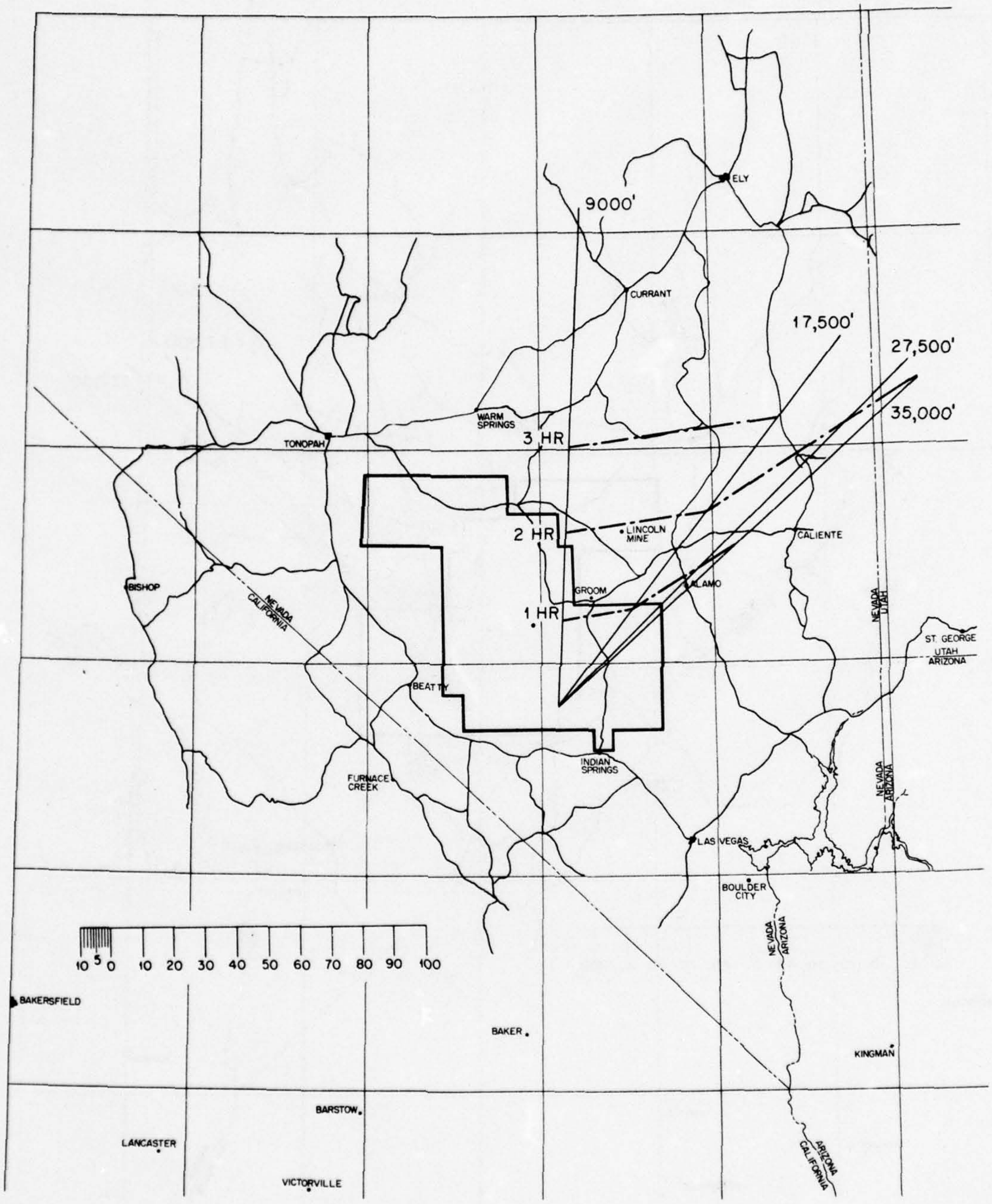

Fig. 40—Fall-out plot for Upshot-Knothole 10, prepared from wind sounding taken at 0200 PDT, 25 May 1953.

[redacted]

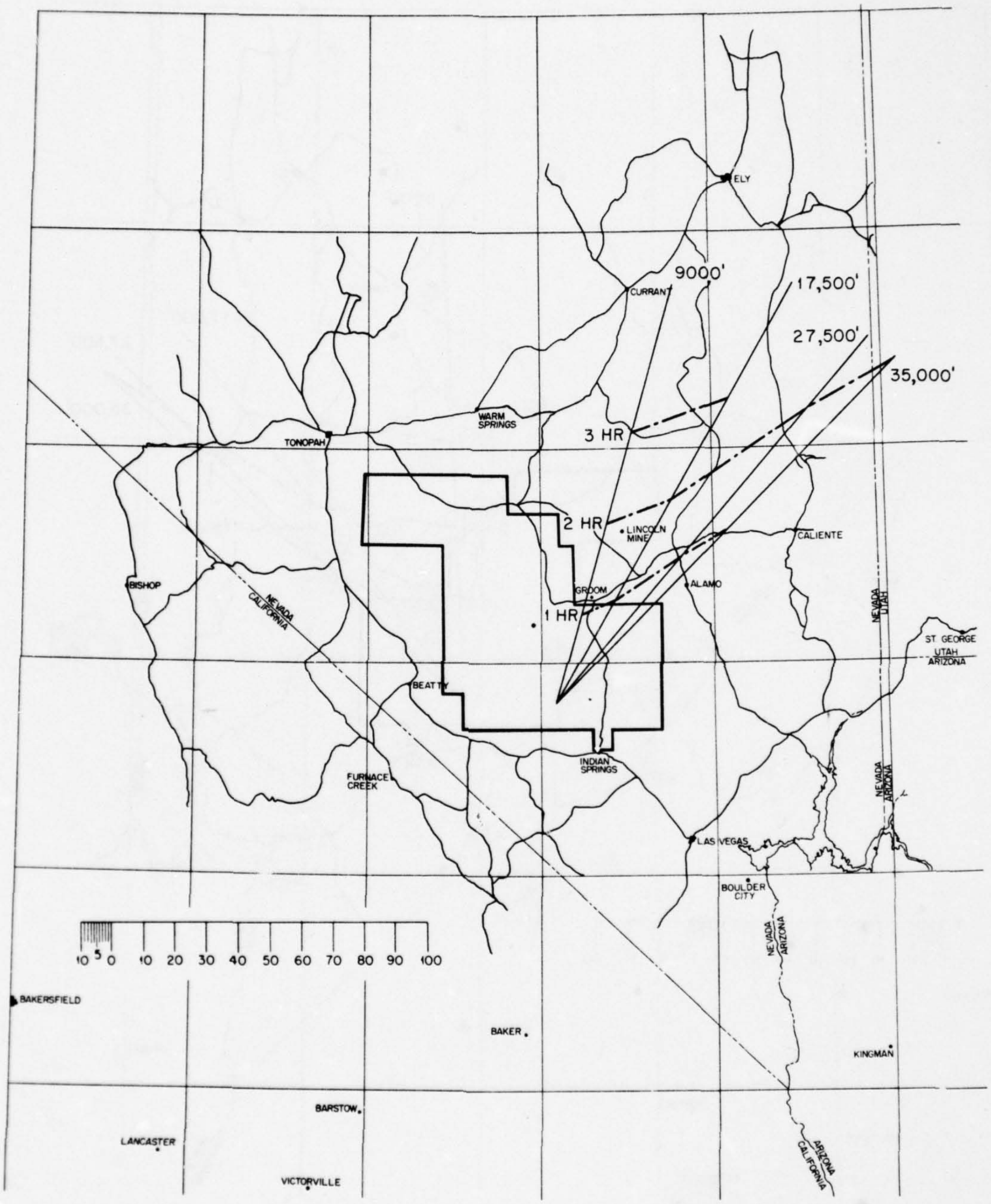

Fig. 41—Fall-out plot for Upshot-Knothole 10, prepared from wind sounding taken at 0400 PDT, 25 May 1953.

RESTRICTED DATA—CONFIDENTIAL—SECURITY INFORMATION

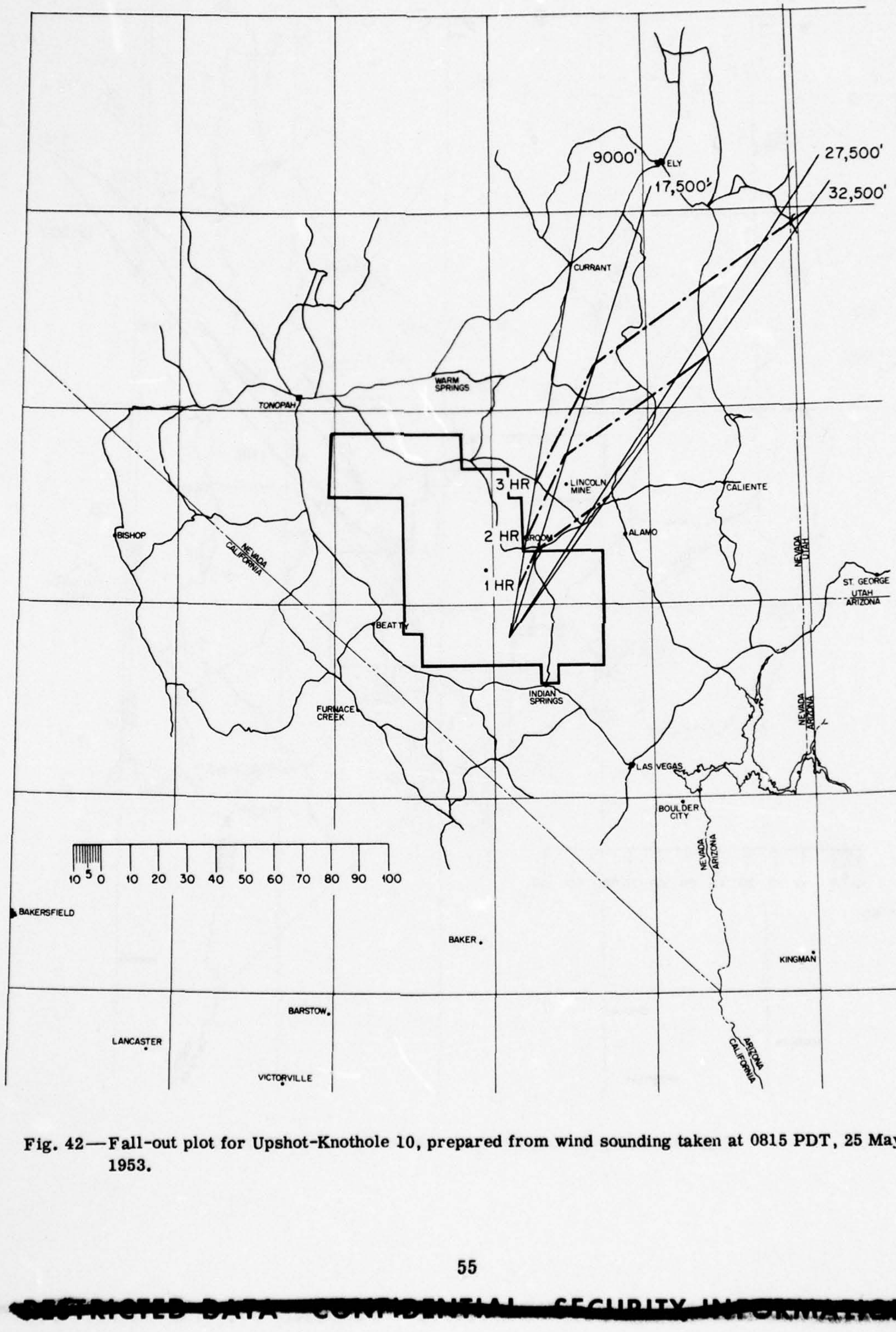

Fig. 42—Fall-out plot for Upshot-Knothole 10, prepared from wind sounding taken at 0815 PDT, 25 May 1953.

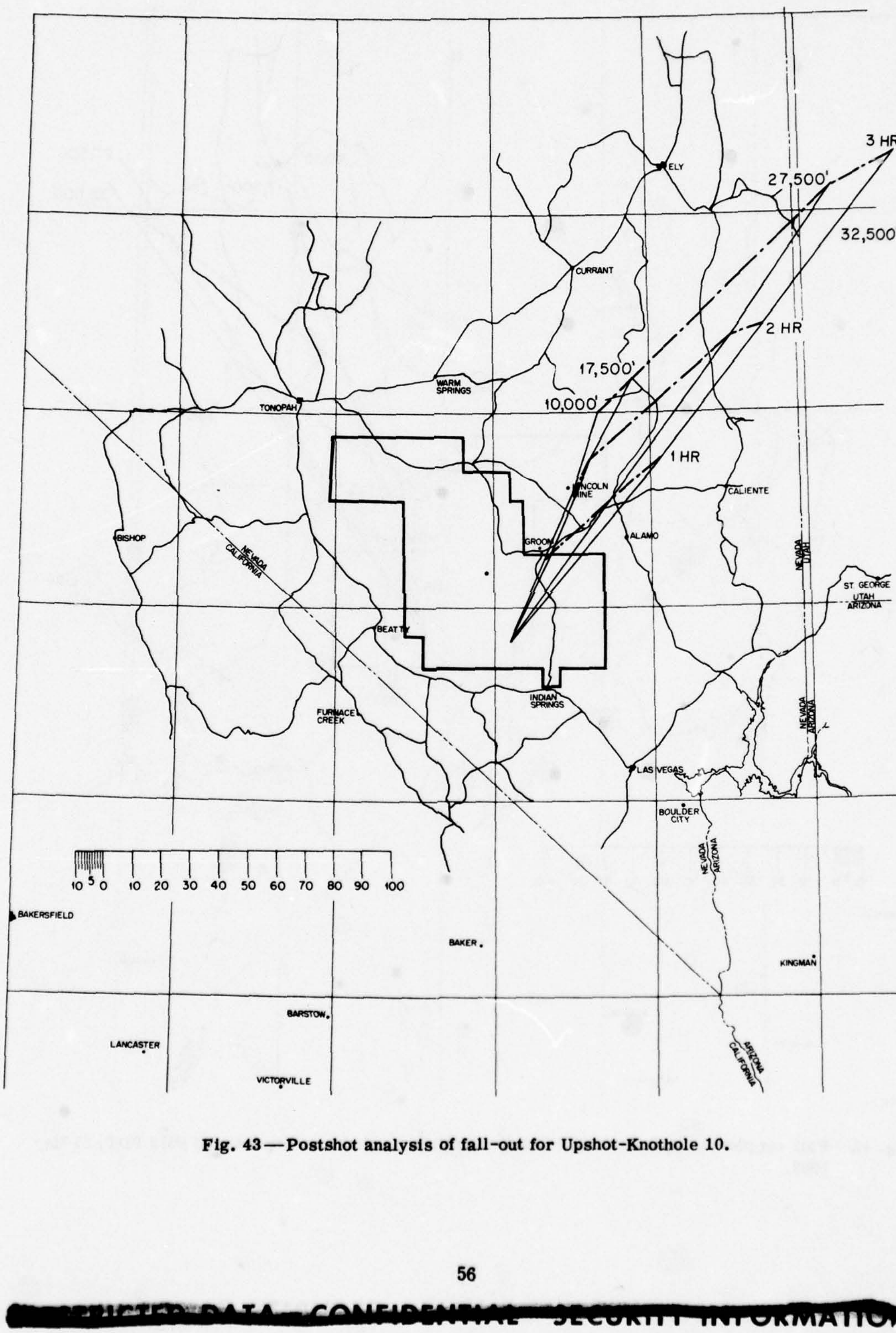

Fig. 43—Postshot analysis of fall-out for Upshot-Knothole 10.

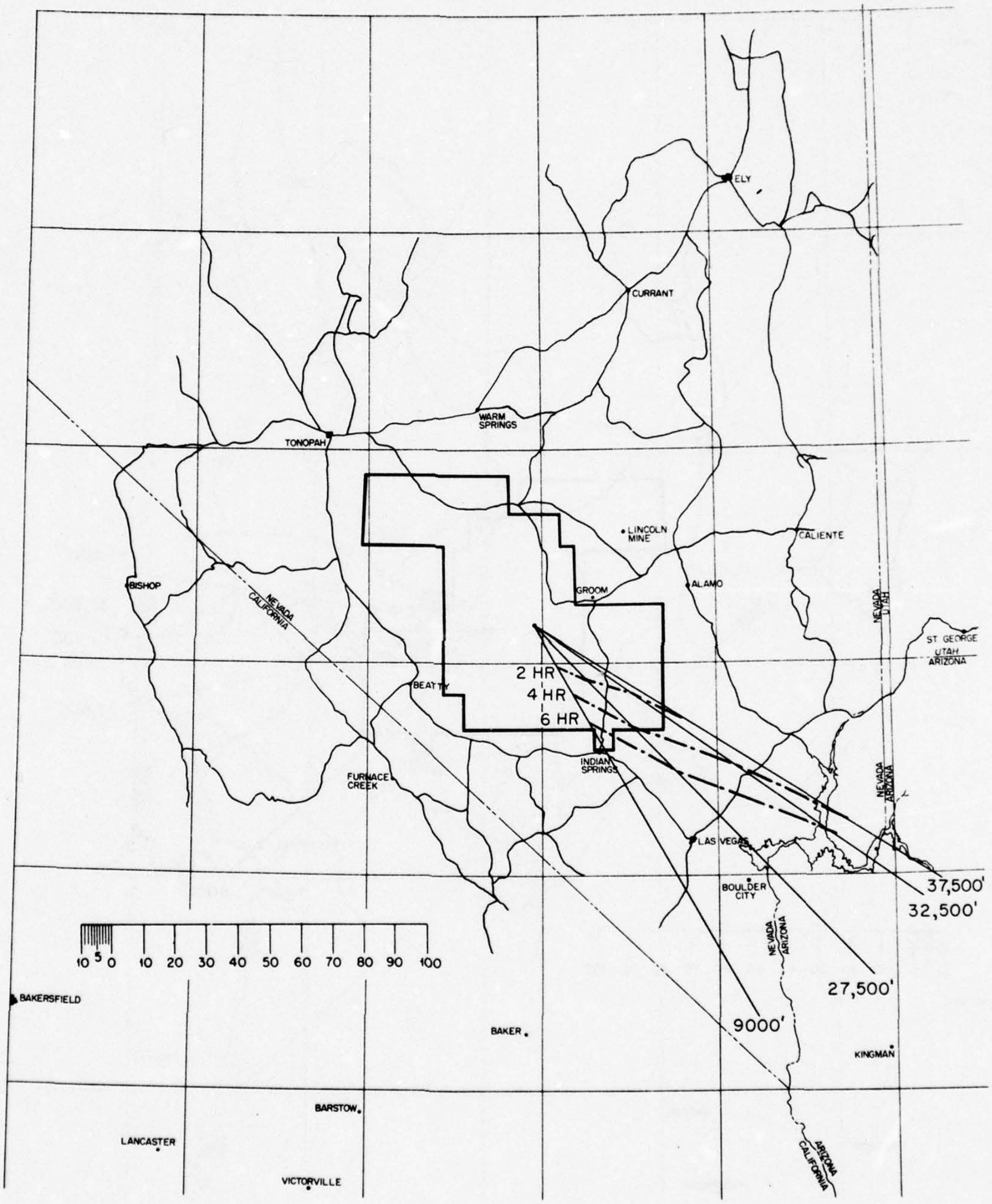

Fig. 44—Fall-out forecast for Upshot-Knothole 11, prepared from briefing wind forecast at 2100 PDT, 3 June 1953, valid at 0415 PDT, 4 June.

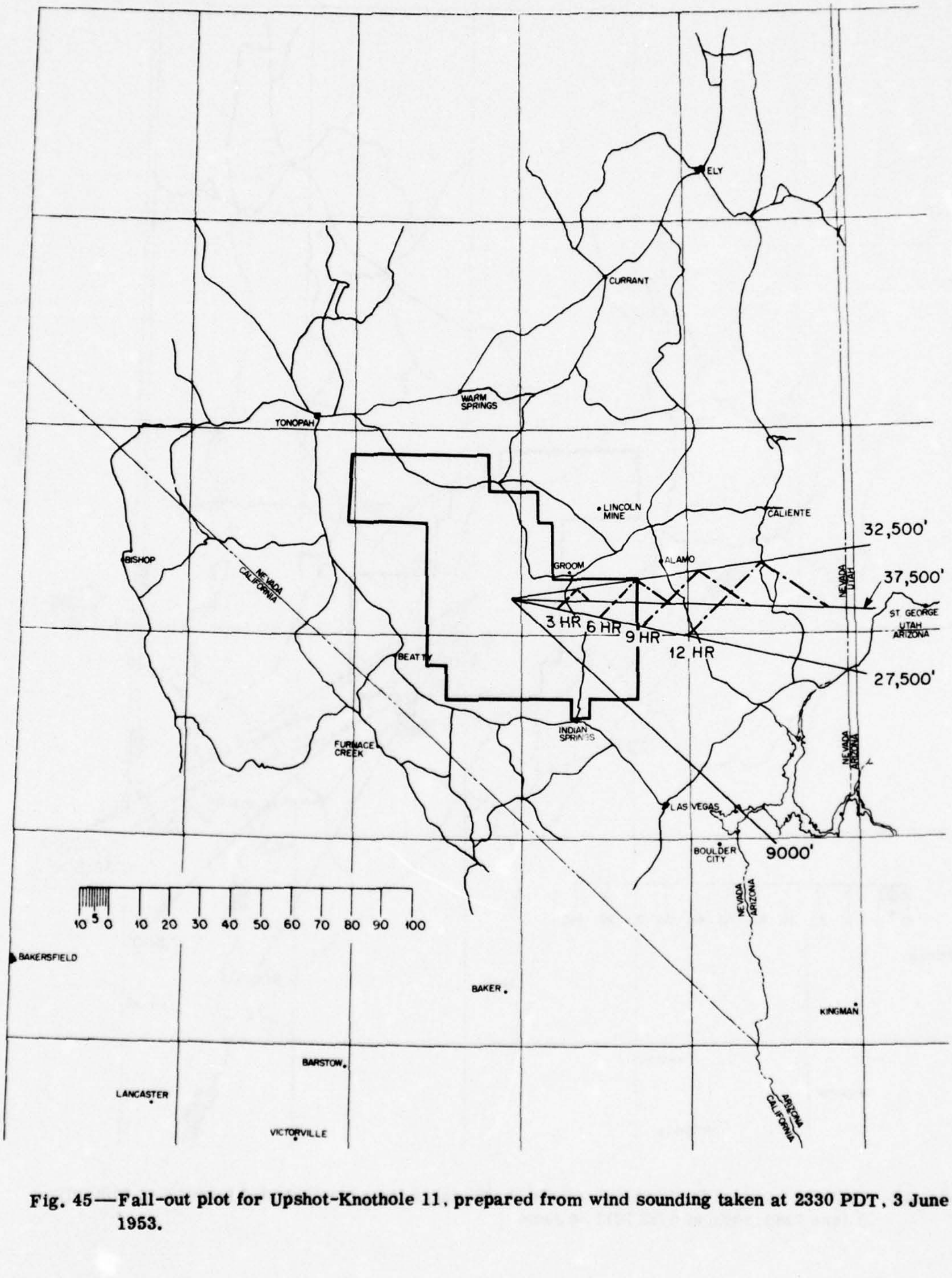

Fig. 45—Fall-out plot for Upshot-Knothole 11, prepared from wind sounding taken at 2330 PDT, 3 June 1953.

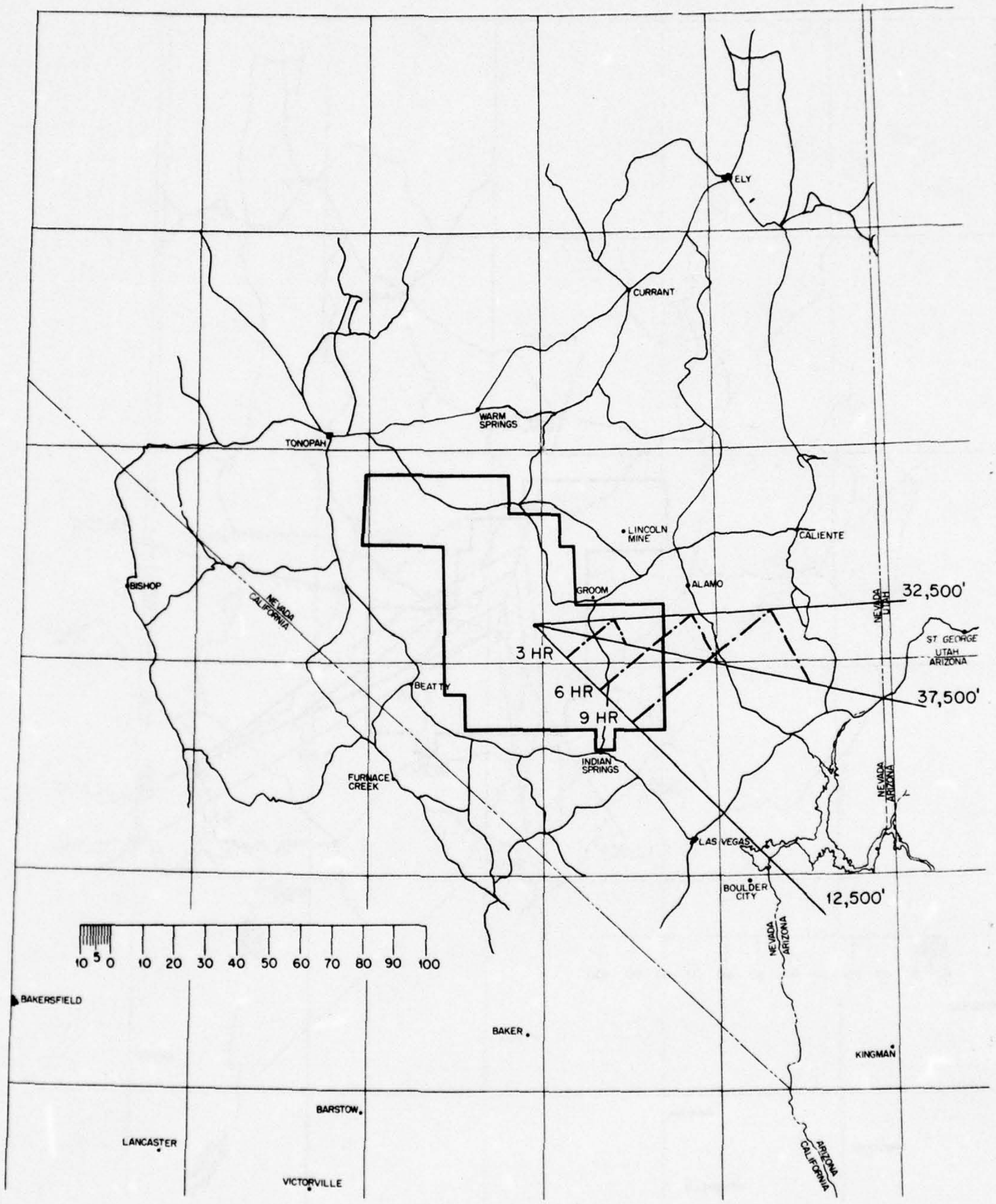

Fig. 46—Fall-out plot for Upshot-Knothole 11, prepared from wind sounding taken at 0130 PDT, 4 June 1953.

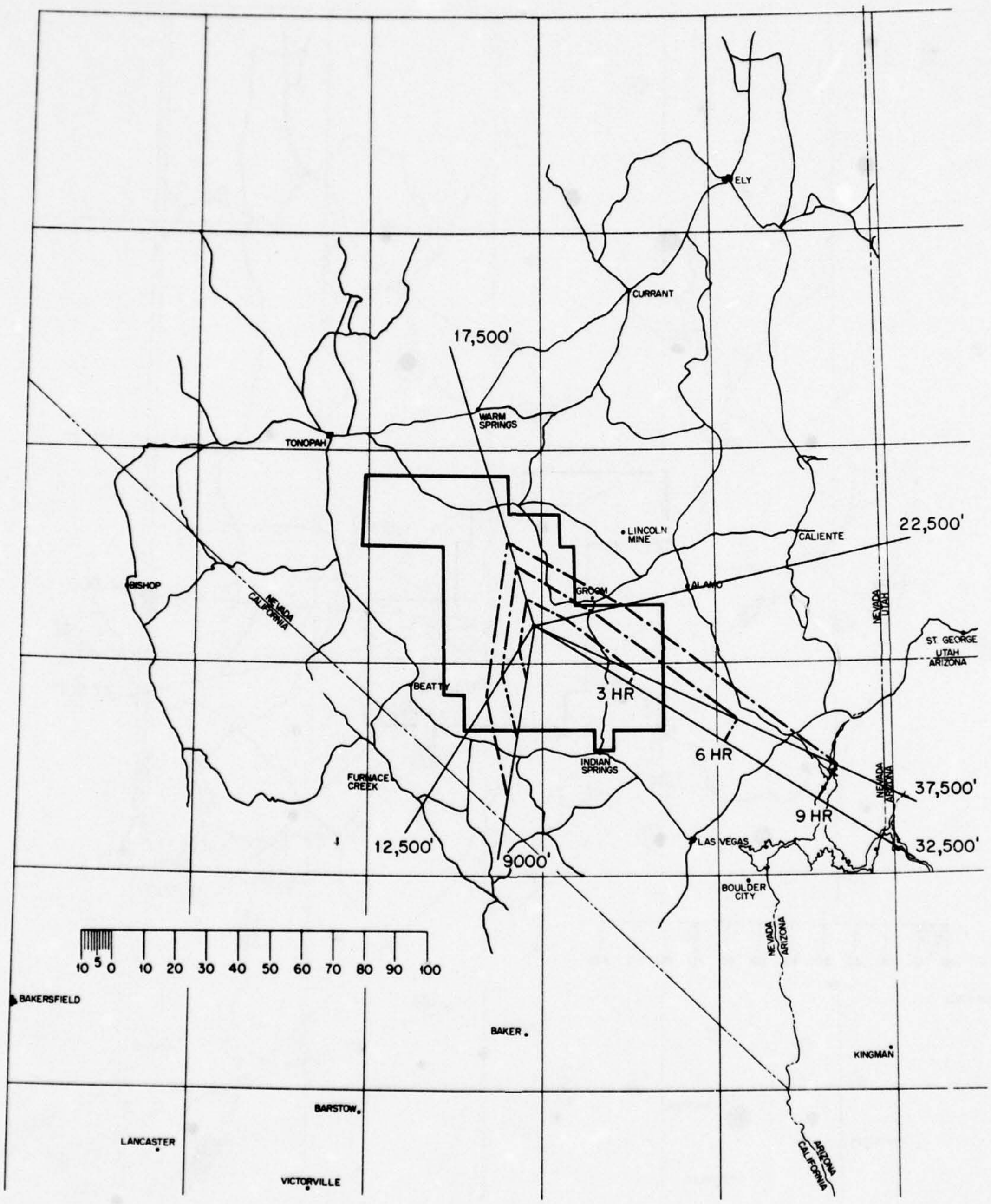

Fig. 47—Fall-out plot for Upshot-Knothole 11, prepared from wind sounding taken at 0500 PDT, 4 June 1953.

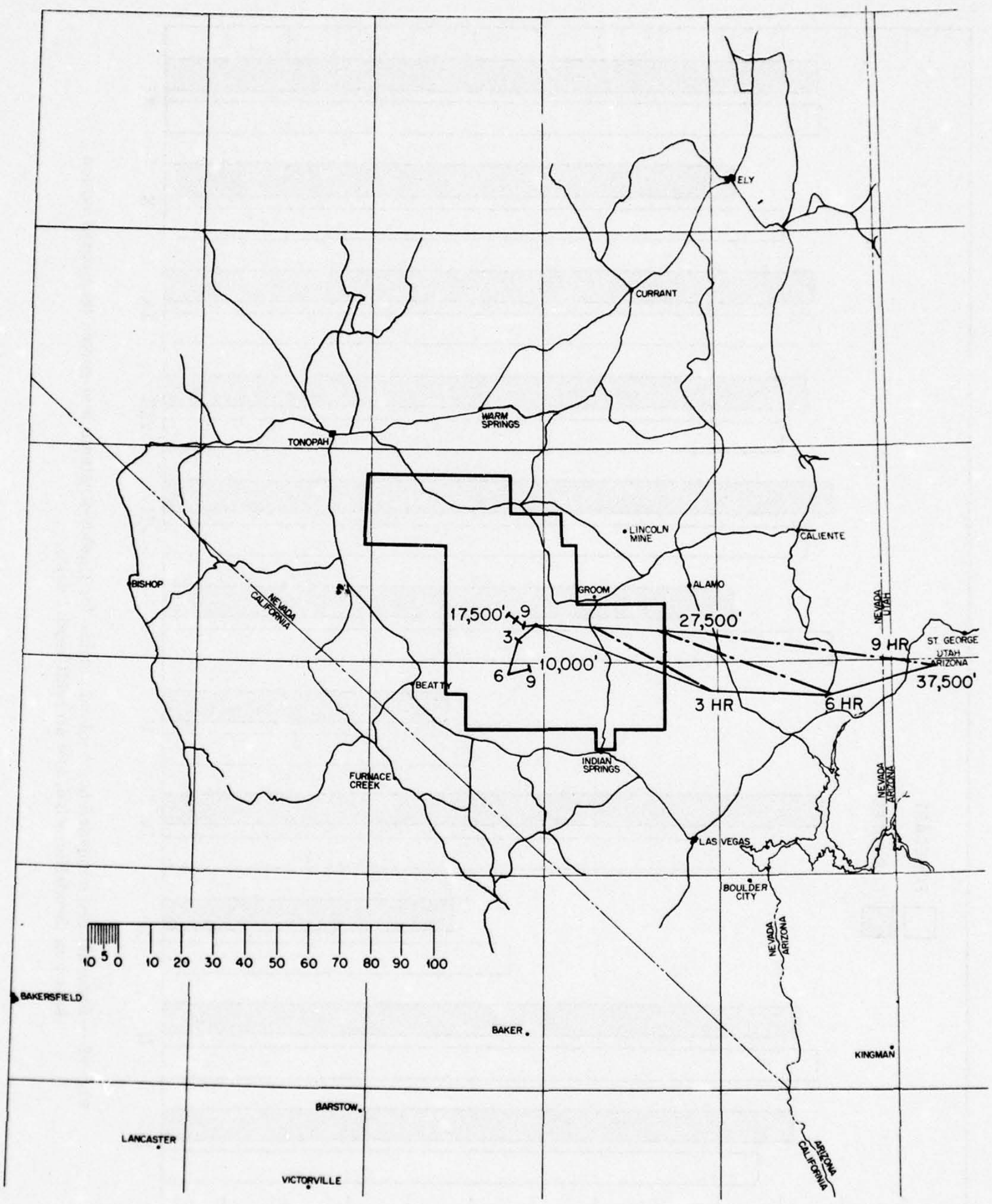

Fig. 48—Postshot analysis of fall-out for Upshot-Knothole 11.

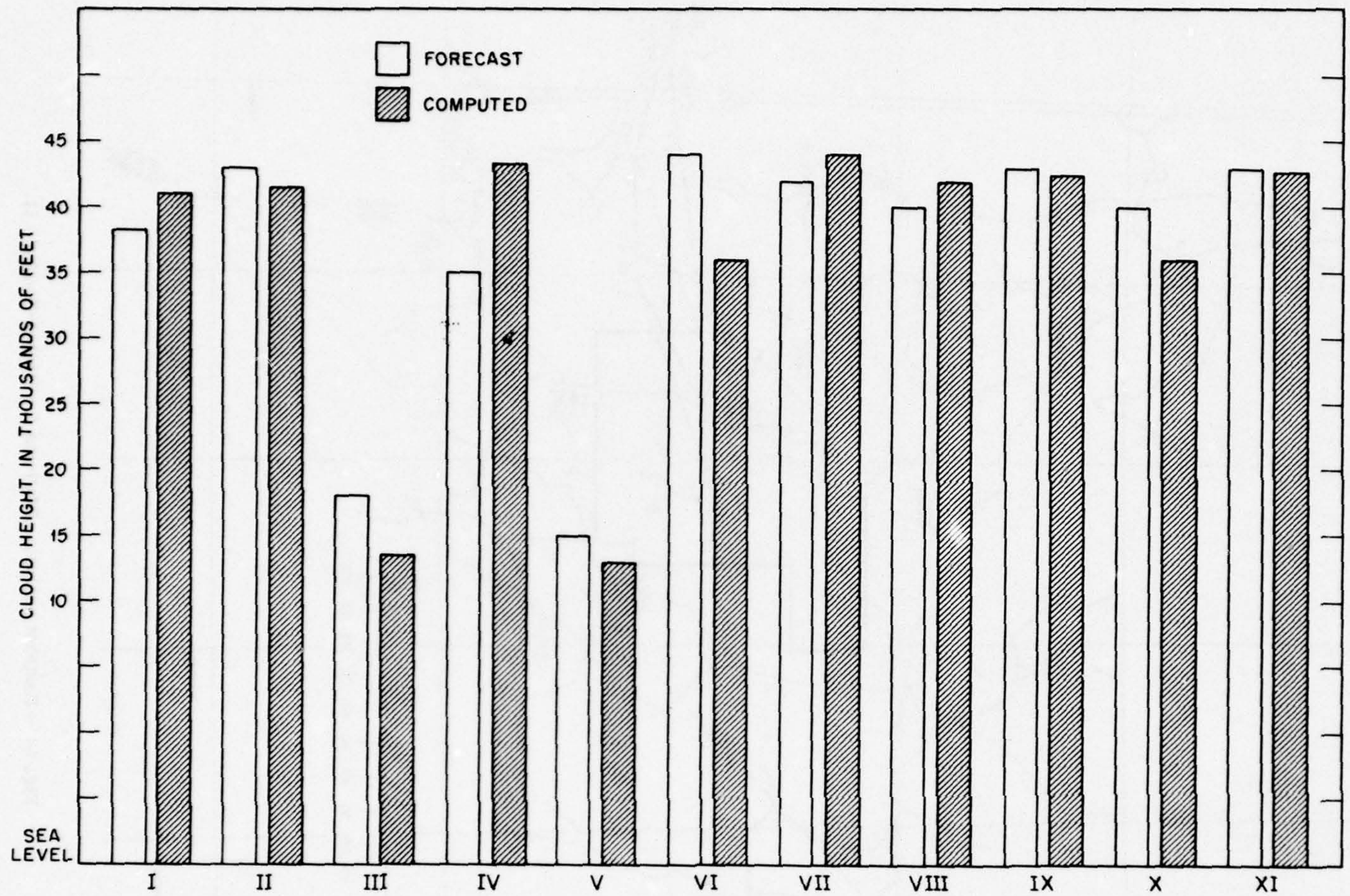

Fig. 49—Forecast and computed bomb-cloud heights for Upshot-Knothole test series (computed values based on theodolite, wind, and aircraft report data).

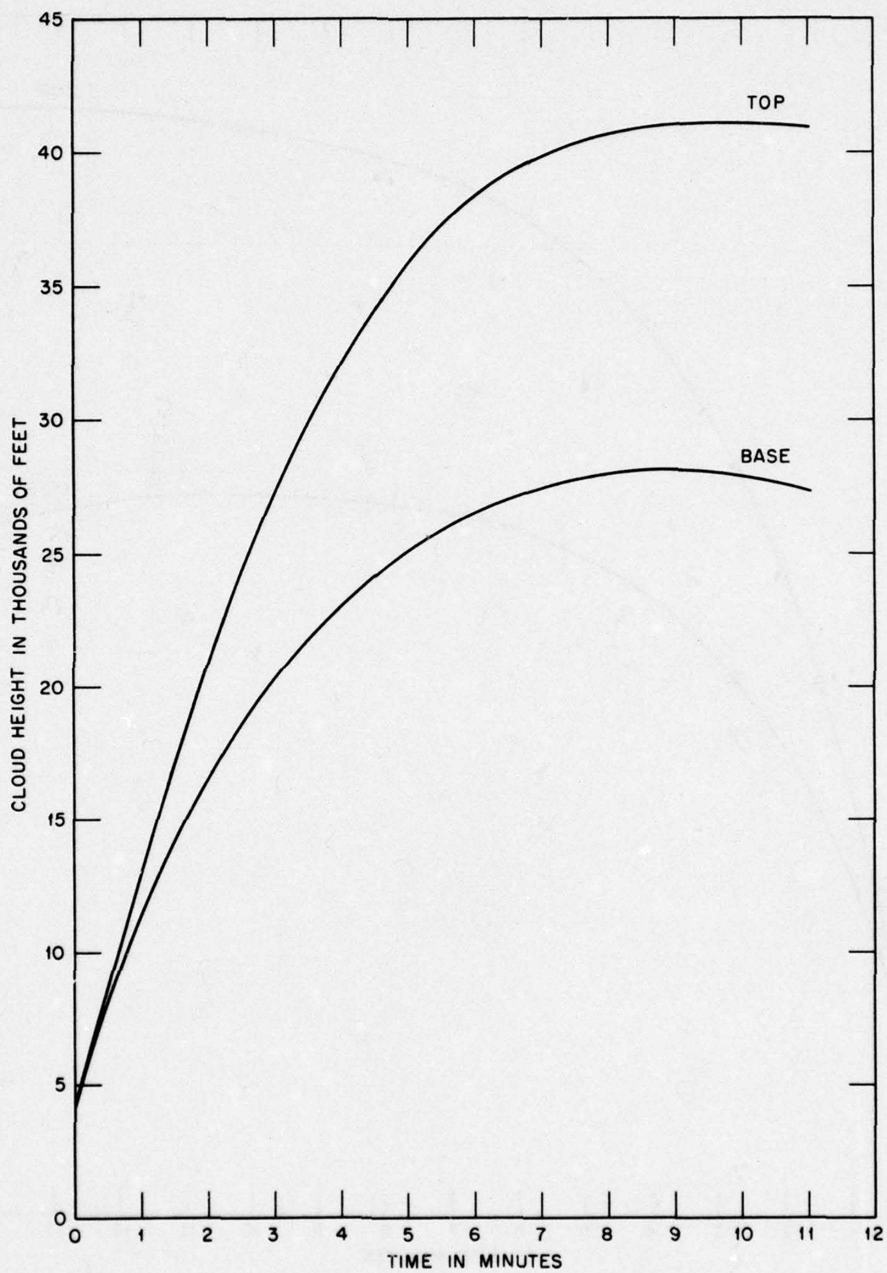

Fig. 50—Cloud rate-of-growth curve for Upshot-Knothole 1.

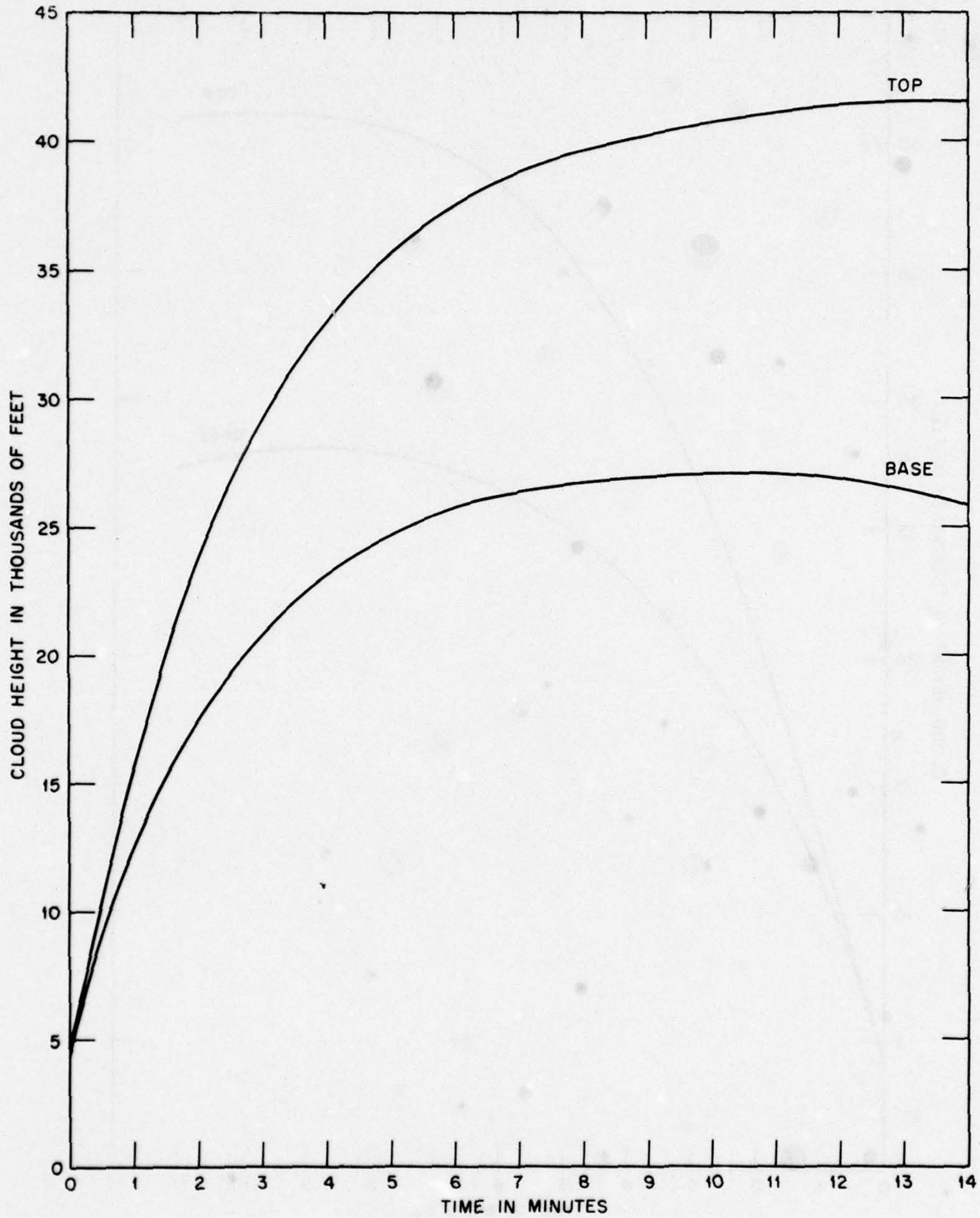

Fig. 51 — Cloud rate-of-growth curve for Upshot-Knothole 2.

[redacted]

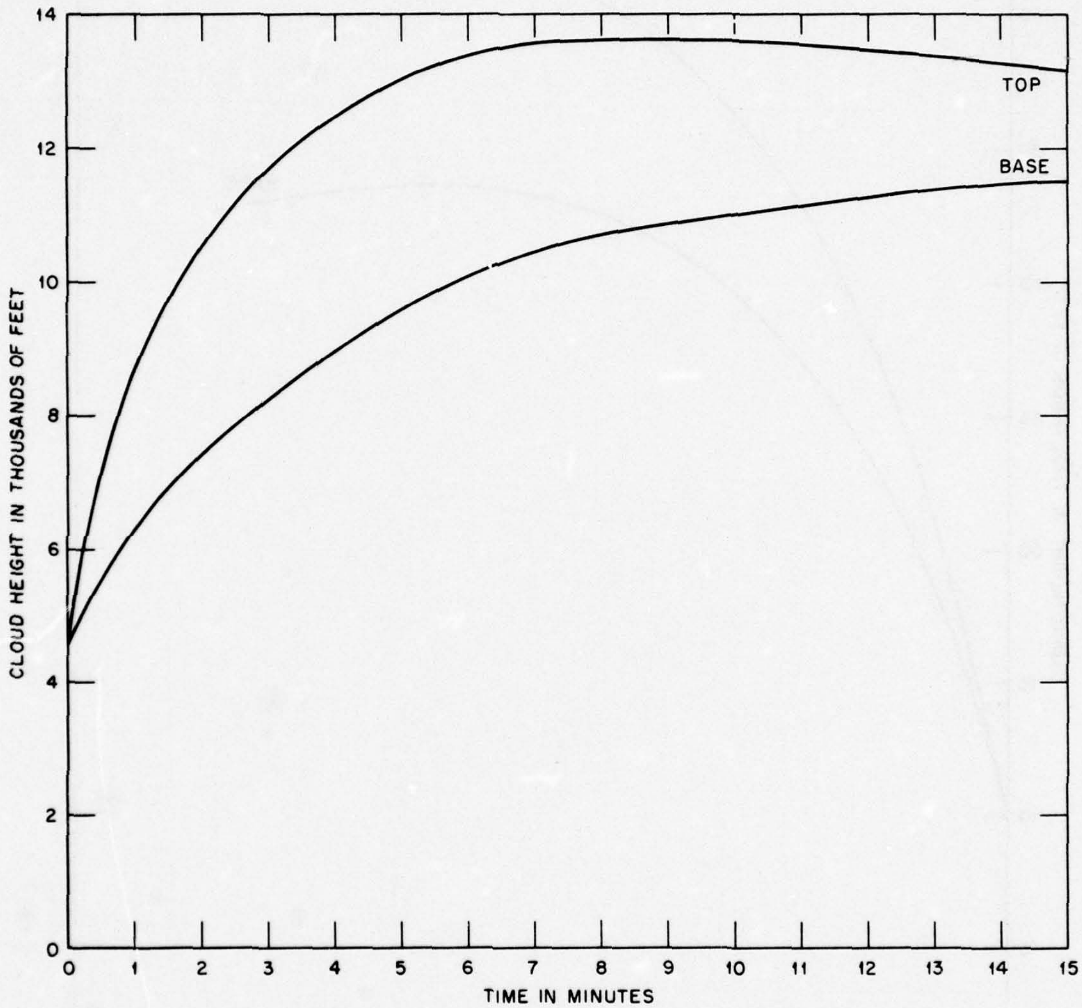

Fig. 52—Cloud rate-of-growth curve for Upshot-Knothole 3.

[redacted]

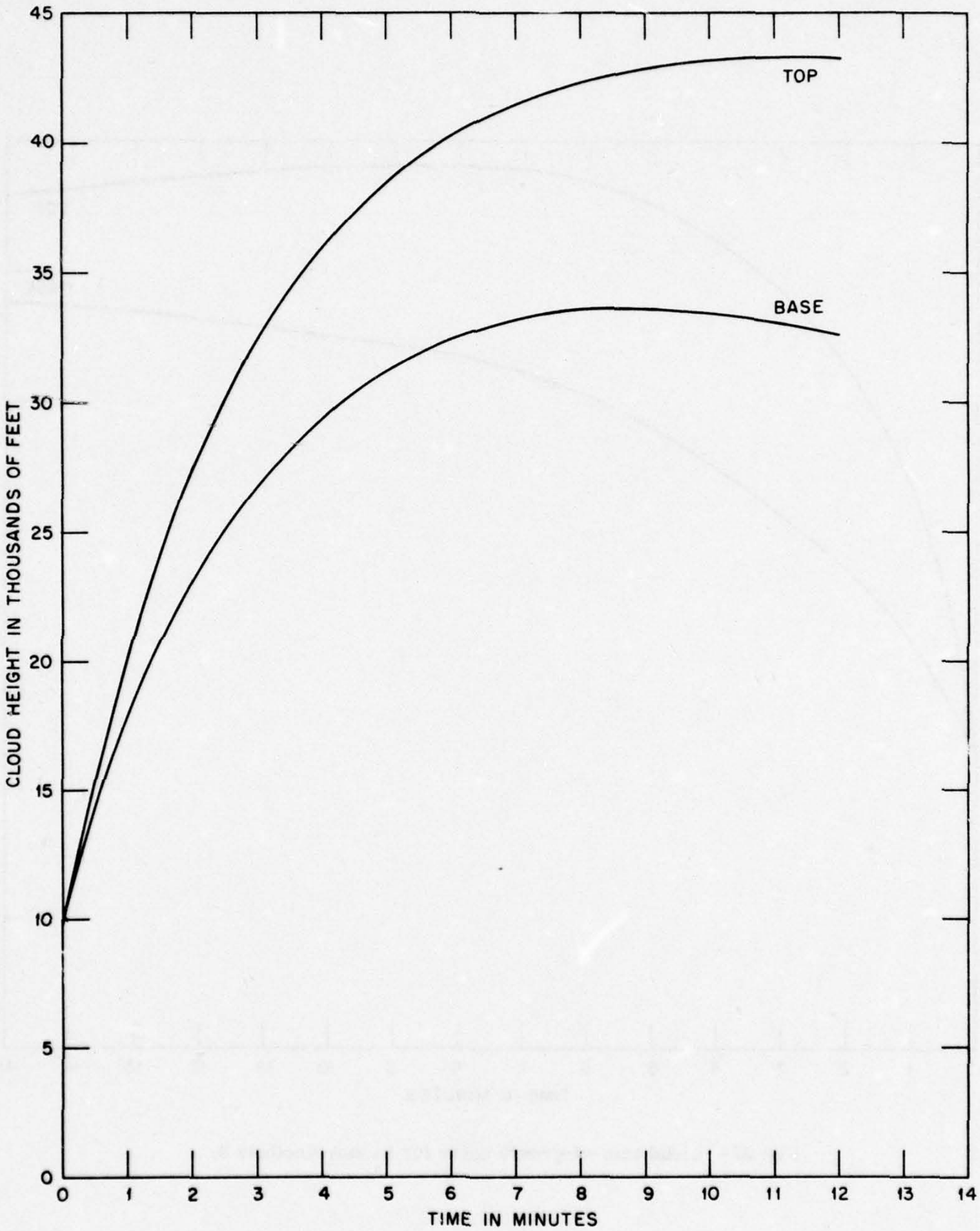

Fig. 53—Cloud rate-of-growth curve for Upshot-Knothole 4.

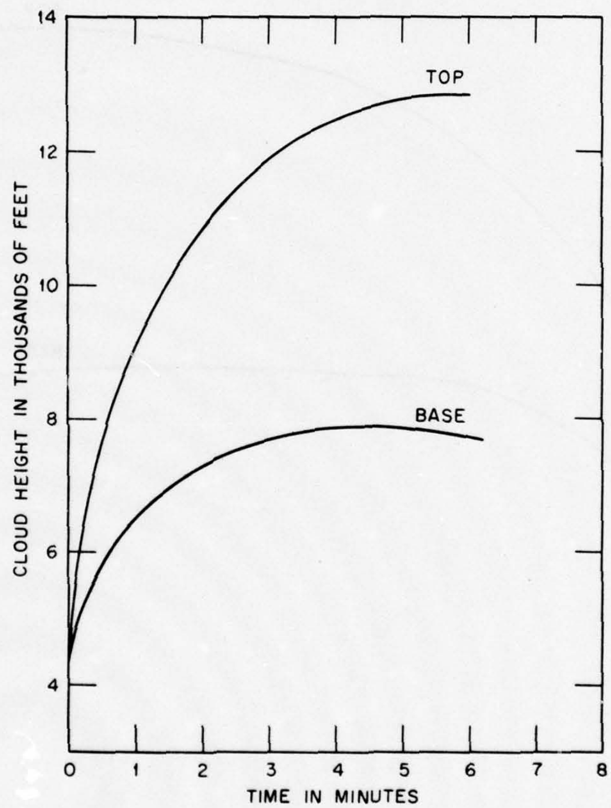

Fig. 54—Cloud rate-of-growth curve for Upshot-Knothole 5.

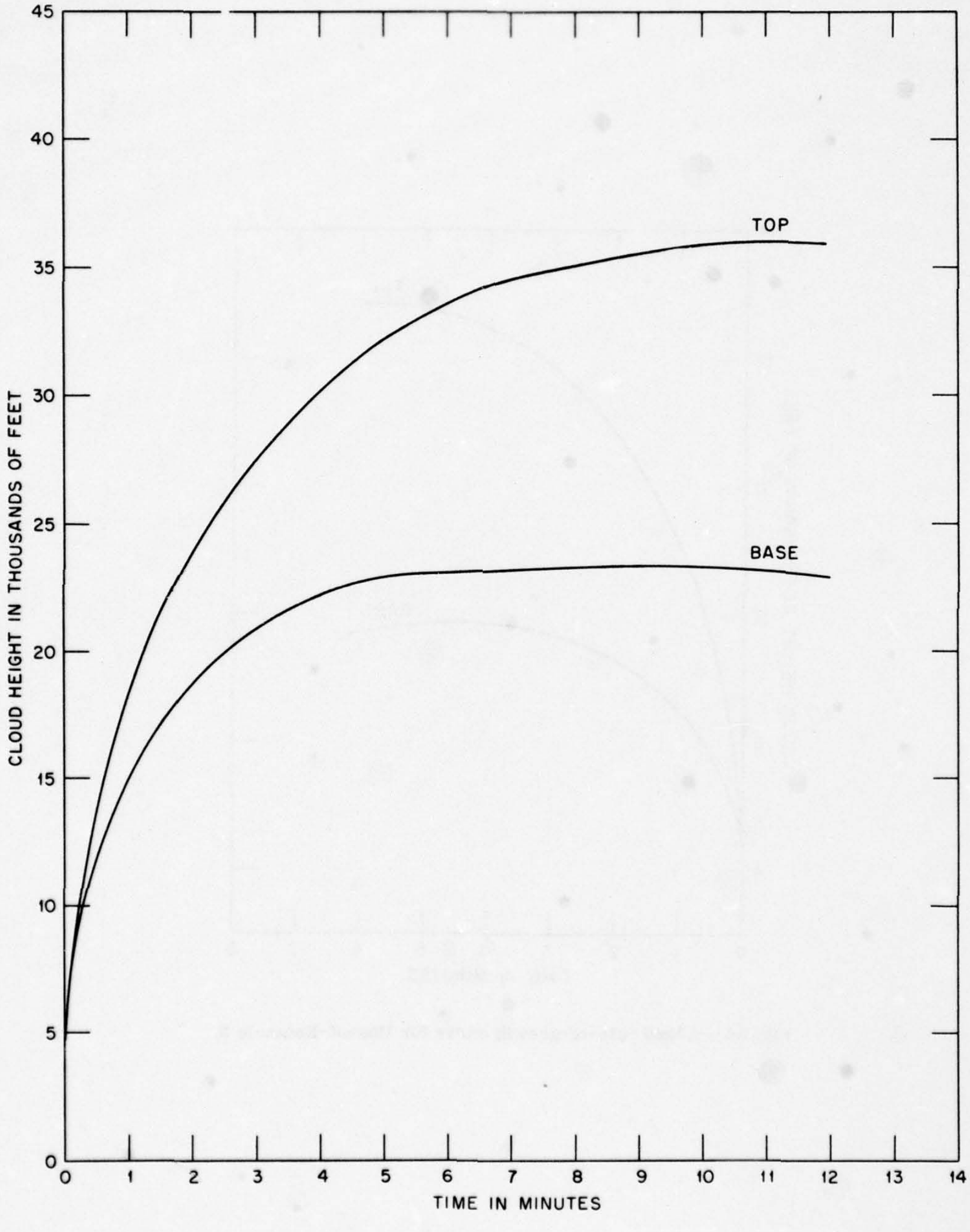

Fig. 55—Cloud rate-of-growth curve for Upshot-Knothole 6.

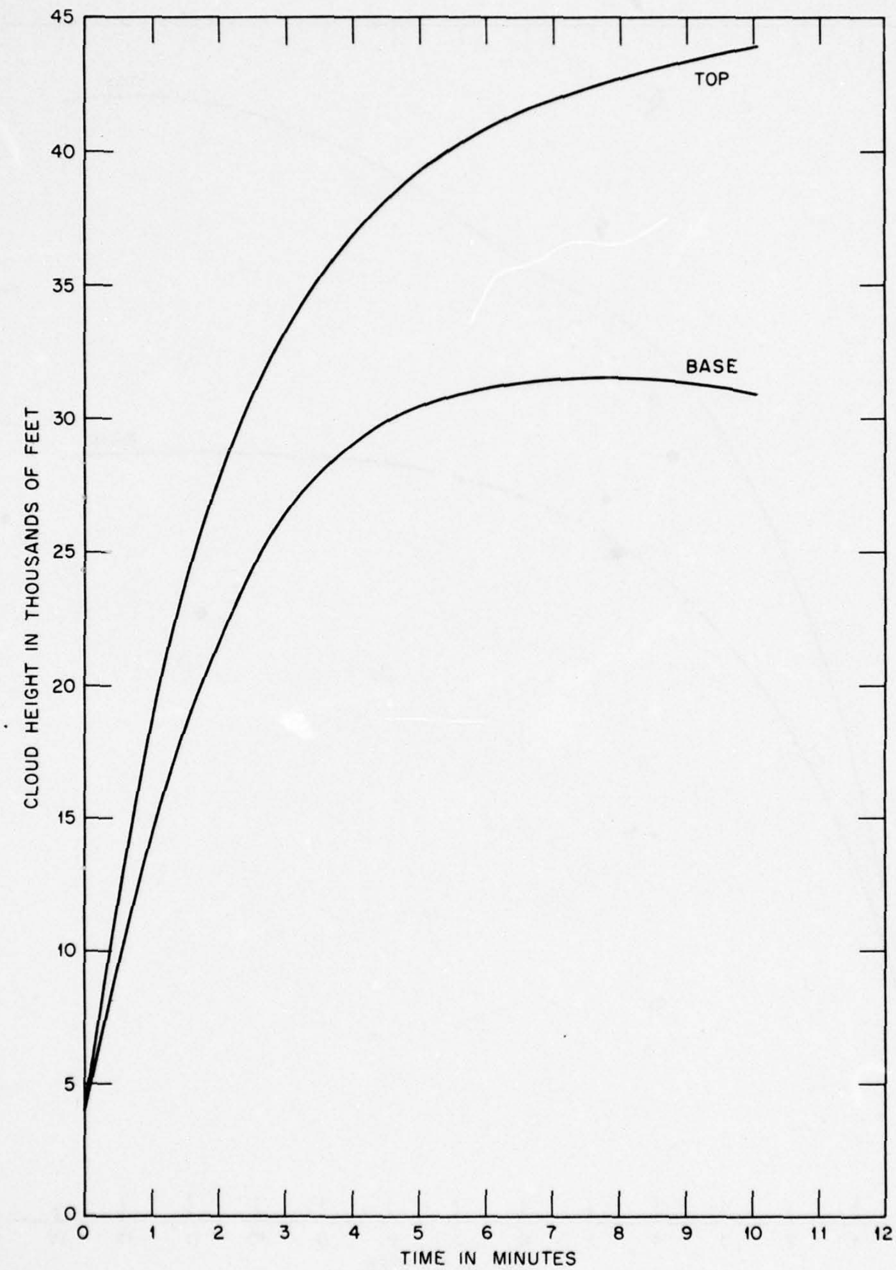

Fig. 56—Cloud rate-of-growth curve for Upshot-Knothole 7.

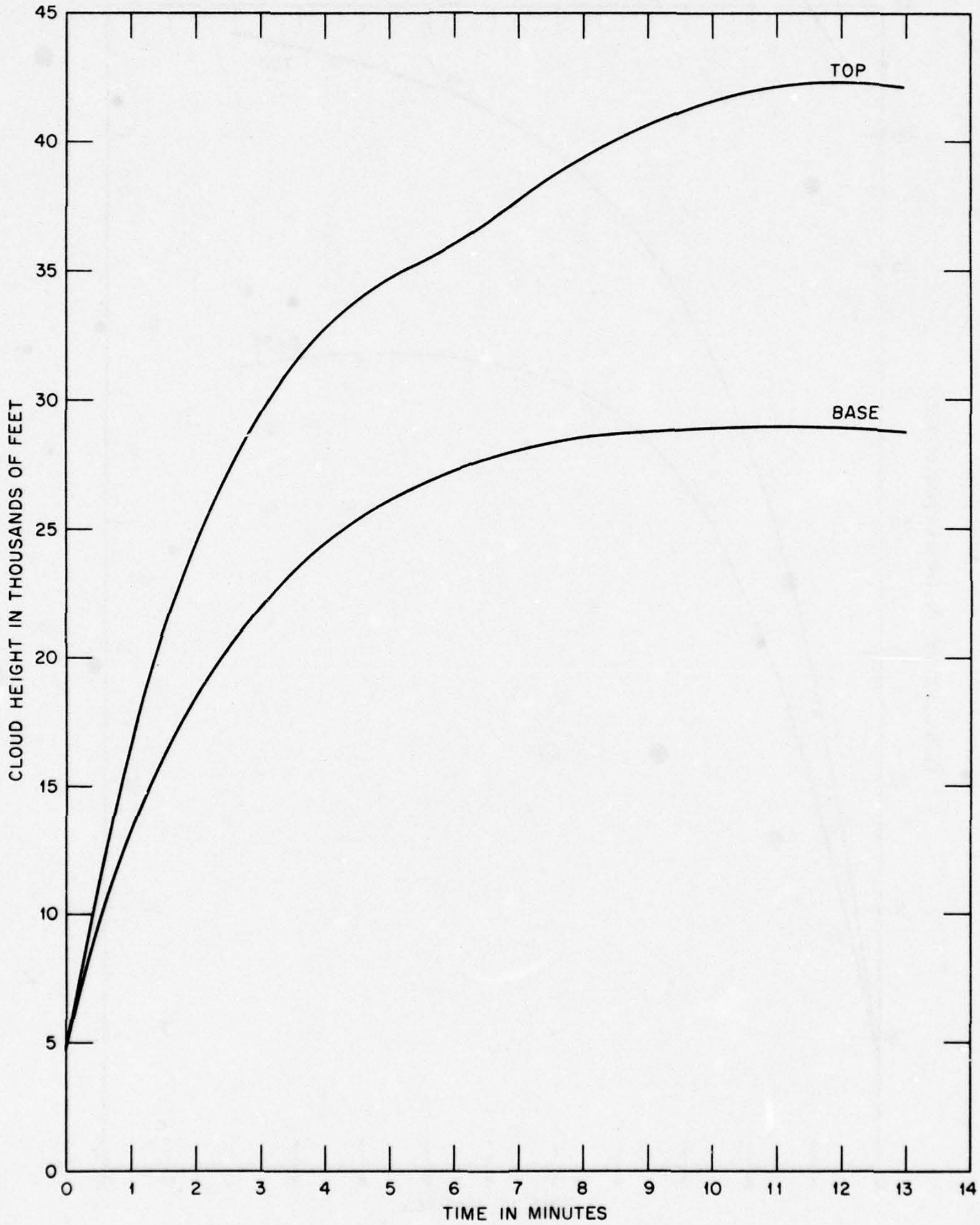

Fig. 57—Cloud rate-of-growth curve for Upshot-Knothole 8.

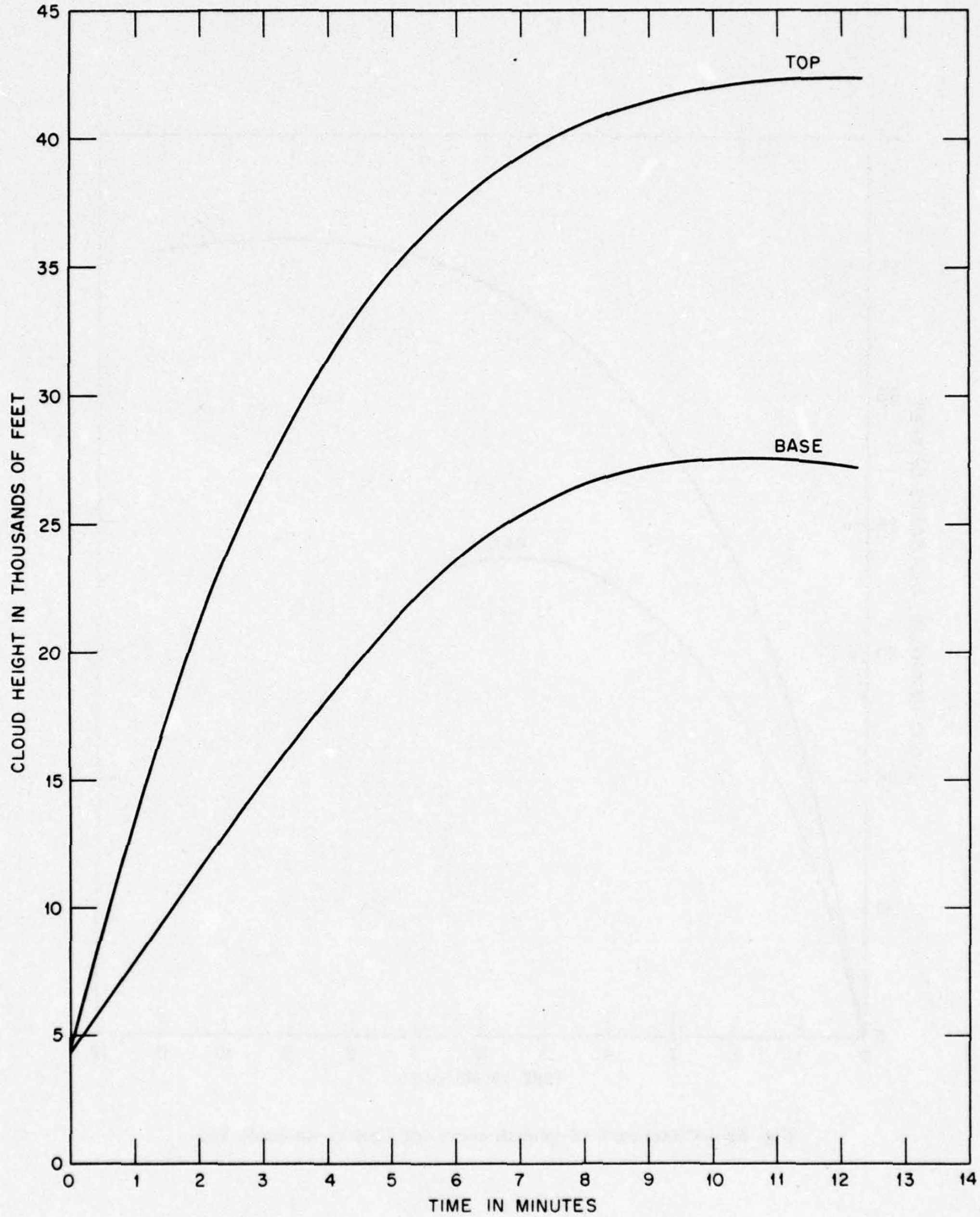

Fig. 58—Cloud rate-of-growth curve for Upshot-Knothole 9.

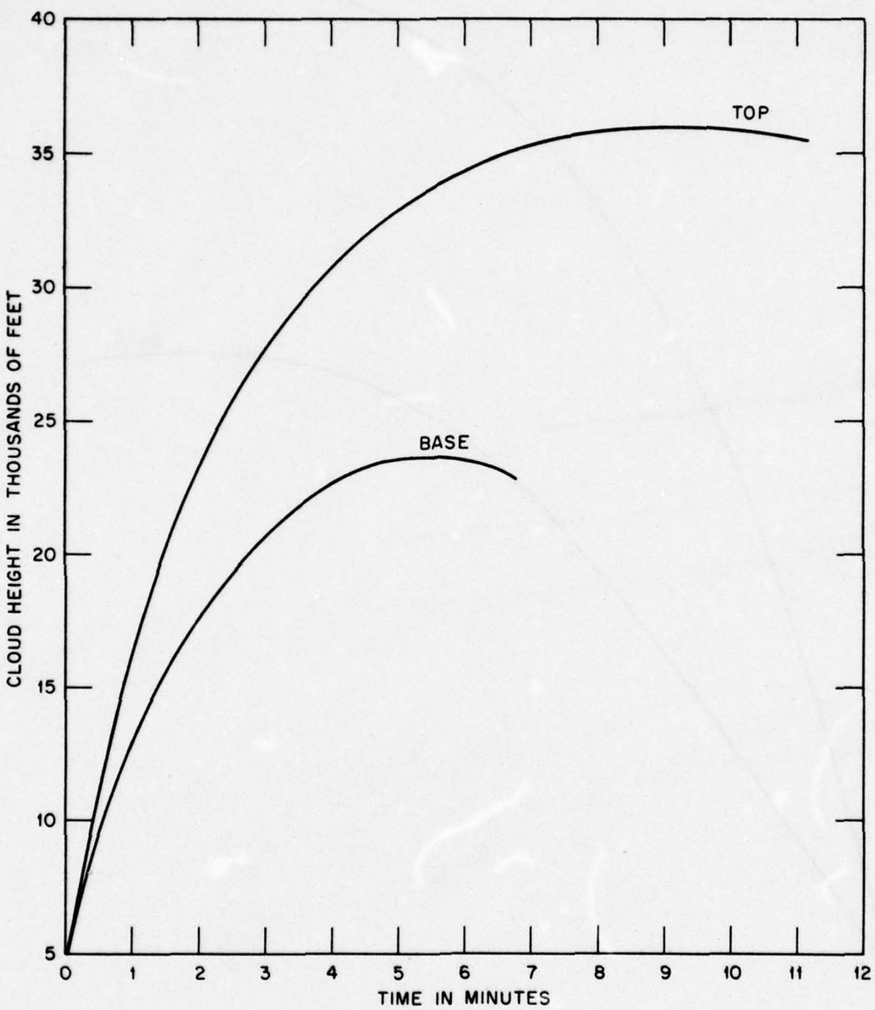

Fig. 59—Cloud rate-of-growth curve for Upshot-Knothole 10.

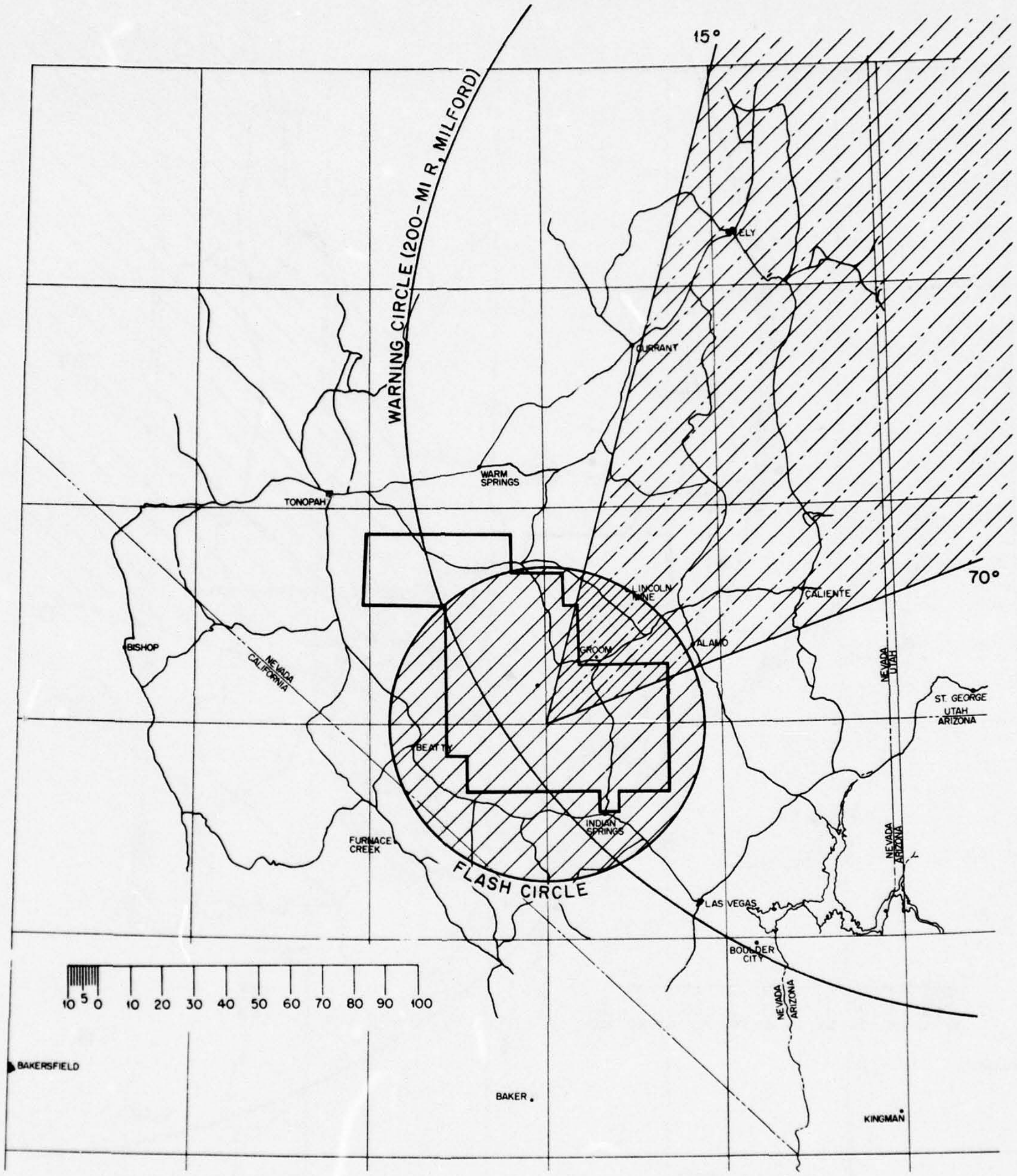

Fig. 60—CAA airspace closure plan for Upshot-Knothole 1, 2200 PST on D−1 day. ——, Flash circle, closed all altitudes, 0500 to 0600; –·–, low sector (15° to 70°), to radius 150 miles, closed 8,000 to 20,000 ft, 0500 to 1100, except Amber 2 airways closed only 0900 to 1100; –··–, high sector (15° to 70°), to radius 300 miles, closed 21,000 ft and up, 0500 to 1400.

Correction to Closure Plan:

0500 D Day: High- and low-sector bearings changed to 60° to 110°. Low-sector radius extended to 300 miles, 0630 to 1100, except Amber 2 and Red 6 airways closed only 0630 to 1100. High-sector radius extended to 450 miles. Warning circle radius extended to 250 miles from Milford.

0825 D Day: Amber 2 and Red 6 airways opened 12,000 ft and below.

1040 D Day: Low-sector closure extended to 1400.

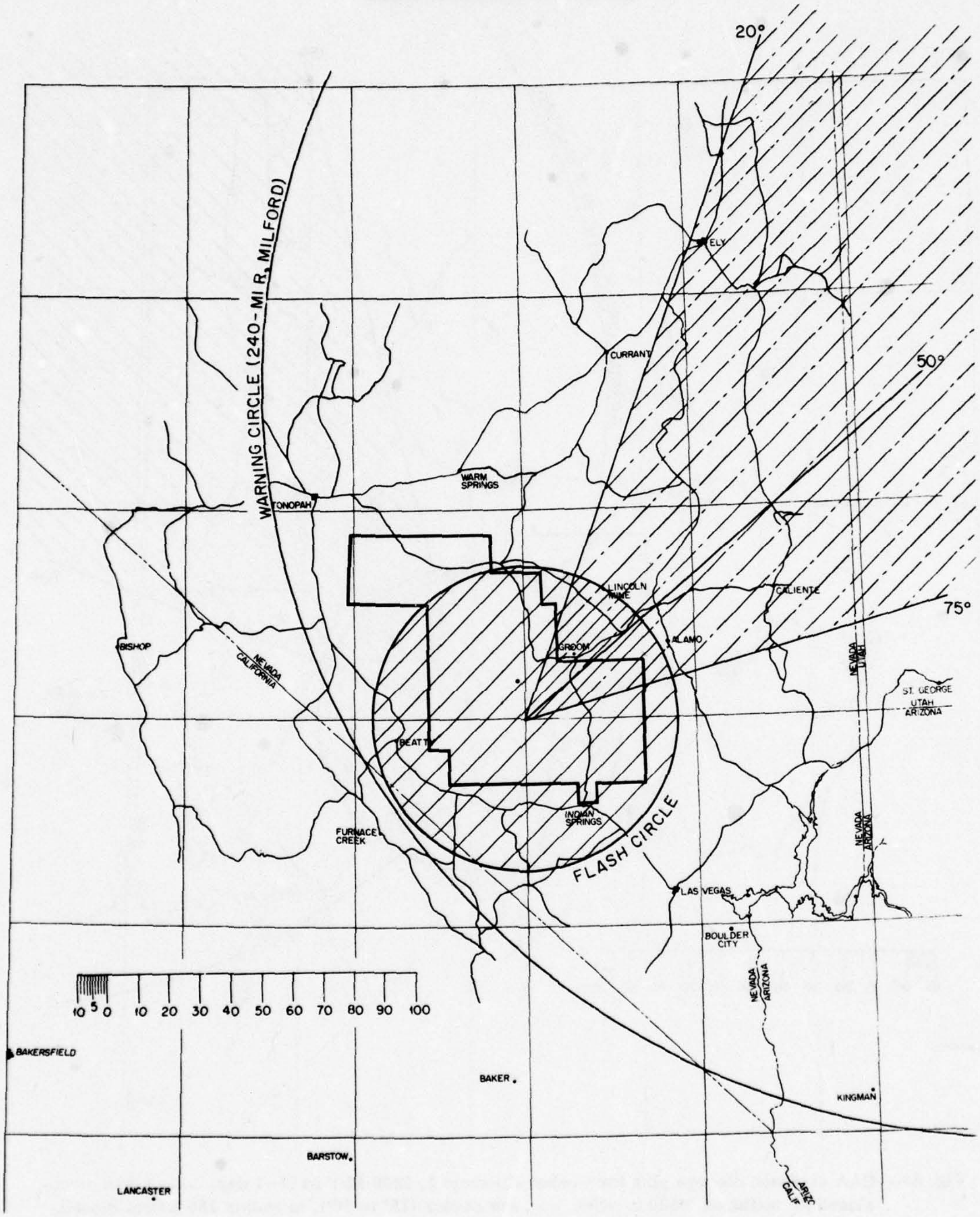

Fig. 61—CAA airspace closure plan for Upshot-Knothole 2, 2200 PST on D−1 day. ——, Flash circle, closed all altitudes, 0430 to 0600; –·–, low sector (20° to 50°), to radius 210 miles, closed 20,000 ft and below, 0500 to 1100; –·–, high sector (50° to 75°), to radius 350 miles, closed 21,000 ft and up, 0500 to 1400.

Correction to Closure Plan:

0430 D Day: Low-sector bearings changed to 330° to 50°.

0900 D Day: High-sector bearings changed to 10° to 75°.

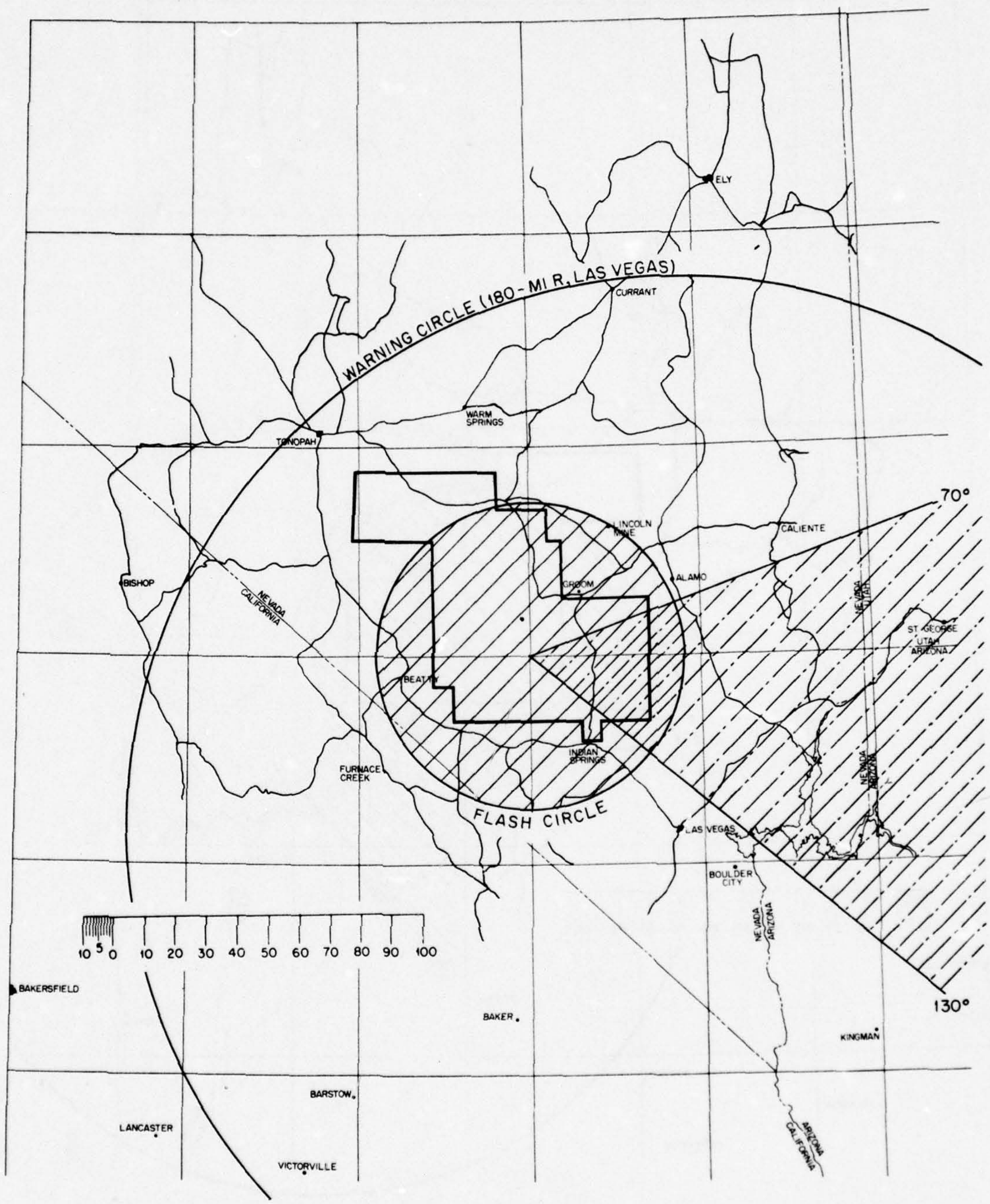

Fig. 62—CAA airspace closure plan for Upshot-Knothole 3, 2200 PST on D−1 day. ——, Flash circle, closed all altitudes, 0430 to 0630; –·–, sector (70° to 130°), to radius 200 miles, closed 21,000 ft and below, 0630 to 1130.

Correction to Closure Plan:

0530 D Day: 17,000 ft and above opened.

0540 D Day: Amber 2 airways opened.

[redacted]

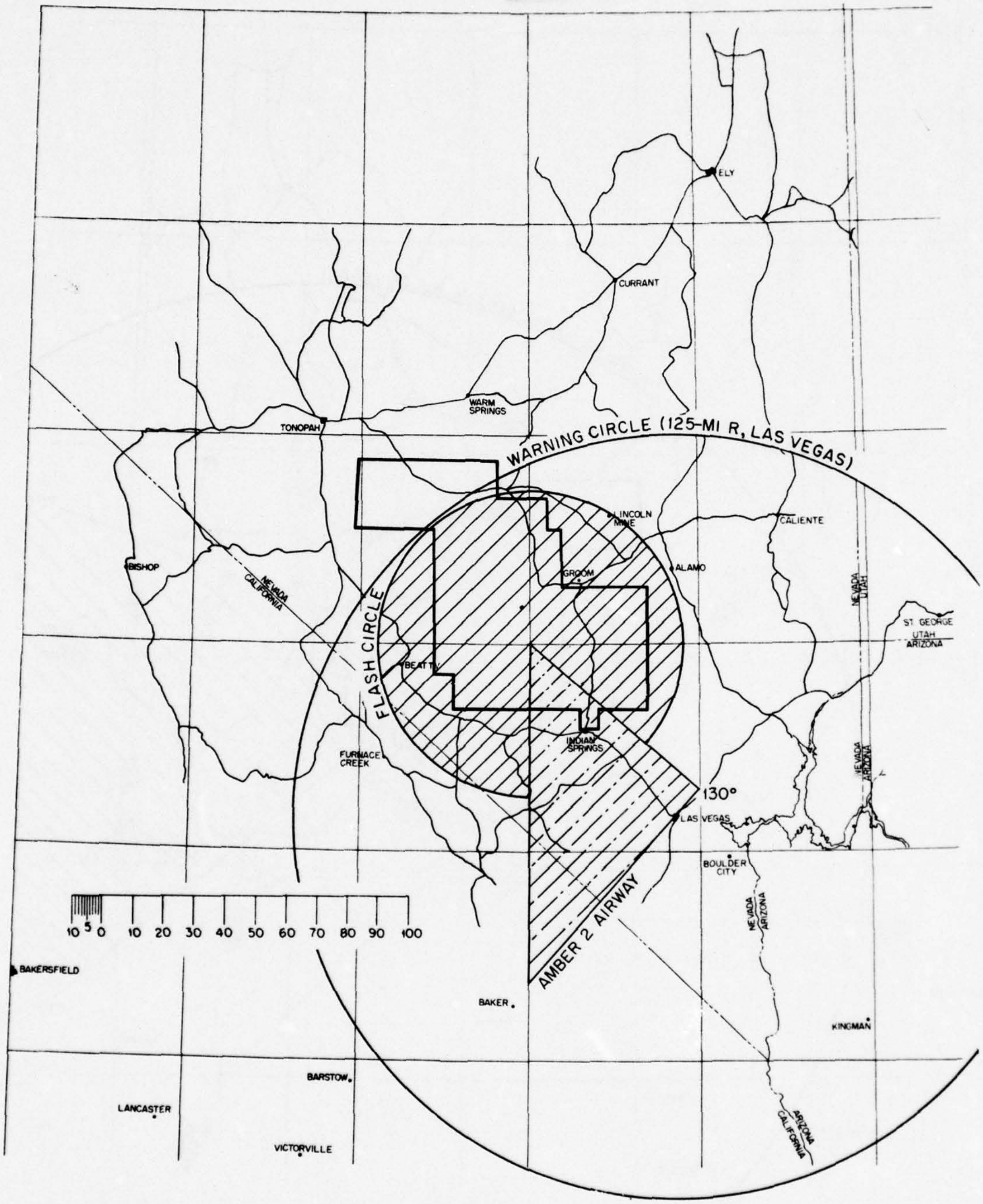

Fig. 63—CAA airspace closure plan for Upshot-Knothole 4, 2200 PST on D−1 day. ——, Flash circle, closed all altitudes, 0700 to 0830; –·–, low sector (130° to 180°), west of Amber 2 airways, closed 23,000 ft and below, 0830 to 0930. High sector, Las Vegas–Yuma–Nogales–Las Vegas, closed 24,000 ft and above, 0830 to 1330.

Correction to Closure Plan:

0620 D Day: High sector changed to Las Vegas–Yuma–Nogales–Albuquerque–Las Vegas.

0830 D Day: High sector changed to include area 35°N to 37°N between Prescott and Albuquerque.

[redacted]

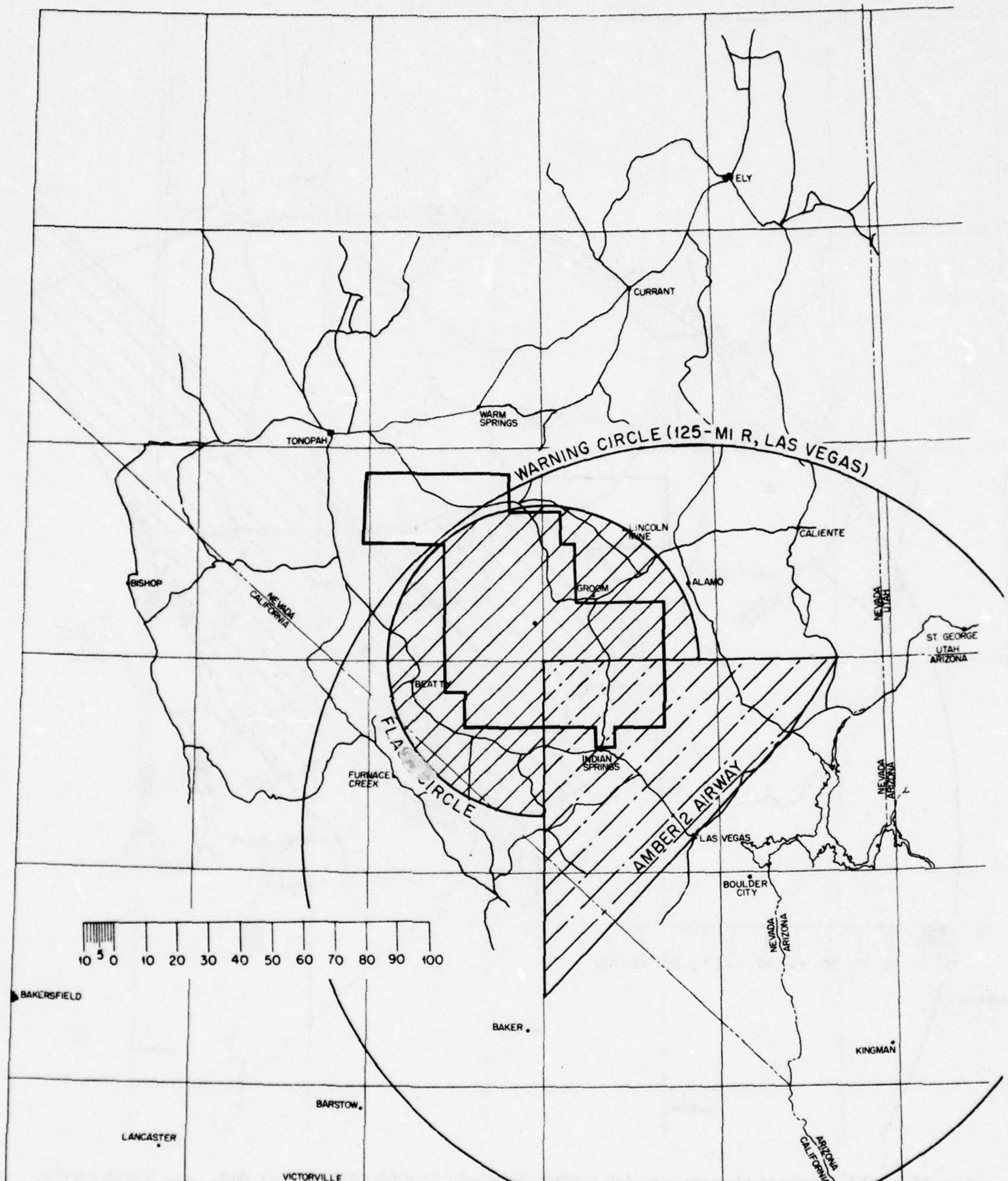

Fig. 64—CAA airspace closure plan for Upshot-Knothole 5, 2200 PST on D−1 day. ——, Flash circle, and -.-., sector (90° to 180°), north of Amber 2 airways, closed 20,000 ft and below 0430 to 0700.

Correction to Closure Plan:

0600 D Day: 180° bearing of sector changed to 200°.

[redacted]

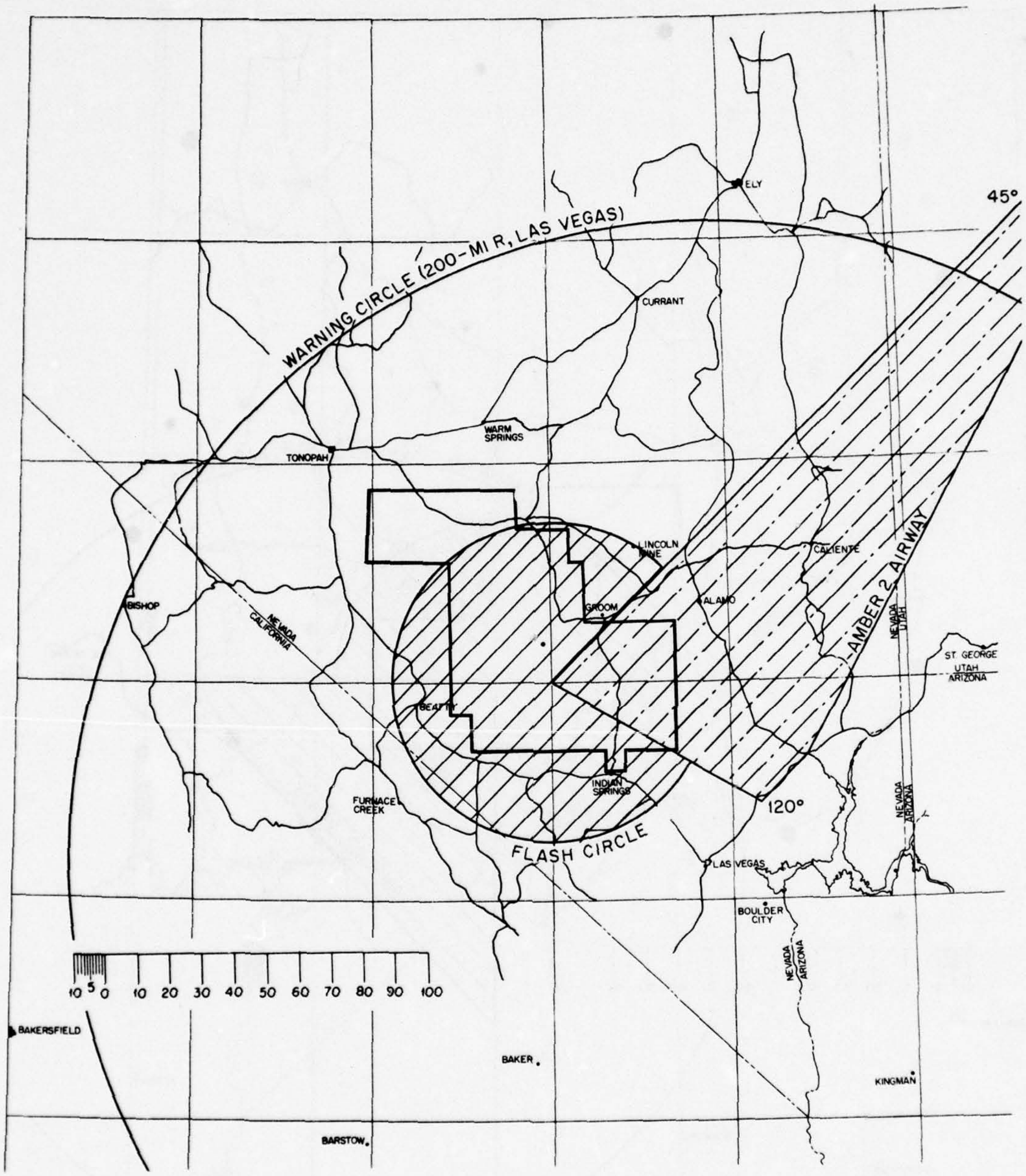

Fig. 65—CAA airspace closure plan for Upshot-Knothole 6, 2200 PST on D−1 day. ——, Flash circle, and –·–, sector (45° to 120°), north of Amber 2 airways, closed all altitudes, 0400 to 0530. High sector No. 1, 21,000 ft and above, Las Vegas–Albuquerque–Grand Junction–Milford–Las Vegas, closed 0500 to 1100. High sector No. 2, 21,000 ft and above, Durango–Albuquerque–Hobbs–Fort Worth–Durango, closed 1100 to 1700.

Correction to Closure Plan:

0530 D Day: Base of high sectors raised to 27,000 ft.

0610 D Day: High sector No. 1 boundaries changed to Las Vegas–El Paso–Durango–Las Vegas. High sector No. 2 boundaries changed to Durango–El Paso–Fort Worth–Durango.

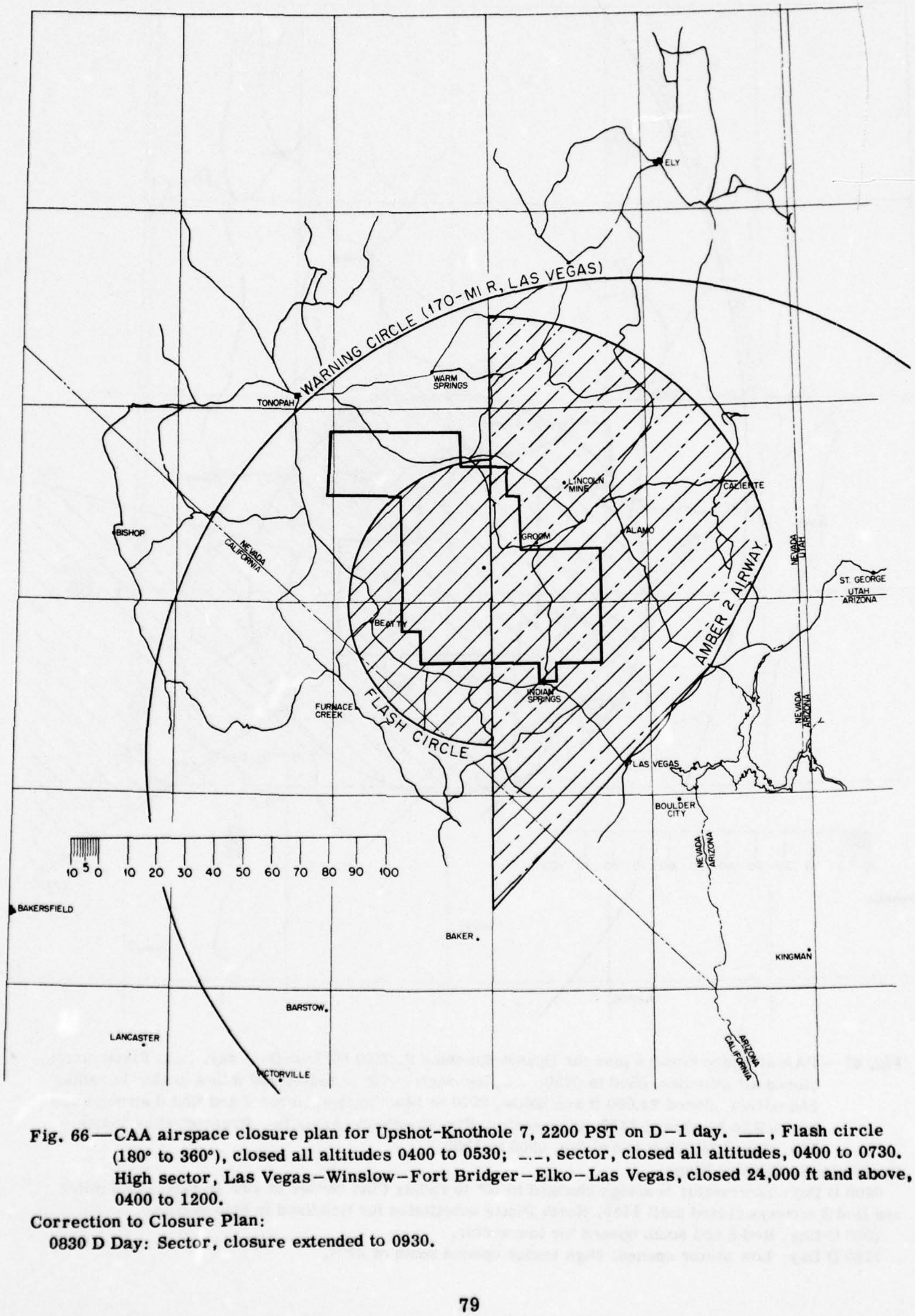

Fig. 66—CAA airspace closure plan for Upshot-Knothole 7, 2200 PST on D−1 day. ——, Flash circle (180° to 360°), closed all altitudes 0400 to 0530; –·–, sector, closed all altitudes, 0400 to 0730. High sector, Las Vegas–Winslow–Fort Bridger–Elko–Las Vegas, closed 24,000 ft and above, 0400 to 1200.

Correction to Closure Plan:

0830 D Day: Sector, closure extended to 0930.

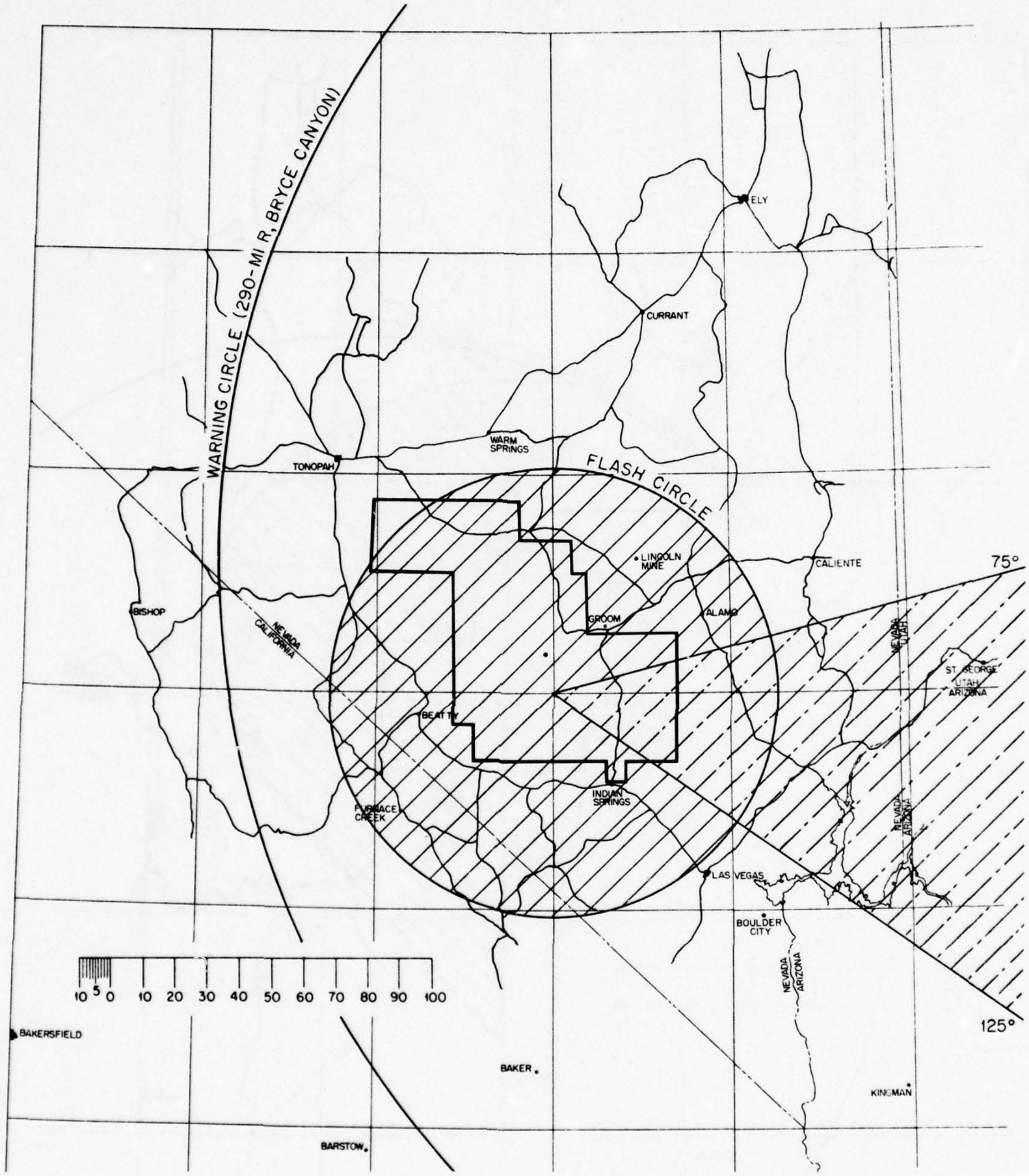

Fig. 67—CAA airspace closure plan for Upshot-Knothole 8, 2200 PDT on D−1 day. ——, Flash circle, closed all altitudes, 0800 to 0930; –·–, low sector (75° to radius 490 miles to 125° to radius 245 miles), closed 24,000 ft and below, 0900 to 1430, except Amber 2 and Red 6 airways and all west to be opened 1130. High sector, Ely–Goodland–Amarillo–Prescott–Las Vegas–Ely, closed 24,000 ft and above, 0900 to 1500.

Correction to Closure Plan:

0900 D Day: Low-sector bearings changed to 50° to radius Utah border to 100° to radius 245 miles and Red 6 airways closed until 1430. North Platte substituted for Goodland in high sector.

1030 D Day: Red 6 and south opened for low sector.

1130 D Day: Low sector opened. High sector opened south of 37°N.

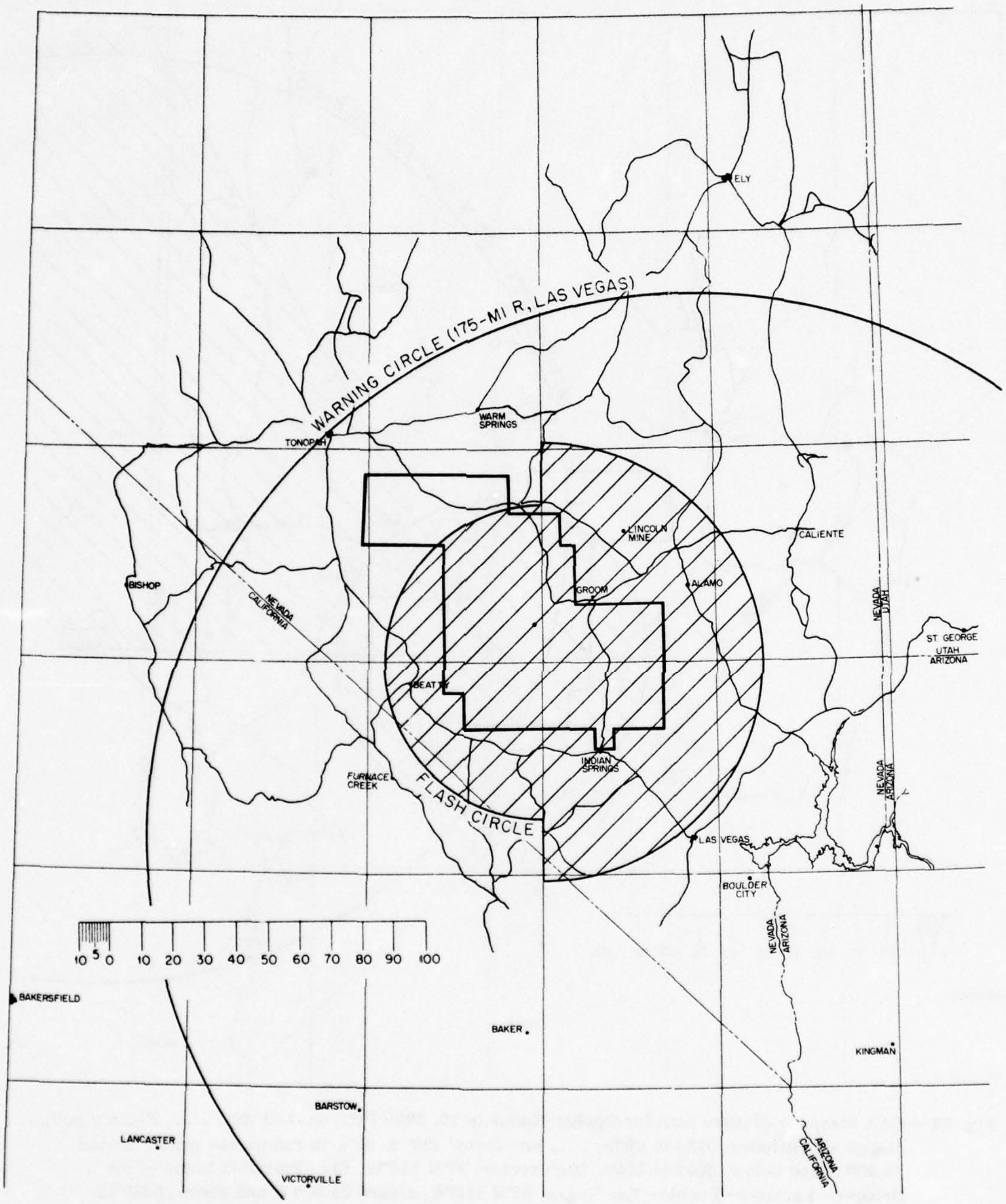

Fig. 68—CAA airspace closure plan for Upshot-Knothole 9, 2200 PDT on D−1 day. ——, Flash circle (0° to 180° to radius 70 miles, 180° to 360° to radius 50 miles), closed all altitudes, 0430 to 0600; —·—, low sector, bounded by vector 70° to radius 100 miles then east along 37° 30′N to 112° 30′W then to Prescott then along north side Green 4 and Red 15 airways to 37°N 116°W, closed at 25,000 ft and below, 0600 to 1130. High sector, 37°N 116°W, Blythe–Douglas–Albuquerque–St. George, 37°N 116°W, closed at 25,000 ft and above, 0530 to 1330.

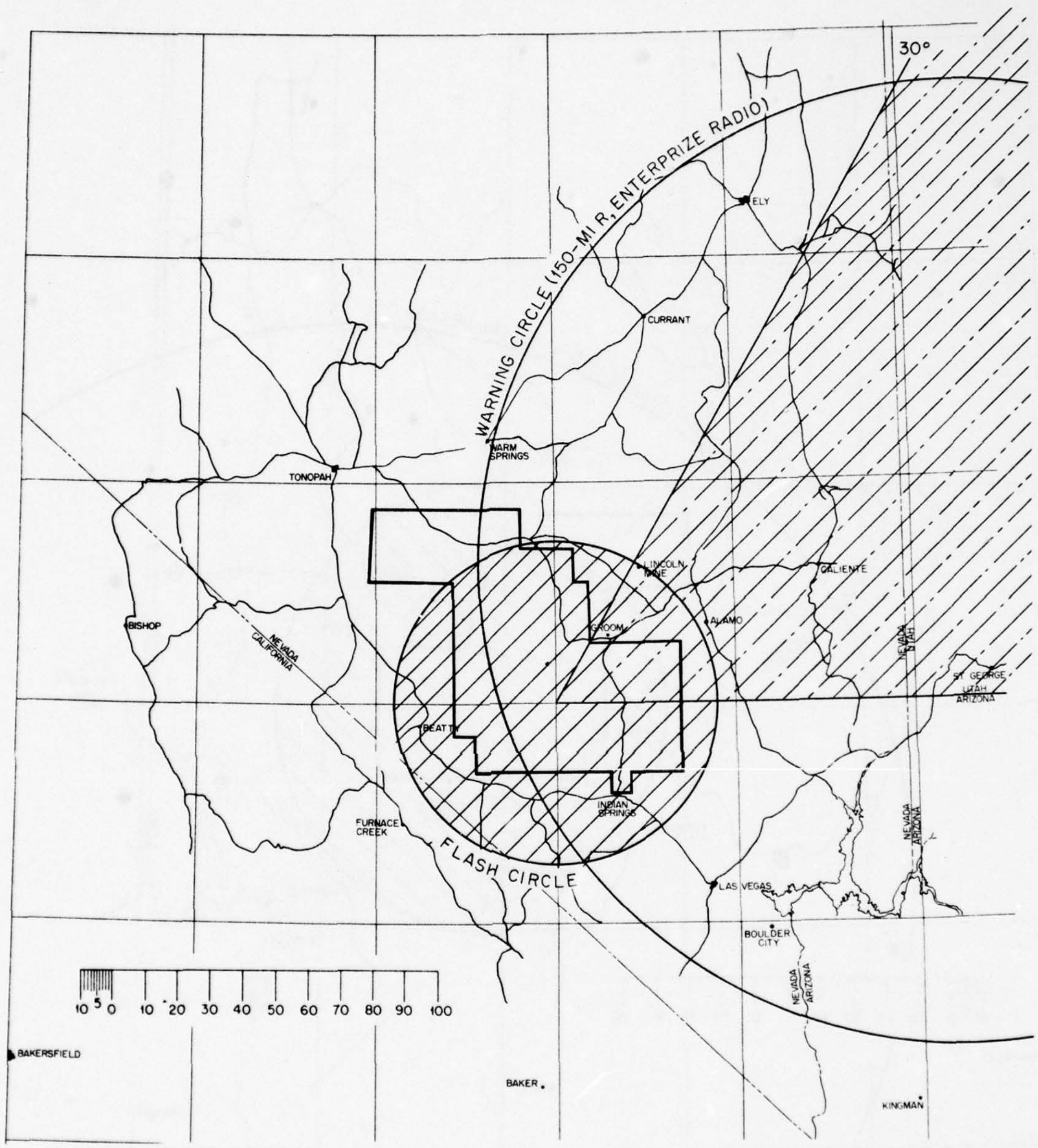

Fig. 69—CAA airspace closure plan for Upshot-Knothole 10, 2200 PDT on D−1 day. ——, Flash circle, closed all altitudes, 0730 to 0900; —·—, low sector (30° to 90°), to radius 250 miles, closed 25,000 ft and below, 0900 to 1200. High sector, 37°N 116°W, Ely−Fairfield Radio−Fort Bridger−Laramie−Pueblo−Las Vegas, 37°N 116°W, closed 25,000 ft and above, 0830 to 1430.

Correction to Closure Plan:

1000 D Day: 90° bearing of low sector changed to 60° and radius extended to 325 miles except Red 49 airway to remain clear. High sector changed to 37°N 116°W, Fairfield−Fort Bridger−Cheyenne, 37°N 116°W.

1140 D Day: Radius of low sector extended to 500 miles and time extended to 1400. Additional high sector added, Salt Lake City−Price−Rapid City−Miles City−Salt Lake City, closed 1200 to 1500.

CONFIDENTIAL

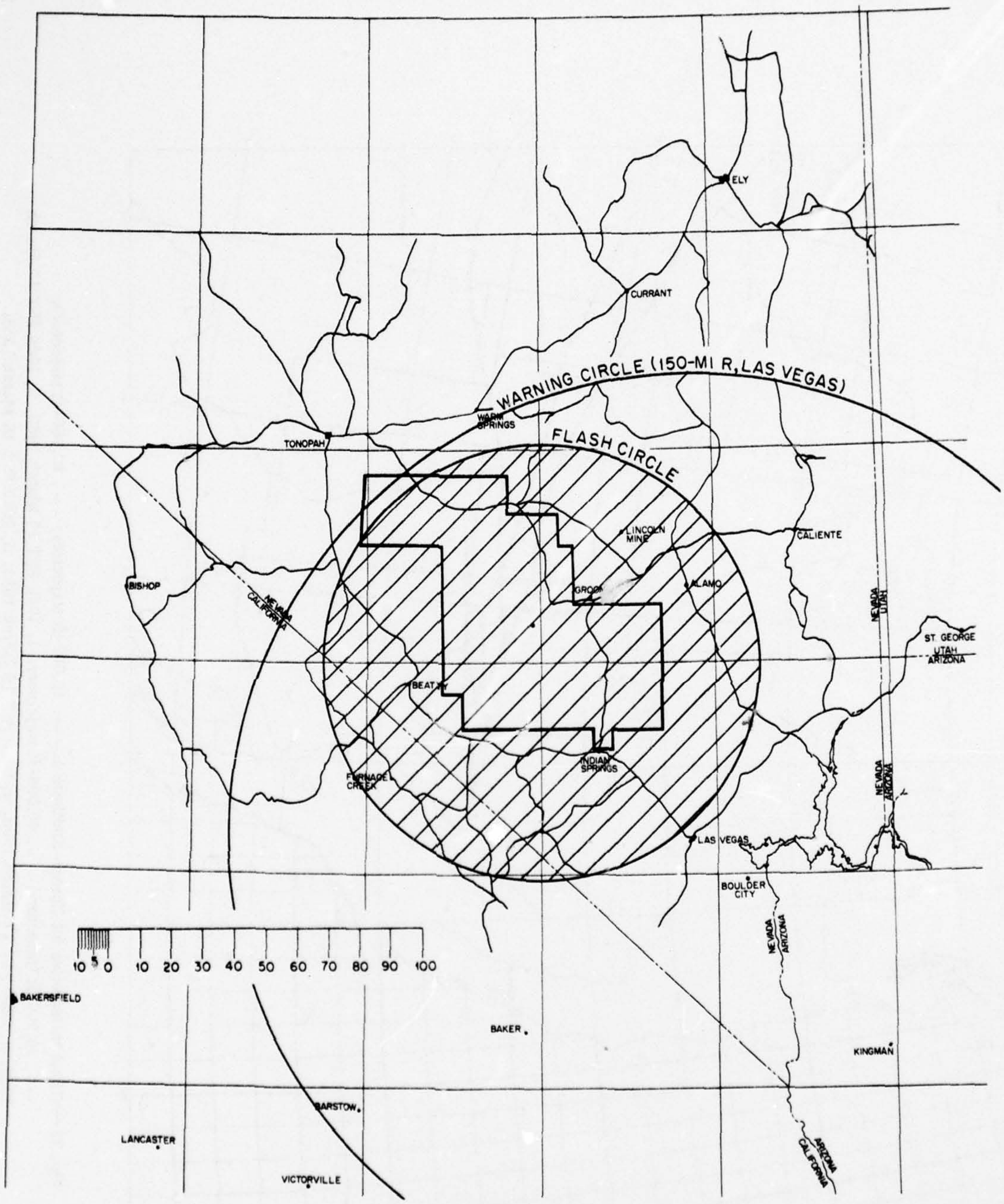

Fig. 70—CAA airspace closure plan for Upshot-Knothole 11, 2200 PDT on D−1 day. ——, Flash circle, closed all altitudes, 0345 to 0515. 0° to 180° sector of flash circle closed to 0800. No low sector. High sector, 37°N 116°W, Delta−Grand Junction−Acomita−Truth or Consequences−Needles, 37°N 116°W, closed 25,000 ft and above, 0500 *to 1500*.

Correction to Closure Plan:

0500 D Day: Closure of flash circle extended to 0800.

RESTRICTED DATA—CONFIDENTIAL—SECURITY INFORMATION

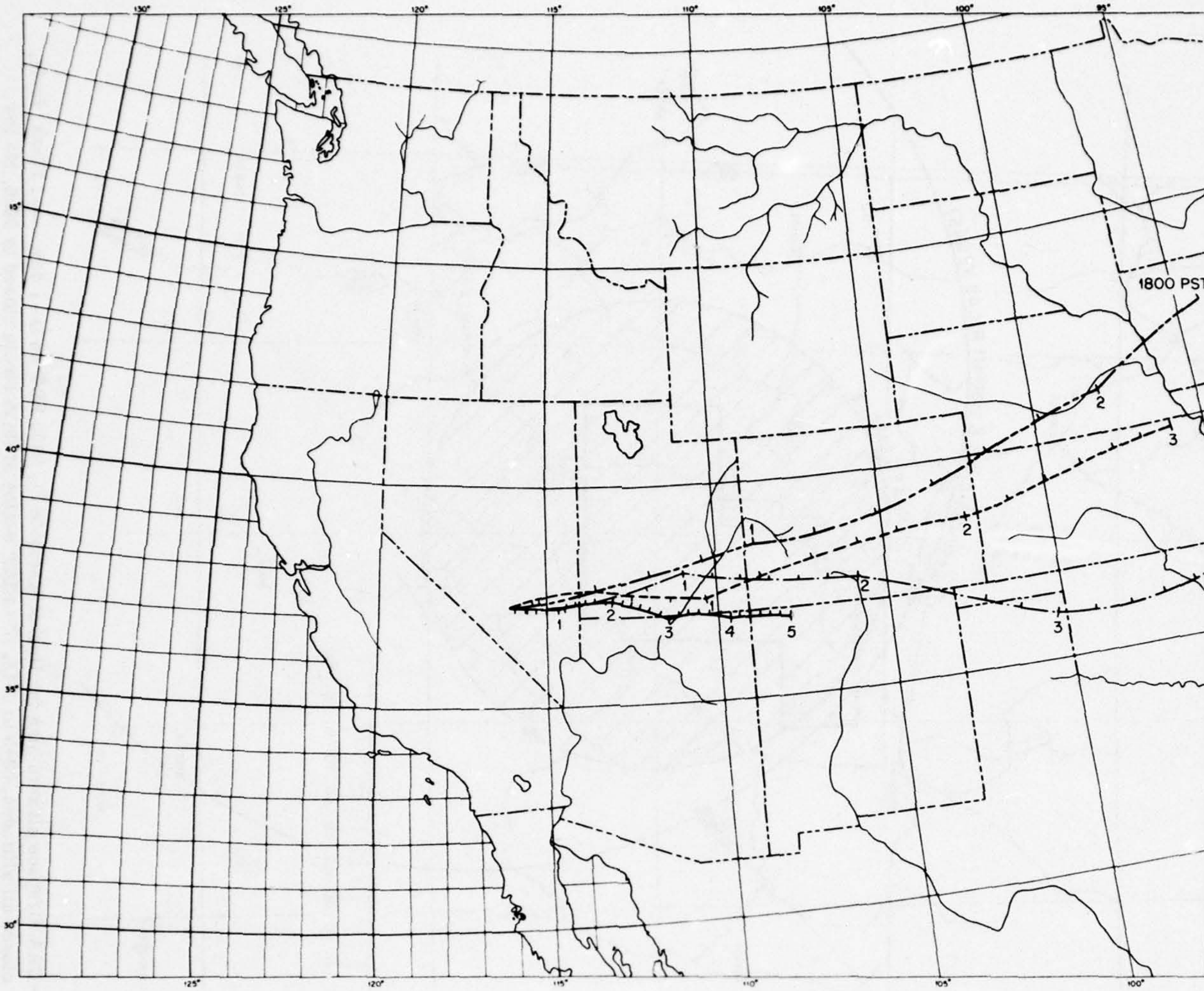

Fig. 71—Cloud trajectories for Upshot-Knothole 1. ——, 10,000-ft trajectory; ---, 20,000-ft trajectory; ---, 30,000-ft trajectory; -·-·-, 40,000-ft trajectory. 1, 1000 PST 17 March 1953. 2, 1600 PST 17 March 1953. 3, 2200 PST 17 March 1953. 4, 0400 PST 18 March 1953. 5, 1000 PST 18 March 1953.

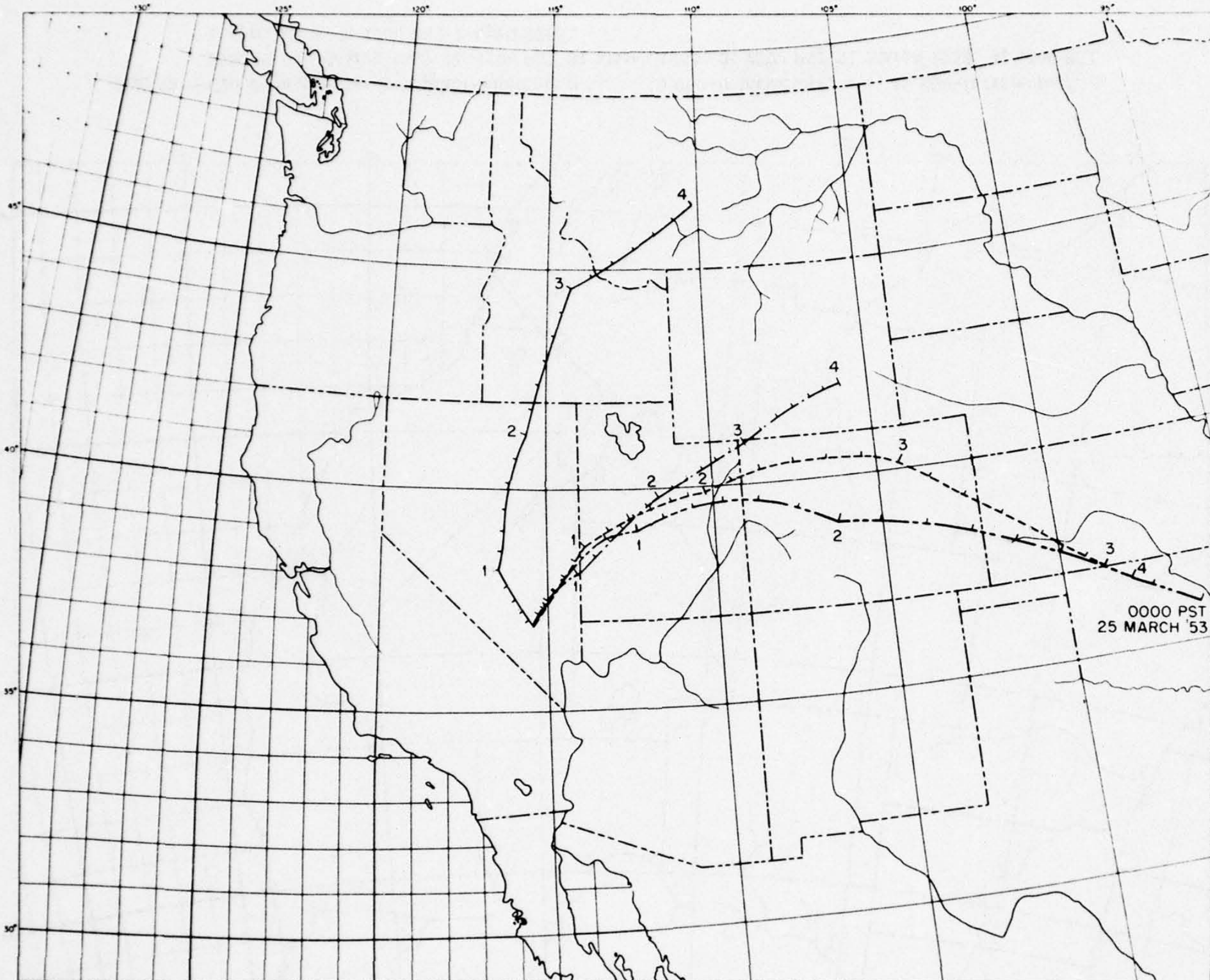

Fig. 72—Cloud trajectories for Upshot-Knothole 2. ——, 10,000-ft trajectory; -·-·, 20,000-ft trajectory; ---, 30,000-ft trajectory; -··-, 40,000-ft trajectory. 1, 1000 PST 24 March 1953. 2, 1600 PST 24 March 1953. 3, 2200 PST 24 March 1953. 4, 0400 PST 25 March 1953.

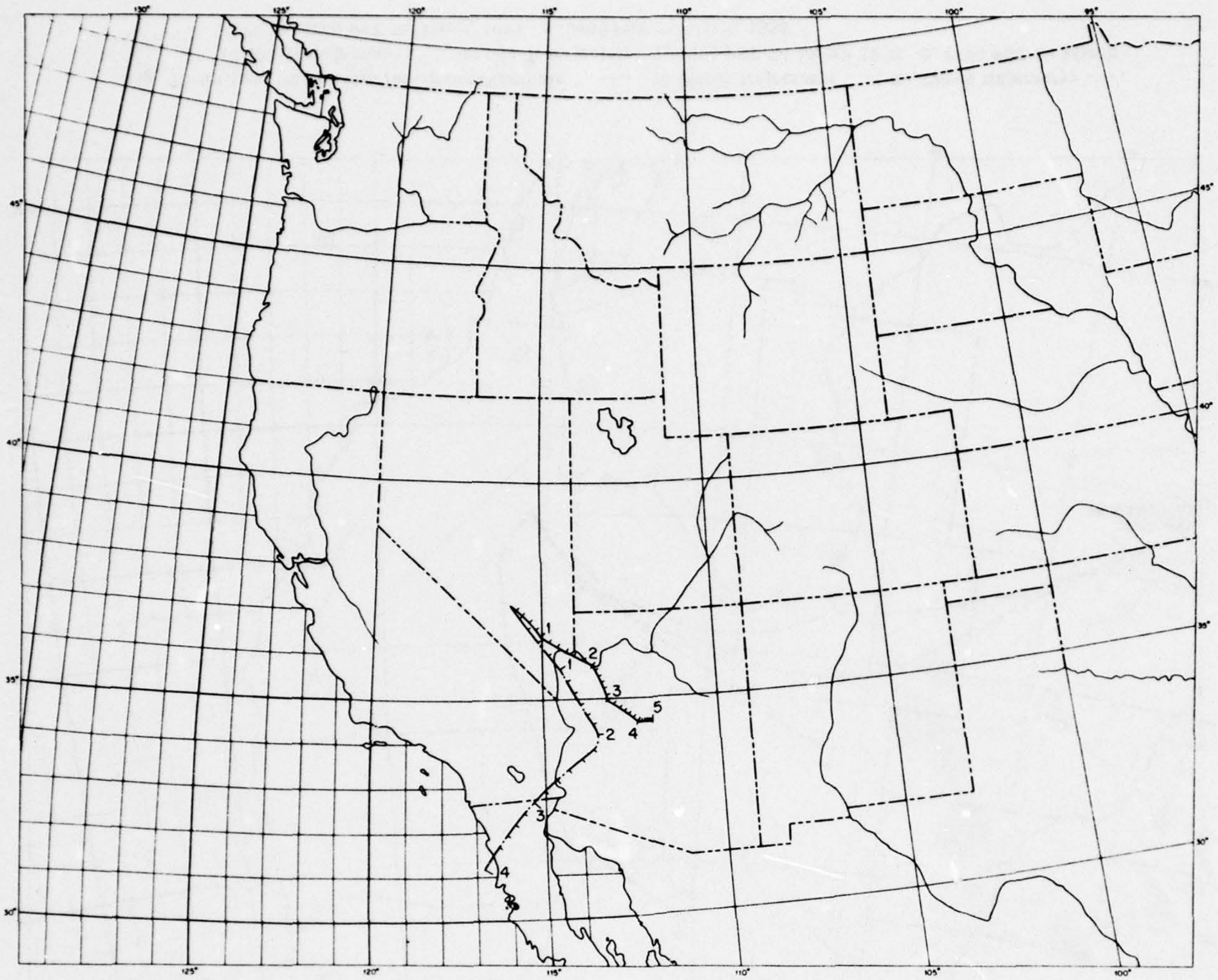

Fig. 73 —Cloud trajectories for Upshot-Knothole 3. ——, 10,000-ft trajectory; -·-·-, 16,000-ft trajectory. 1, 1000 PST 31 March 1953. 2, 1600 PST 31 March 1953. 3, 2200 PST 31 March 1953. 4, 0400 PST 1 April 1953. 5, 1000 PST 1 April 1953.

[redacted]

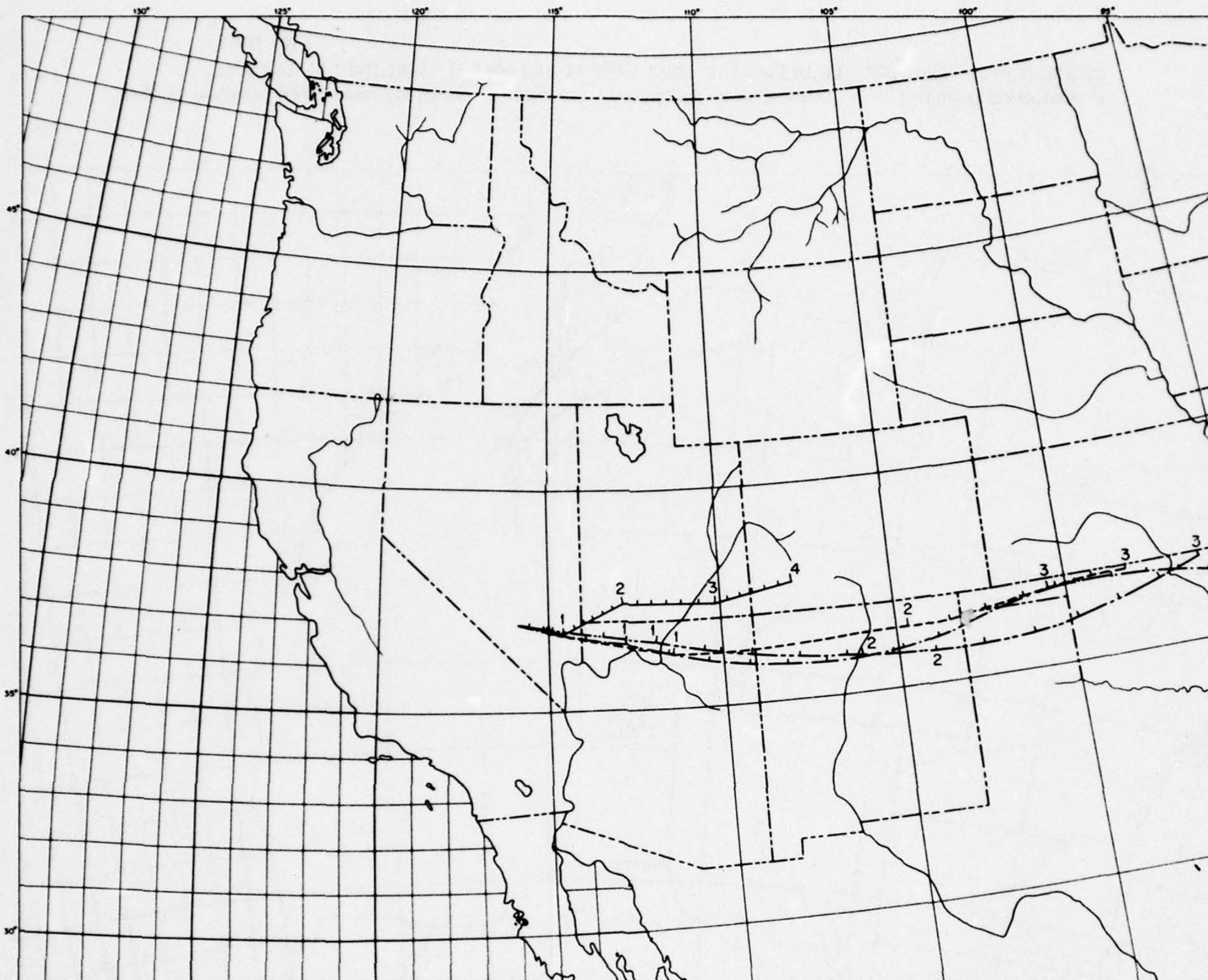

Fig. 74—Cloud trajectories for Upshot-Knothole 4. ——, 10,000-ft trajectory; —·—, 20,000-ft trajectory; ---, 30,000-ft trajectory; ----, 40,000-ft trajectory. 1, 1000 PST 6 April 1953. 2, 1600 PST 6 April 1953. 3, 2200 PST 6 April 1953. 4, 0400 PST 7 April 1953.

[redacted]

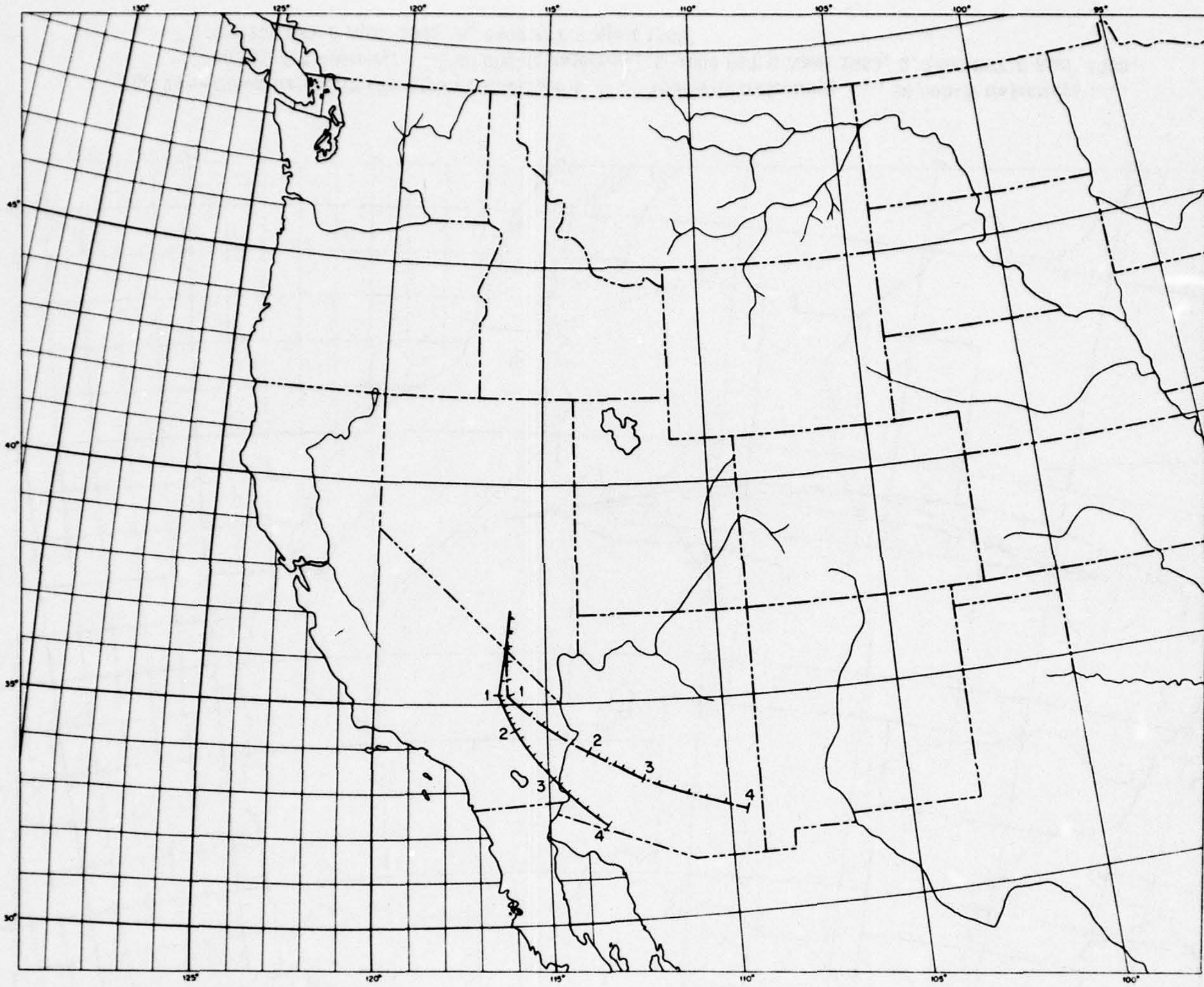

Fig. 75—Cloud trajectories for Upshot-Knothole 5. ——, 8,000-ft trajectory; -·-·, 12,000-ft trajectory. 1, 1000 PST 11 April 1953. 2, 1600 PST 11 April 1953. 3, 2200 PST 11 April 1953. 4, 0400 PST 12 April 1953.

[redacted]

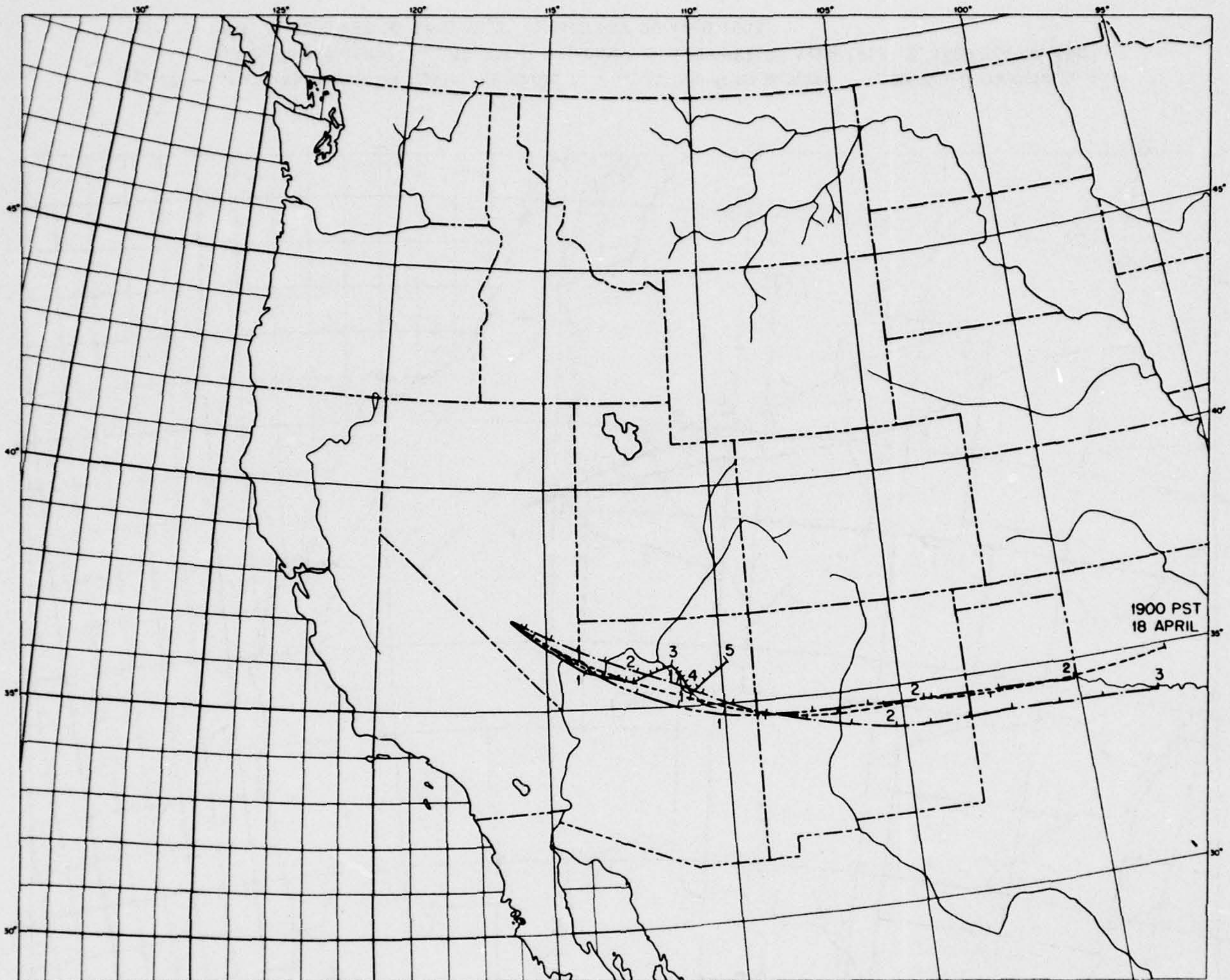

Fig. 76—Cloud trajectories for Upshot-Knothole 6. ——, 10,000-ft trajectory; ---, 20,000-ft trajectory; ---, 30,000-ft trajectory; —·—, 35,000-ft trajectory. 1, 1000 PST 18 April 1953. 2, 1600 PST 18 April 1953. 3, 2200 PST 18 April 1953. 4, 0400 PST 19 April 1953. 5, 1000 PST 19 April 1953.

[redacted]

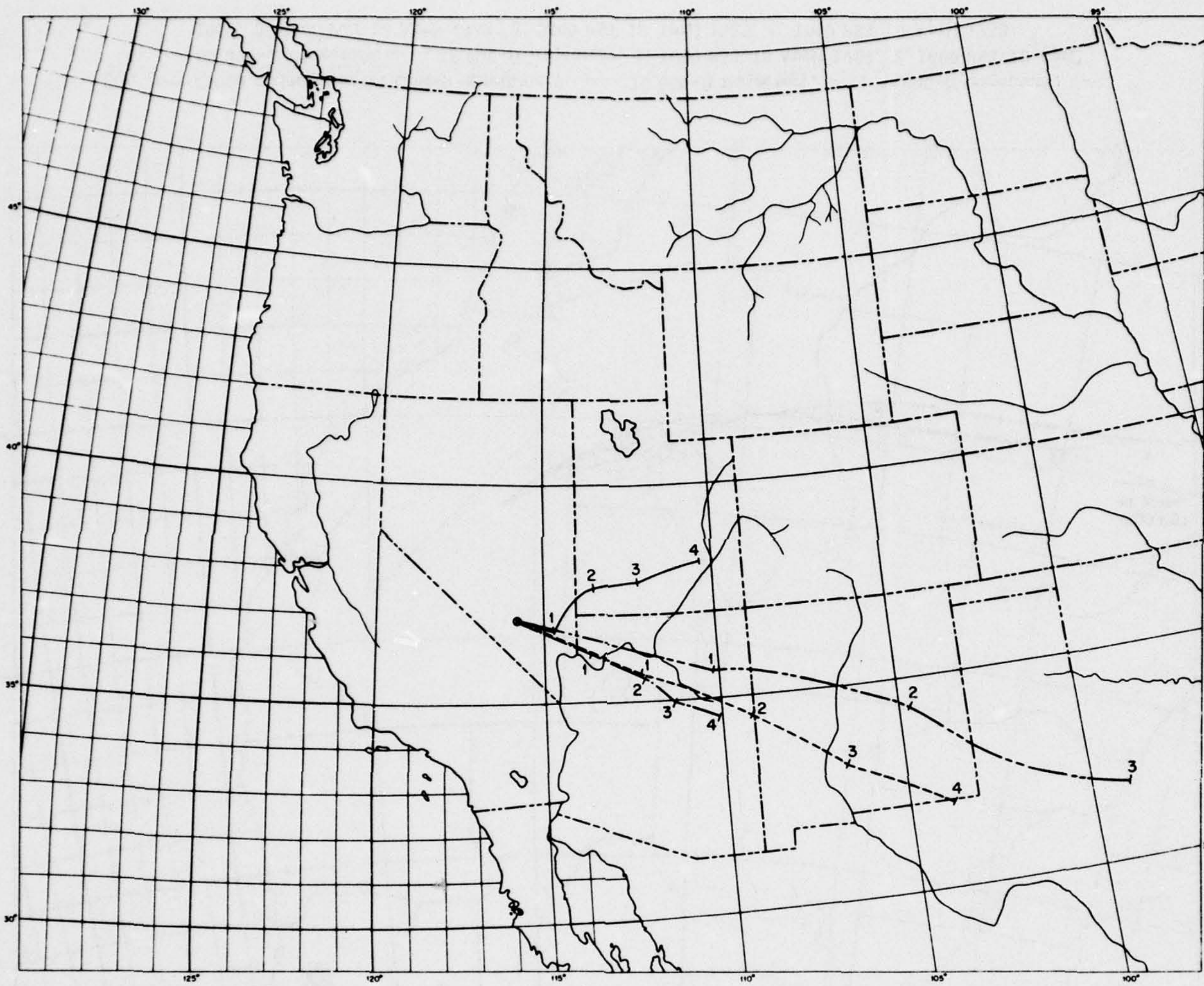

Fig. 77—Cloud trajectories for Upshot-Knothole 7. ——, 10,000-ft trajectory; , 20,000-ft trajectory; - - -, 30,000-ft trajectory; -·-·-, 40,000-ft trajectory. 1, 1000 PST 25 April 1953. 2, 1600 PST 25 April 1953. 3, 2200 PST 25 April 1953. 4, 0400 PST 26 April 1953.

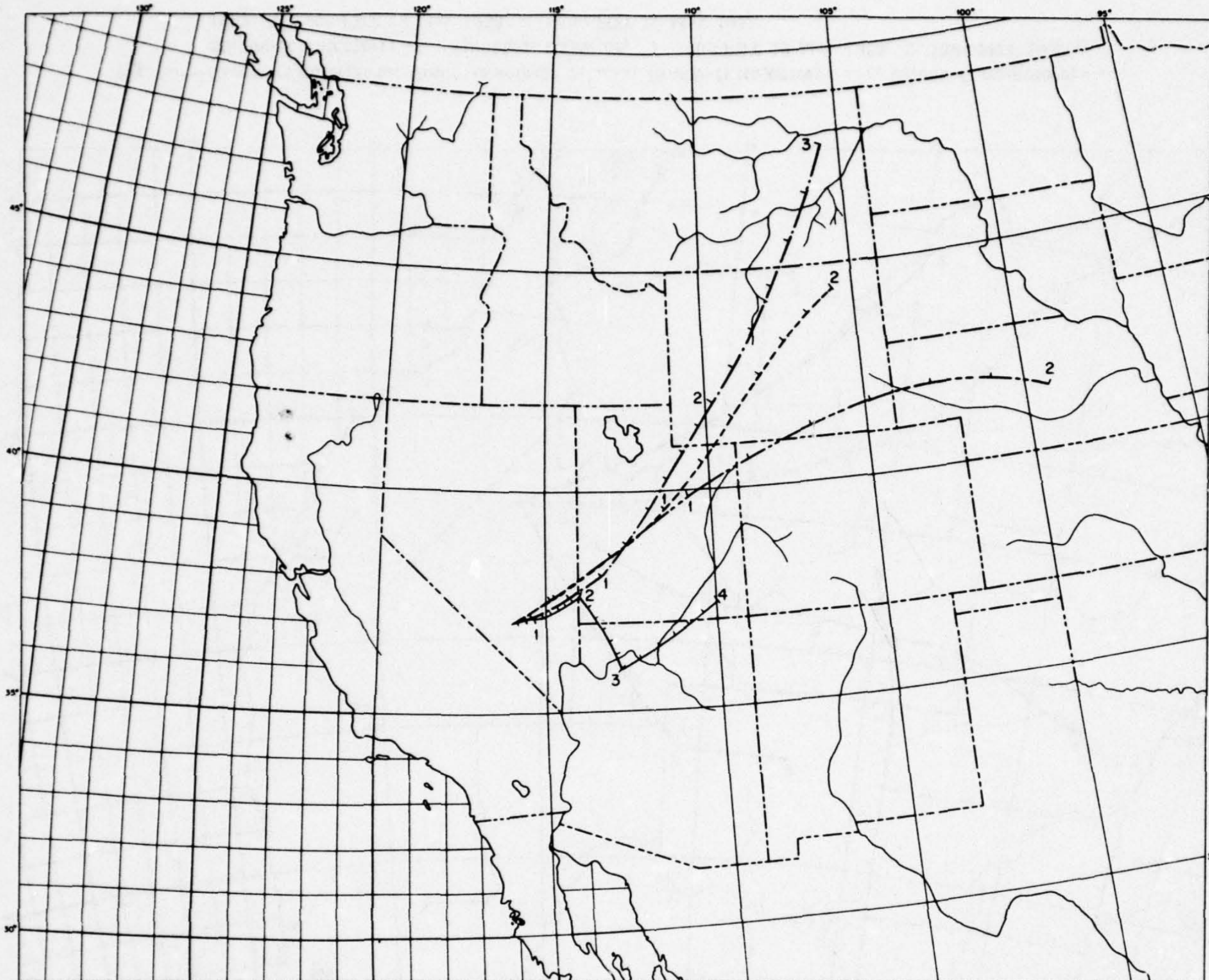

Fig. 78—Cloud trajectories for Upshot-Knothole 8. ——, 10,000-ft trajectory; –·–, 20,000-ft trajectory; ---, 30,000-ft trajectory; —·—, 40,000-ft trajectory. 1, 1100 PDT 8 May 1953. 2, 1700 PDT 8 May 1953. 3, 2300 PDT 8 May 1953. 4, 0500 PDT 9 May 1953.

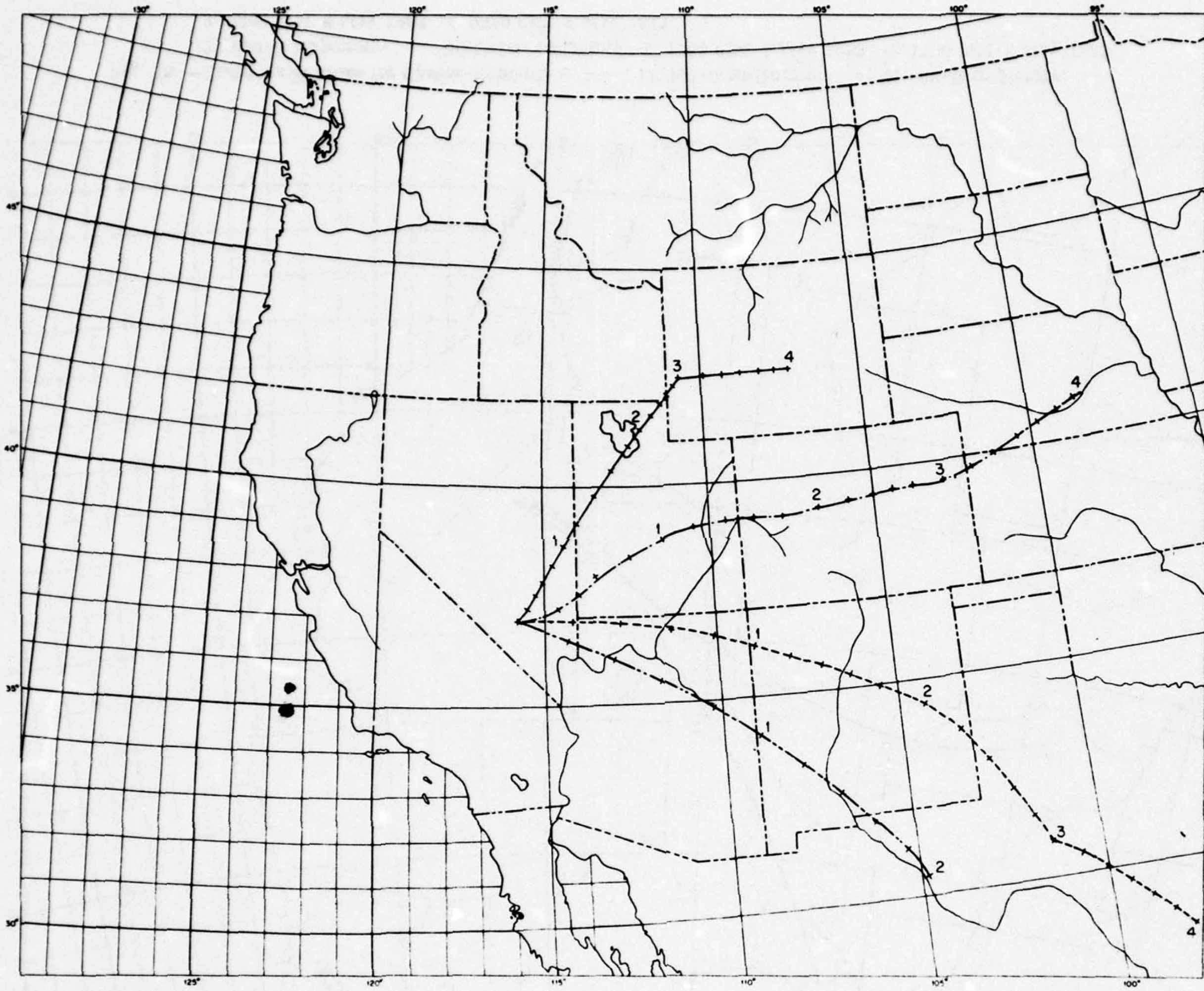

Fig. 79—Cloud trajectories for Upshot-Knothole 9. ——, 10,000-ft trajectory; -·-·-, 20,000-ft trajectory; - - -, 30,000-ft trajectory; -··-··-, 40,000-ft trajectory. 1, 1000 PDT 19 May 1953. 2, 1500 PDT 19 May 1953. 3, 2000 PDT 19 May 1953. 4, 0200 PDT 20 May 1953.

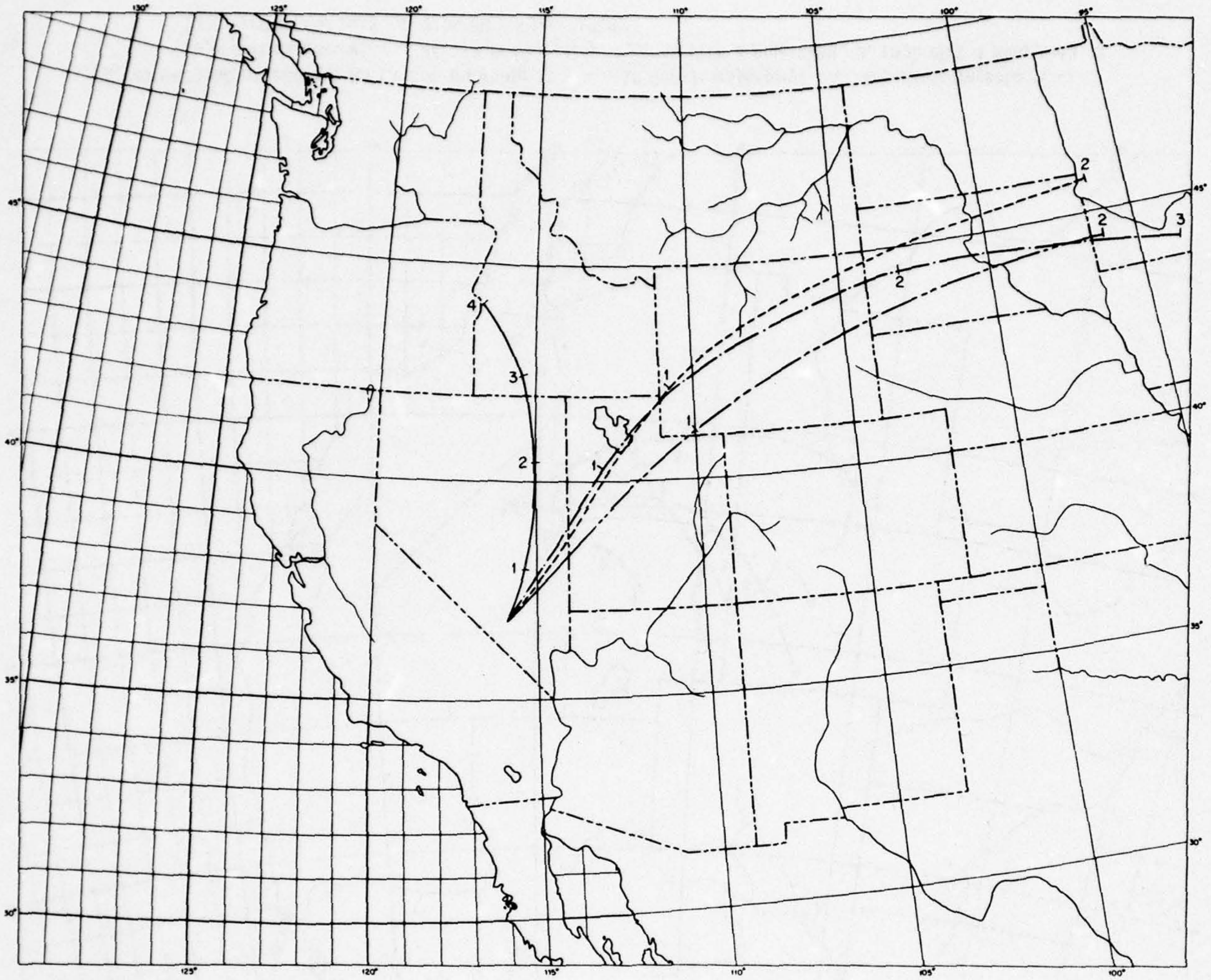

Fig. 80—Cloud trajectories for Upshot-Knothole 10. ——, 10,000-ft trajectory; –·–, 20,000-ft trajectory; ---, 30,000-ft trajectory; –··–, 35,000-ft trajectory. 1, 1130 PDT 25 May 1953. 2, 1730 PDT 25 May 1953. 3, 2330 PDT 25 May 1953. 4, 0530 PDT 26 May 1953.

UNCLASSIFIED

~~CONFIDENTIAL~~

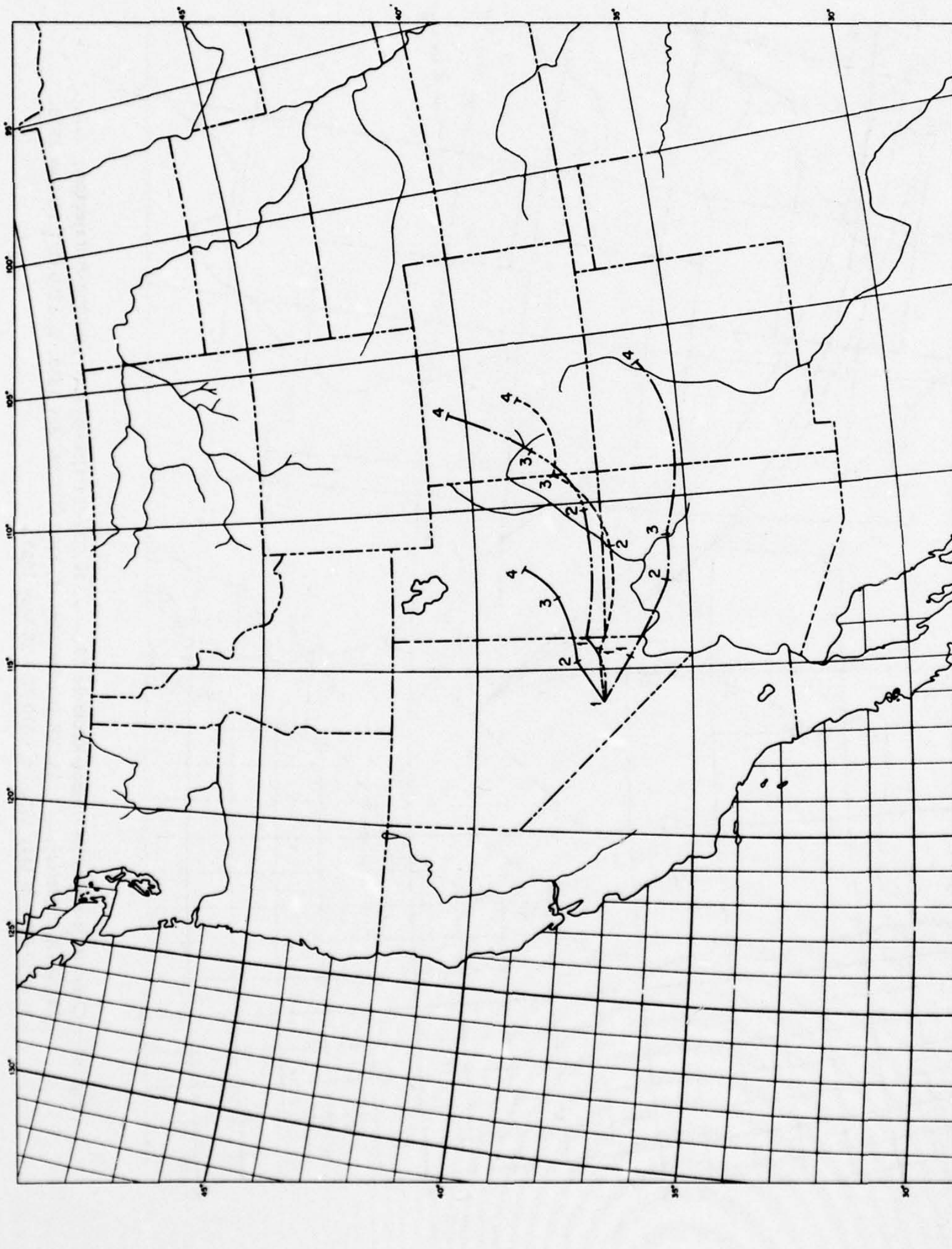

Fig. 81 —Cloud trajectories for Upshot-Knothole 11. ——, 10,000-ft trajectory; - - -, 20,000-ft trajectory; — - —, 30,000-ft trajectory; —··—, 40,000-ft trajectory. 1, 0700 PDT 4 June 1953. 2, 1300 PDT 4 June 1953. 3, 1900 PDT 4 June 1953. 4, 0100 PDT 5 June 1953.

~~RESTRICTED DATA CONFIDENTIAL SECURITY INFORMATION~~

UNCLASSIFIED

DISTRIBUTION

	Copy
ARMY ACTIVITIES	
Asst. Chief of Staff, G-2, D/A, Washington 25, D. C.	1
Asst. Chief of Staff, G-3, D/A, Washington 25, D. C., ATTN: Dep. CofS, G-3, (RR&SW)	2
Asst. Chief of Staff, G-4, D/A, Washington 25, D. C.	3
Chief of Ordnance, D/A, Washington 25, D. C., ATTN: ORDTX-AR	4
Chief Signal Officer, D/A, P&O Division, Washington 25, D. C., ATTN: SIGOP	5–7
The Surgeon General, D/A, Washington 25, D. C., ATTN: Chairman, Medical R&D Board	8
Chief Chemical Officer, D/A, Washington 25, D. C.	9–10
Chief of Engineers, D/A, Military Construction Division, Protective Construction Branch, Washington 25, D. C., ATTN: ENGEB	11
Chief of Engineers, D/A, Civil Works Division, Washington 25, D. C., ATTN: Engineering Division, Structural Branch	12
The Quartermaster General, CBR, Liaison Office, Research and Development Division, D/A, Washington 25, D. C.	13–14
Chief of Transportation, Military Planning and Intelligence Division, D/A, Washington 25, D. C.	15
Chief, Army Field Forces, Ft. Monroe, Virginia	16–19
Army Field Forces Board #1, Ft. Bragg, N. C.	20
Army Field Forces Board #4, Ft. Bliss, Tex.	21
Commanding General, First Army, Governor's Island, New York 4, N. Y., ATTN: G-1	22
Commanding General, First Army, Governor's Island, New York 4, N. Y., ATTN: G-2	23
Commanding General, First Army, Governor's Island, New York 4, N. Y., ATTN: G-3	24
Commanding General, First Army, Governor's Island, New York 4, N. Y., ATTN: G-4	25–26
Commanding General, Second Army, Ft. George G. Meade. Md., ATTN: AIABB	27
Commanding General, Second Army, Ft. George G. Meade, Md., ATTN: AIAME	28
Commanding General, Second Army, Ft. George G. Meade, Md., ATTN: AIACM	29
Commanding General, Third Army, Ft. McPherson, Ga., ATTN: ACofS, G-3	30–31
Commanding General, Fourth Army, Ft. Sam Houston, Tex., ATTN: G-3 Section	32–33
Commanding General, Fifth Army, 1660 E. Hyde Park Blvd., Chicago 15, Ill., ATTN: ALFEN	34
Commanding General, Fifth Army, 1660 E. Hyde Park Blvd.. Chicago 15, Ill., ATTN: ALFCM	35
Commanding General, Fifth Army, 1660 E. Hyde Park Blvd., Chicago 15, Ill., ATTN: ALFGA-MS	36
Commanding General, Sixth Army, Presidio of San Francisco, Calif., ATTN: AMGCT-4	37
Commanding General, Trieste US Troops, APO 209, c/o PM, New York, N. Y., ATTN: ACofS, G-3	38–40
Commanding General, US Forces Austria, APO 168, c/o PM, New York, N. Y., ATTN: ACofS, G-3	41
Commander-in-Chief, Far East Command, APO 500, c/o PM, San Francisco, Calif., ATTN: ACofS, J-3	42–43
Commanding General, US Army Forces Far East (Main), APO 343, c/o PM, San Francisco, Calif., ATTN: ACofS, G-3	44–46

Commanding General, U. S. Army Alaska, APO 942, c/o PM, Seattle, Wash.	47
Commanding General, U. S. Army Caribbean, Fort Amador, C. Z., ATTN: Cml. Off.	48
Commanding General, USARFANT & MDPR, Fort Brooke, Puerto Rico	49
Commanding General, U. S. Army Europe, APO 403, c/o PM, New York, N. Y., ATTN: OPOT Division, Com. Dev. Branch	50-51
Commanding General, U. S. Army Pacific, APO 958, c/o PM, San Francisco, Calif., ATTN: Cml. Off.	52-53
Commandant, Command and General Staff College, Ft. Leavenworth, Kan., ATTN: ALLIS(AS)	54
Commandant, Army War College, Carlisle Barracks, Pa., ATTN: Library	55
Commandant, The Infantry School, Ft. Benning, Ga., ATTN: C.D.S.	56-57
Commandant, The Artillery School, Ft. Sill, Okla.	58
Commandant, The AA&GM Branch, The Artillery School, Ft. Bliss, Tex.	59
Commandant, The Armored School, Ft. Knox, Ky., ATTN: Classified Document Section, Evaluation and Res. Division	60-61
Commanding General, Medical Field Service School, Brooke Army Medical Center, Ft. Sam Houston, Tex.	62
Director of Special Weapons Developments, OCAFF, Ft. Bliss, Tex., ATTN: Major Hale Mason, Jr.	63
Commandant, Army Medical Service Graduate School, Walter Reed Army Medical Center, Washington 25, D. C., ATTN: Dept. of Biophysics	64
Commanding General, The Transportation Center and Ft. Eustis, Ft. Eustis, Va., ATTN: Asst. Commandant, Military Science and Tactics Bd.	65
The Superintendent, U. S. Military Academy, West Point, N. Y., ATTN: Professor of Ordnance	66
Commandant, Chemical Corps School, Chemical Corps Training Command, Ft. McClellan, Ala.	67
Commanding General, Research and Engineering Command, Army Chemical Center, Md., ATTN: Special Projects Officer	68-69
Commanding General, The Engineer Center, Ft. Belvoir, Va., ATTN: Asst. Commandant, Engineer School	70-72
Commanding Officer, Engineer Research and Development Laboratory, Ft. Belvoir, Va., ATTN: Chief, Technical Intelligence Branch	73
Commanding Officer, Picatinny Arsenal, Dover, N. J., ATTN: ORDBB-TK	74
Commanding Officer, Frankford Arsenal, Philadelphia 37, Pa., ATTN: RD Control Off.	75
Commanding Officer, Army Medical Research Laboratory, Ft. Knox, Ky.	76
Commanding Officer, Chemical Corps Chemical and Radiological Laboratory, Army Chemical Center, Md., ATTN: Technical Library	77-78
Commanding Officer, Transportation R&D Station, Ft. Eustis, Va.	79
Director, Technical Documents Center, Evans Signal Laboratory, Belmar, N. J.	80
Director, Waterways Experiment Station, PO Box 631, Vicksburg, Miss., ATTN: Library	81
Director, Operations Research Office, Johns Hopkins University, 6410 Connecticut Ave., Chevy Chase, Md., ATTN: Library	82

NAVY ACTIVITIES

Chief of Naval Operations, D/N, Washington 25, D. C., ATTN: OP-36	83-84
Chief, Bureau of Medicine and Surgery, D/N, Washington 25, D. C., ATTN: Special Weapons Defense Division	85-86
Chief, Bureau of Ordnance, D/N, Washington 25, D. C.	87
Chief of Naval Personnel, D/N, Washington 25, D. C., ATTN: Pers C123	88
Chief of Naval Personnel, D/N, Washington 25, D. C., ATTN: Pers C	89
Chief of Naval Personnel, D/N, Washington 25, D. C., ATTN: Pers 15	90
Chief, Bureau of Ships, D/N, Washington 25, D. C., ATTN: Code 348	91-92
Chief, Bureau of Supplies and Accounts, D/N, Washington 25, D. C.	93
Chief, Bureau of Yards and Docks, D/N, Washington 25, D. C., ATTN: P-312	94
Chief, Bureau of Aeronautics, D/N, Washington 25, D. C.	95-96
Commander-in-Chief, U. S. Atlantic Fleet, U. S. Naval Base, Norfolk 11, Va	97-98
Commander-in-Chief, U. S. Pacific Fleet, Fleet Post Office, San Francisco, Calif.	99-100

AD-A077 504 LOS ALAMOS SCIENTIFIC LAB N MEX F/G 4/2
ACTIVITIES OF THE SPECIAL WEATHER ADVISORY SERVICE.(U)
JUL 53 G J NEWGARDEN

UNCLASSIFIED AEC-WT-705 NL

2 OF 2
ADA
077504

END
DATE
FILMED
12-79
DDC

END
DATE
FILMED
12-79
DDC

Commandant, U. S. Marine Corps, Washington 25, D. C., ATTN: Code A03H	101–104
President, U. S. Naval War College, Newport, Rhode Island	105
Superintendent, U. S. Naval Postgraduate School, Monterey, Calif.	106
Commanding Officer, U. S. Naval Schools Command, U. S. Naval Station, Treasure Island, San Francisco, Calif.	107–108
Director, USMC Development Center, USMC Schools, Quantico, Va., ATTN: Tactics Board	109
Director, USMC Development Center, USMC Schools, Quantico, Va., ATTN: Equipment Board	110
Commanding Officer, U. S. Fleet Training Center, Naval Base, Norfolk 11, Va., ATTN: Special Weapons School	111
Commanding Officer, U. S Fleet Training Center, Naval Station, San Diego 36, Calif., ATTN: (SPWP School)	112
Commanding Officer, U. S. Naval Damage Control Training Center, Naval Base, Philadelphia 12, Pa., ATTN: ABC Defense Course	113
Commanding Officer, U. S. Naval Unit, Chemical Corps School, Army Chemical Training Center, Ft. McClellan, Ala.	114
Commander, U. S. Naval Ordnance Laboratory, Silver Spring 19, Md., ATTN: E	115
Commander, U. S Naval Ordnance Laboratory, Silver Spring 19, Md., ATTN: EE	116
Commander, U. S. Naval Ordnance Laboratory, Silver Spring 19, Md., ATTN: R	117–118
Commander, U. S. Naval Ordnance Test Station, Inyokern, China Lake, Calif.	119
Officer-in-Charge, U. S. Naval Civil Engineering Research and Evaluation Laboratory, Construction Battalion Center, Port Hueneme, Calif., ATTN: Code 753	120–121
Commanding Officer, U. S. Naval Medical Research Institute, National Naval Medical Center, Bethesda 14, Md.	122
Director, U. S. Naval Research Laboratory, Washington 25, D. C.	123
Commanding Officer and Director, U. S. Navy Electronics Laboratory, San Diego 52, Calif., ATTN: Code 250	124
Commanding Officer and Director, U. S. Navy Electronics Laboratory, San Diego 52, Calif., ATTN: Code 310	125
Commanding Officer, U. S. Naval Radiological Defense Laboratory, San Francisco 24, Calif., ATTN: Technical Information Division	126–129
Commanding Officer and Director, David W. Taylor Model Basin, Washington 7, D. C., ATTN: Library	130
Commanding Officer, U. S. Naval Photographic Center, Anacostia, D. C.	131–132
Commander, U. S. Naval Air Development Center, Johnsville, Pa.	133
Director, Office of Naval Research Branch Office, 1000 Geary Street, San Francisco 9, Calif.	134–135

AIR FORCE ACTIVITIES

Asst. for Atomic Energy, Headquarters, USAF, Washington 25, D. C., ATTN: DCS/O	136
Asst. for Development Planning, Headquarters, USAF, Washington 25, D. C	137
Director of Operations, Headquarters, USAF, Washington 25, D. C.	138
Director of Operations, Headquarters, USAF, Washington 25, D. C., ATTN: Operations Analysis Division	139
Director of Plans, Headquarters, USAF, Washington 25, D. C., ATTN: War Plans Division	140
Directorate of Requirements, Headquarters, USAF, Washington 25, D. C., ATTN: AFDRQ-SA/M	141
Directorate of Research and Development, Armament Division, DCS/D, Headquarters, USAF, Washington 25, D. C.	142
Directorate of Intelligence, Headquarters, USAF, Washington 25, D. C., ATTN: AFOIN-1B2	143–144
The Surgeon General, Headquarters, USAF, Washington 25, D. C., ATTN: Bio. Def. Br., Pre. Med. Div.	145
Commander, U. S. Air Forces Europe, APO 633, c/o PM, New York, N. Y.	146
Commander, Far East Air Forces, APO 925, c/o PM, San Francisco, Calif.	147
Commander, Alaskan Air Command, APO 942, c/o PM, Seattle, Wash., ATTN: AAOTN	148–157

OTHER DEPT. OF DEFENSE ACTIVITIES

ATOMIC ENERGY COMMISSION ACTIVITIES